NTNU – Trondheim
Norwegian University of
Science and Technology

Applying Time-Lapse Seismic Inversion In Reservoir Management: A Case Study Of The Norne Field

Anass Nii-Armah Ammah

Petroleum Geosciences
Submission date: June 2012
Supervisor: Egil Tjåland, IPT

Norwegian University of Science and Technology
Department of Petroleum Engineering and Applied Geophysics

APPLYING TIME-LAPSE SEISMIC INVERSION IN RESERVOIR MANAGEMENT:

A CASE STUDY OF THE NORNE FIELD

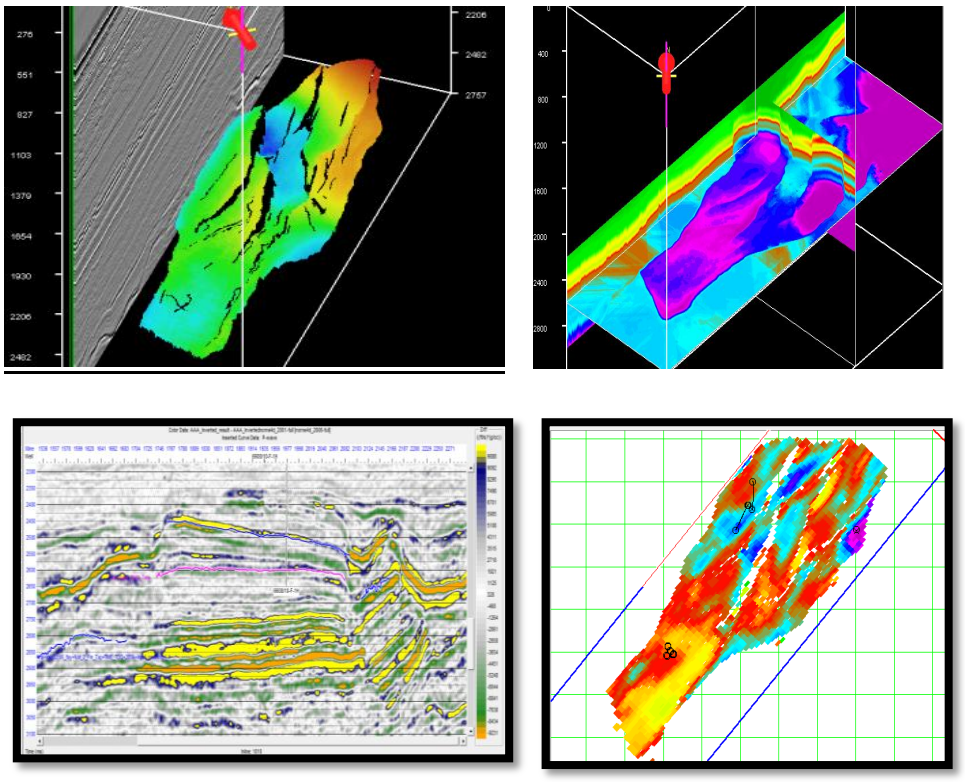

By Anass Nii-Armah Ammah

(Department of Petroleum Engineering and Applied Geophysics, 2012)

Declaration

This thesis is the result of research work undertaken by Anass Nii-Armah Ammah in the Department of Petroleum Engineering and Applied Geophysics, Norwegian University of Science and Technology (NTNU), under the supervision of Associate Professor Egil Tjåland in partial fulfilment of the requirements for the degree of Master of Science in Petroleum Geoscience (Geophysics Specialization).

Date: _____ Signed: _____

Anass Nii-Armah Ammah

Date: _____ Approved: _____

Associate Professor Egil Tjåland

(Thesis Supervisor)

Abstract

Time-lapse seismic inversion approach to reservoir management has proven to be a vital tool in the industry today because of its effectiveness in tracking the movement of fluid front within the reservoir as well as identifying isolated bypassed accumulations.

A base (2001) and three monitor (2003, 2004 and 2006) seismic surveys from the Norne field were inverted during this research. Water and gas have been injected into the reservoir to maintain the initial pressure within the field. These seismic surveys were analyzed for time-lapse impedance changes due to the differences in the produced hydrocarbons and the injected fluids. Check-shot corrected well data as well as interpreted horizons were integrated in the inversion process. Two independent wavelets were extracted from base and monitor surveys and combined to form an all-encompassing frequency and amplitude wavelet. The base and monitors were jointly inverted. This is because of the reduction in inconsistencies that are associated with independent inversions of surveys and the production related changes expected in time-lapse inverted seismic data.

The results of the inversion show the impedance difference across the field for the various monitor surveys. Areas surrounding producer wells show slight changes in impedance while great impedance difference are observed around injector wells. A statistical analysis of the inversion results also shows steady increase in impedance across the field for the subsequent monitors. Structural and stratigraphic interpretation of the time-lapse inverted data also confirmed the sealing properties of some formations. This sealing property supported the impedance changes within the field. Fault interpretations as well as its sealing and non-sealing properties were inferred from the impedance differences across various discontinuities.

Time-lapse acoustic impedance inversion of the Norne post-stack seismic data has revealed the impacts of production, dynamic fluid changes across main identified geologic structures, fluid front migration, fluid communication across structures and segments and other identified stratigraphic elements.

Acknowledgements

I wish to above all things thank God Almighty for His mercies and love towards me during my period of study in Norway. His guidance and grace have been sufficient for me.

My appreciation goes to my supervisor, Associate Professor Egil Tjåland, Department of Petroleum Engineering and Applied Geophysics for his fruitful discussions and review throughout the period of the thesis.

Special thanks to Richard Rwechungura, research scientist, Department of Petroleum Engineering and Applied Geophysics for his guidance, counsel and support during my stay in Norway and also for assisting me in getting access to the Norne database.

I am grateful to Professors Alexey Stovas and Martin Landrø for their willingness to assist me whenever I called on them and in providing literary materials for my thesis. To Våtevika and Knut Backe, thanks for your software assistance and technical help.

To all friends who took time off their busy schedules to assist me in various ways during my thesis I am grateful especially to Achel, David and Samson. To the Wilsons, Fionuala, Angela, Jemimah, Matilda, Ganaahs and all other colleagues, I say thanks.

I finally wish to thank the Integrated Operations Center (IOC), Statoil and their partners in the Norne field for making the various databasets available during the period of the thesis.

Dedication

I wish to dedicate this thesis to my parents Oliver Camel-Din Teiko Ammah and Beatrice Tsotsoo Anang. I am greatly indebted to you for your love, care and support for me. Thanks for helping me find my feet in academia and respecting my choices.

Table of Contents

Table of Figures

List of Table

1. Chapter One

1.1 Introduction

The drive for finding economically viable hydrocarbon reserves has led to various developments in the exploration industry. Since the time of first discoveries of hydrocarbon accumulation in simple anticlinal structures, there has been a complexity which one has to now deal with since the more obvious traps have been explored and produced. This complexity in the discovery of hydrocarbons has led to the integration of various fields of study. Some of these fields of study are petrophysics, geology, geophysics and reservoir engineering. The integration of these various disciplines can be classified as formation evaluation. Formation evaluation has been used over the years in the hydrocarbon exploration and production industry. It aims to integrate, analyze and interpret various datasets in order to be able to tell the nature of the reservoir and be able to quantitatively establish the volume of hydrocarbon contents in the reservoir and to determine the most effective means of recovery of our hydrocarbons.

The use of seismic data in the exploration of hydrocarbons both on land and in marine conditions cannot be overemphasized in geophysics. Seismic data has been the pivoting tool around which the exploration industry has strived. The introduction of 3D seismic surveys revolutionized the exploration industry. With its efficiency in providing a volume of closely spaced three-dimensional time migrated data, improved signal to noise ratio and its ability to collapse diffraction from unconformity boundaries to their point of origin (Gaarenstroom, L. 1984) , the 3D seismic data became a vital tool over potential fields and had a significant advantage over 2D surveys. A repeated seismic survey is classified as 4D or time-lapse seismic survey with time being the fourth dimension. According to Landrø, 2010, a repeated 2D seismic survey can still be classified as a time-lapse survey since the fourth dimension, time, is incorporated. With the use of time-lapse seismic being mainly used in the monitoring of hydrocarbon reservoirs to track production, it can also be used for the monitoring of underground storage of CO_2 gas as well as the monitoring geohazards. One of the first and best known examples of time-lapse monitoring was by Greaves and Fulp, 1987, where they showed its use in a thermal recovery process.

The main aim of a seismic survey is to interpret the geometry of subsurface reflectors, their continuity and the depths at which they are located. This is possible due to the differences in

acoustic properties of the subsurface materials. The use of conventional methods in the interpretation of seismic data is getting considerably complex and thus the need for other methods to be employed in the identification of potential reservoirs. Seismic inversion is one of these methods which can effectively be used to aid interpretation in more complex reservoirs and increase productivity.

Forward modeling process according to Menke, 1989, involves predicting the results of measurements on the basics of a principle or model and a set of specific conditions relevant to the problem to be solved. Seismic inversion or simply, inversion is the opposite of forward modeling process. An accurately inverted data gives a model of physical measurements of the earth which is representative of the real earth after the wavelet effect has been deconvolved from the measured seismic data to get acoustic impedances.

Inversion of seismic data requires the use of well logs which are essentially used in the process. A well log is a continuous recording of a petrophysical parameter along a borehole (Asquith and Gibson, 1983). Almost all measurements taken during a well logging exercise can be used as supplementary data in the inversion process but the most important of these logs are the acoustic/sonic and density logs.

The combined use of time-lapse seismic survey and inversion will be utilized in the monitoring of changes which occur within the reservoir of the Norne field. Most of the changes which occur within the reservoirs are usually production related changes and this would be explored during this research.

1.2 Aim and Objective

The aim of this thesis is to invert post-stack measured seismic data from the Norne field and access the time-lapse effect of the inverted data due to production related changes. The time-lapse changes within a reservoir can mostly be in terms of saturations and pressures due to production. Acoustic Impedance (AI) change is another effect which comes along with time-lapse seismic. The inverted seismic data could also be transformed into reservoir properties which can be used by reservoir engineers during simulation and optimization processes to enhance the effective monitoring and extraction of hydrocarbons.

1.3 Methodology

Various methodologies have been proposed for the inversion of time-lapse seismic data. Sarkar et al., 2003, supports the inversion of a base and monitor survey separately and the difference calculated by subtraction one inverted result from the other. Lorenzen, 2000, coupled the inversion of base and monitor by the use of a single low-frequency for both surveys. Lafet et al., 2005, also proposed the inversion of a base survey and an initial model generated from this to invert the subsequent monitor survey. The direct inversion of amplitude differences for elastic changes has also been suggested by Buland and El Ouair, 2006 but in this case we explore the approach suggested by El Ouair and Strønen, 2006, where there is a simultaneous inversion of all vintages. The uniqueness in the simultaneous inversion is the trace by trace comparison which effectively means that non-comparable traces which fall outside the bins are immediately rejected from the time-lapse analysis. Other methods do not have this advantage since most of them just subtract one inverted data from the other, and trace by trace comparison is not done to ascertain the differences in the data before inversion. It has been suggested that coupling the inversion of base and monitor surveys is important to obtain representative quantitative estimates of impedance changes and a reduction in the non-uniqueness of the inversion process. The algorithm for the simultaneous inversion of base and monitors has been explained in the workflow in chapter 4.

The seismic inversion was carried out mainly using an application of the Hampson Russell 9 Software package, Pro4D with supporting applications such as eLog, Well explorer and SeisLoader. The well explorer was used to load the well data, its deviations, check shot, and picks. The eLog edited and transformed the well data that had been loaded in the well explorer. The SeisLoader package loaded the measured seismic. Wavelet extraction, crosscorrelation, seismic difference mapping, model building and inversion processes were also carried out with the main Pro4D application.

The main application for the inversion has been based on the Pro4D Time-Lapse application which integrates the key elements for the monitoring of time-lapse seismic. Most time-lapse monitoring of reservoirs is to track production related changes in the reservoir and determine areas of bypassed hydrocarbon accumulations. The relevance of the time-lapse seismic is seen in complex geometry and non-homogeneous reservoirs. The complexity and non-communicating

parts of a reservoir indicates that there are areas which are not produced through conventional methods but a time-lapse analysis is the sure way of identifying these areas of the reservoir.

1.4 Geology of the Mid-Norwegian Margin

1.4.1 Structure

The Norne field is located within the Mid-Norwegian Margin (see Figure 1). The margin comprises three main basins; Møre, Vøring and Lofoten-Vesterålen. These are located along the strike of the margin and separated by the East Jan Mayan Fracture Zone and Bivrost Lineament/Transfer Zone (Faleide et al., 2010).

The Møre basin is filled with thick Cretaceous fill steeply dipping basinward with material thickness thinning to <10km. It comprises of sub-basins separated by intra-basinal highs formed during late Jurassic-Early Cretaceous rifting. The structural reliefs are filled with materials from mid-Cretaceous time interlaced with sill intrusions.

The Vøring margin comprises the Trøndelag Platform, the Halten Terrace (HT), the Dønna Terrace (DT), the Vøring Basin and Vøring Marginal High (VMH) from the southeast to the northwest as seen in Figure 1. The Trøndelag Platform comprises of deep basins filled with Triassic and Upper Paleozoic sediments. The platform has been stabilized since Jurassic time. The differential vertical movements within the Vøring basin during the Late Jurassic-Early Cretaceous characterize the sub-basins located within it. The VMH and Vøring Escarpment are contained in the Vøring Plateau. The VMH consist of an outer thick oceanic crust and a landward continental crust which is covered by thick Early Eocene basalts and underplated by mafic intrusions. The Vøring and Lofoten-Vesterålen Margin (LVM) are separated by the Bivrost Lineament. The LVM is characterised by a steep slope and narrower shelf and basins. LVM is less extended compared to the Vøring basin which is largely extended further south.

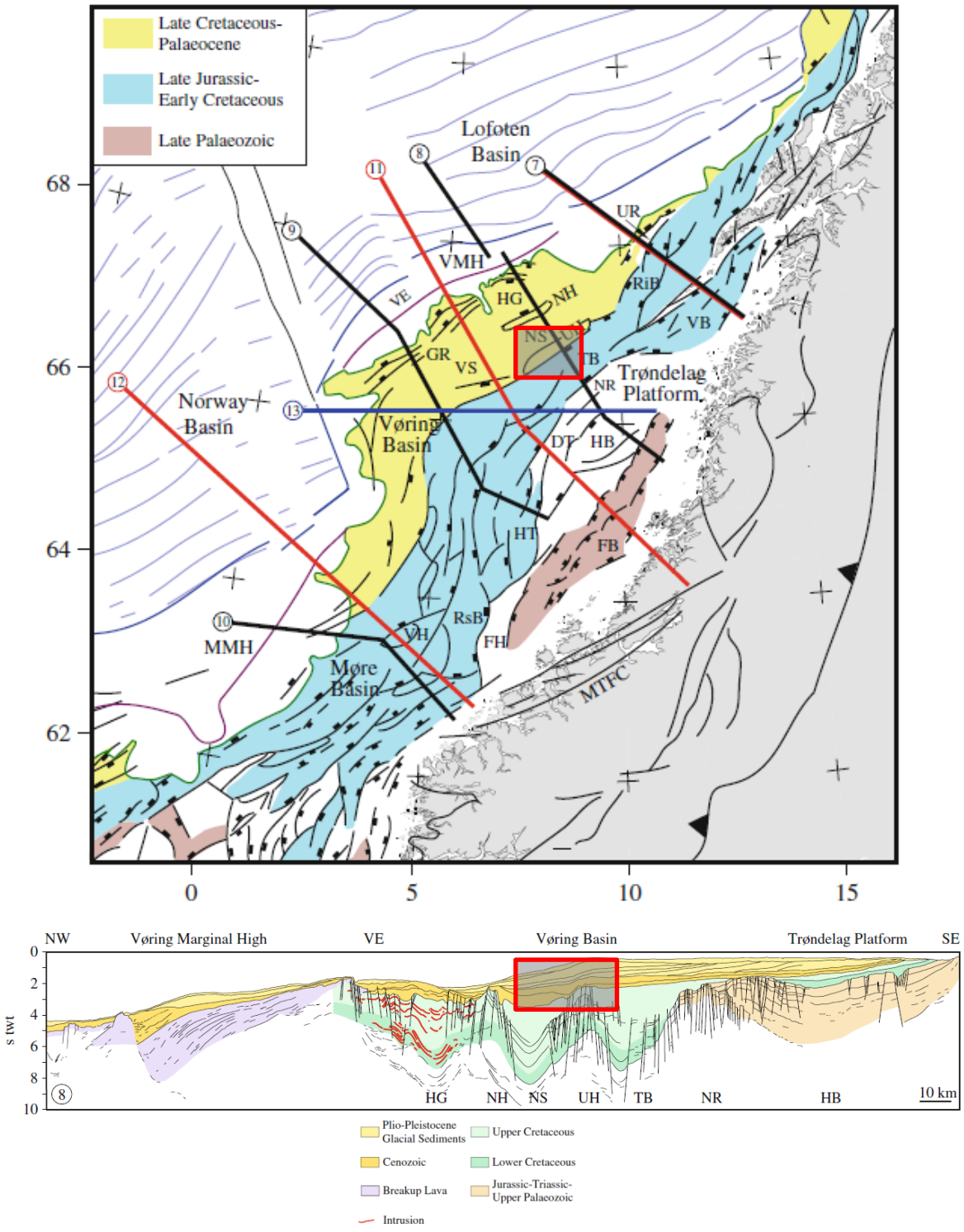

Figure 1: (Top) Main structural elements of the mid-Norwegian modified from (Faleide et al., 2008), (Bottom) Regional profiles across the Mid-Norwegian Margin (modified from Blystad et al., 1995). Insert of Norne field location

1.4.2 Stratigraphy/Evolution

The stratigraphic and evolutionary history of the mid-Norwegian Sea (Faleide et al., 2010) includes Late Paleozoic rift basins formed between Norway and Greenland along the NE-SW Caledonian trend. This has been followed by the NE-Atlantic-Artic Late Jurassic-Early Cretaceous rift episode responsible for the development of major Cretaceous basins like the Vøring and Møre off Mid-Norway.

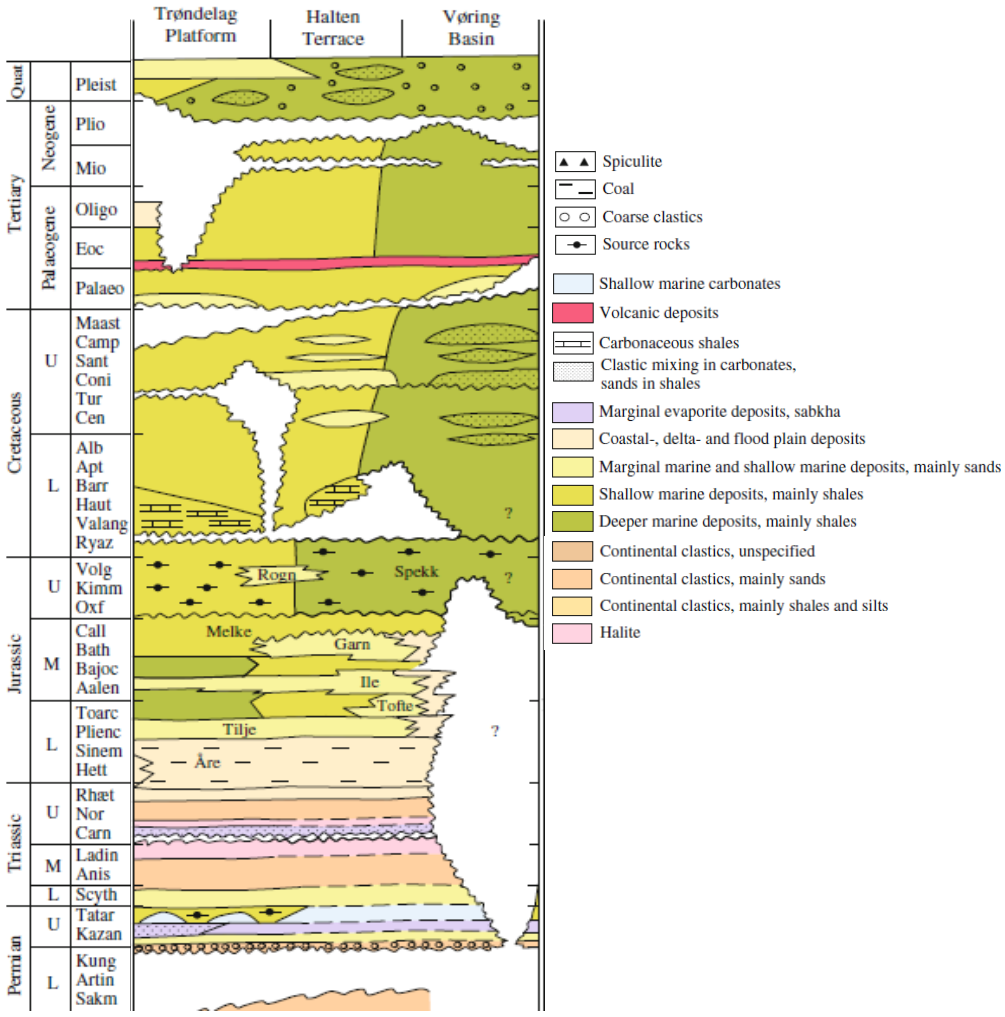

Figure 2: Lithostratigraphic summary for the Norwegian Continental Shelf and adjacent areas (modified from Brekke et al., 2001)

The Trøndelag Platform (Froan Basin) and Vestfjorden Basin have recorded significant fault activity in Permian-Early Triassic time. Permian-Triassic extension is best constrained onshore east Greenland where a major phase of normal faulting took place in the mid-Permian with block faulting occurring in the Early Triassic. There are Lower-Middle Jurassic strata of sandstones which reflect shallow marine deposition to the onset of the next major rift phase. This was followed by extensive crustal extension and thinning which led to the development of the Vøring and Møre basins off mid-Norway in the Cretaceous. During the mid-Cretaceous time, the Vøring basin and Møre basins have been filled in and fine-grained clastics from the Upper Cretaceous have been deposited.

There was a break in the NE Atlantic which was preceded by a prominent Late Cretaceous-Paleocene rifting. The main period of the faulting occurred in the Campanian time followed by smaller scale activity leading to the break-up. The rifting in the Campanian resulted in the updoming of thick Cretaceous sequences at the Vøring margin and LVM.

The break-up of the lithosphere in the Norwegian Margin occurred near the Paleocene-Eocene transition at ~55Ma. This culminated in a 3-6 m.y. period associated with magmatic activity. The mid-Norwegian margin experienced a regional subsidence and modest sedimentation since Middle Eocene time which later developed into a passive rifted margin bordering the oceanic Norwegian-Greenland Sea.

Mid-Cenozoic compressional deformation is well documented on the Vøring margin. This is characterized by domes/anticlines, reverse faults and broad scale inversions. The main phase of this deformation is Miocene with some structures being initiated in earlier times.

1.4.3 The Norne Field

The Norne field is located within block 6608/10 and 6508/1 in the Norwegian Sea. It is an oil field located about 80 kilometres north of the Heidrun field in the Norwegian Sea. The field is currently operated by Statoil ASA and partnered by Petoro AS and Eni Norge AS. The field is located within the Nordland area in the Norwegian Sea. The Norne field covers an approximate area of 9 X 3 km^2 and is both an oil and gas field with a water depth of approximately 380 meters. The field is located on a horst faulted block as are most of the fields in the basin. The

trap type is a rotated fault block of Jurassic age in a horst and graben terrane with complex fault blocks within the major faults zone. The source rock, Spekk Formation, formed during the rifting in the Late Jurassic. Coal beds of the Åre Formation were deposited in the Early Jurassic and may be the source of the gas in the formation (Clayton, 1994). The location of the Norne Field has been indicated in the Figure below.

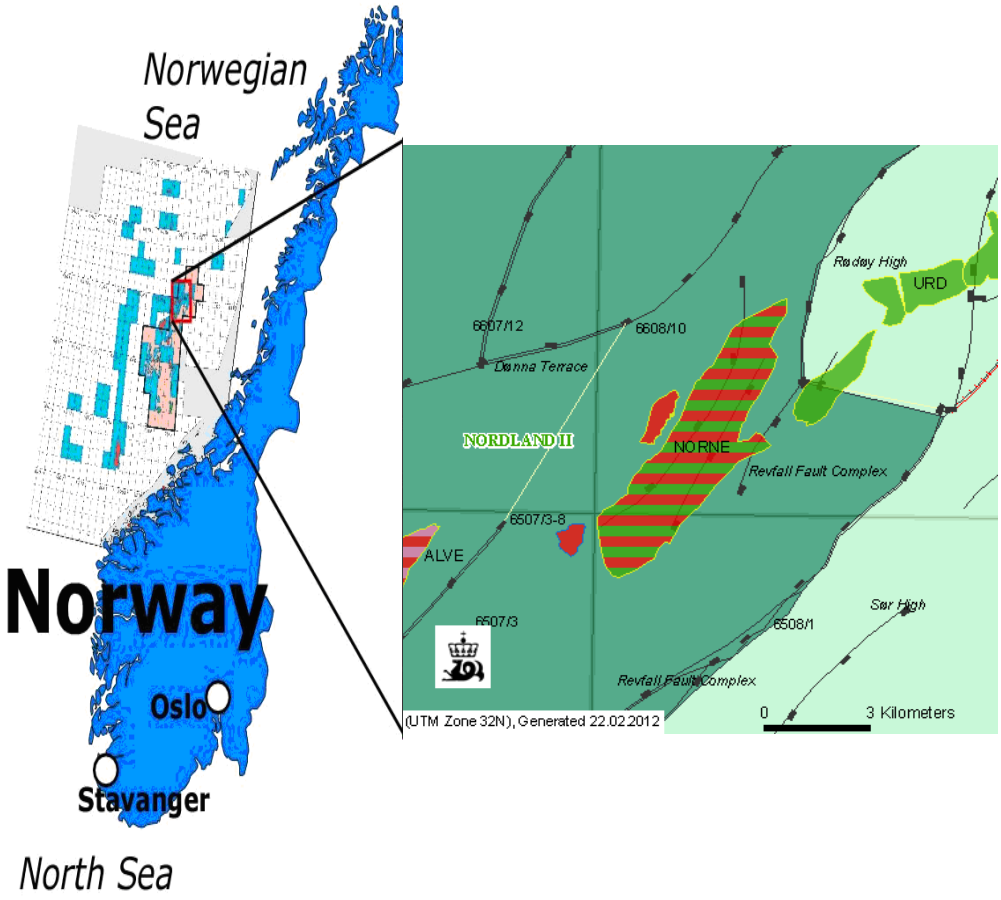

Figure 3: Location of Norne Field within the Norwegian Sea (modified from Statoil, 2006)

The field is made up of two main compartments of C, D, E and G segments. The G-segment is located in the northeastern part of the field with the rest of the segments within the main structure. The field was first awarded in 1986 with the first well drilled in the same year and the first discovery well drilled in 1991. The locations of these segments are presented below

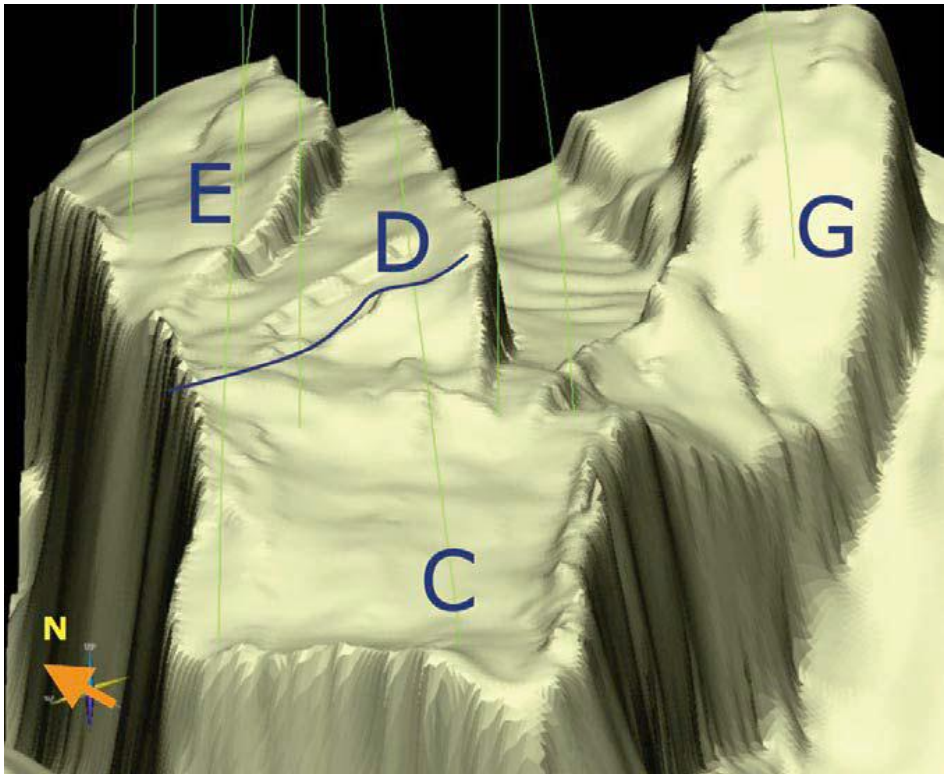

Figure 4: Top reservoir map showing Norne horst block with four segments. (Osdal et al., 2006)

1.4.4 Reservoir Geology

The Early to Middle Jurassic rocks hosts the main reservoirs of the field. There are four main sandstone formations within this area namely; Tilje, Tofte, Ile and Garn formations. There has been varied erosional activity within the area of the reservoir. This affected the Ile and Tilje formations more than the other reservoir rocks (Dalland et al., 1988). The erosional activity is evident in the varied reservoir thickness across the field with the Northern part of the field more eroded. The reservoir sands within the Ile and Tofte are of good quality with porosities in the range of 25 – 30% and permeability in the range of 50 – 3000mD. The reservoir sands are fine grained, well sorted subarkosic arenites (Statoil, 1991)

The Tilje formation is made up of tidally influenced deposits which are subdivided into the Tilje 1 – 4 with their porosities varying from 16 – 25% and a total thickness of about 90m. This was deposited in the Lower Jurassic with sands forming the major part of the reservoir in addition to some clays and conglomerates. This formation is separated from the Tofte formation by an unconformity (Statoil, 1991)

The Tofte formation is less eroded and forms a much laterally uniform formation with sands and shales in the western and eastern parts respectively. Like the Tilje formation there are various subdivisions of the Tofte formation. There are a total of 4 subdivisions with a porosity range from 22 – 28% and a total thickness of 57m. There are channelized sands in the initial layers of this formation (Dalland et al., 1988).

The Ile formation vertically overlies the Tofte formation. The Ile is made up of mostly thick sands with an average porosity of 25% and a total thickness of about 35m. The Ile formation is subdivided into 3 parts. There are channelized sands also present in the Ile formation. There is a great lateral communication between these formations with one on top of the other. There is however a challenge of vertical communication above the Ile formation. This is because of the presence of the Not shale formation which separates the Ile formation from the Garn formation.

The Not formation is thin but it acts as a very effective seal that breaks the communication between the reservoirs above and below it. There are faults and diagenetic carbonates which also tend to prevent the communication between the reservoirs acting as barriers to fluid flow. Some of these diagenetic carbonates are found in various parts of the reservoir column especially within the Tofte and Ile formations (Statoil, 1991).

The Garn formation is made up of near shore sands of about 30m thickness and a porosity range from 18 – 29%. The Garn formation is gas filled with a part of the column also filled with oil (Figure 3). The Garn is vertically overlaid by the Melke and Spekk formation which tend to act as seals for the whole reservoir (Dalland et al., 1988).

1.4.5 Stratigraphic sub- division of the Norne Reservoir

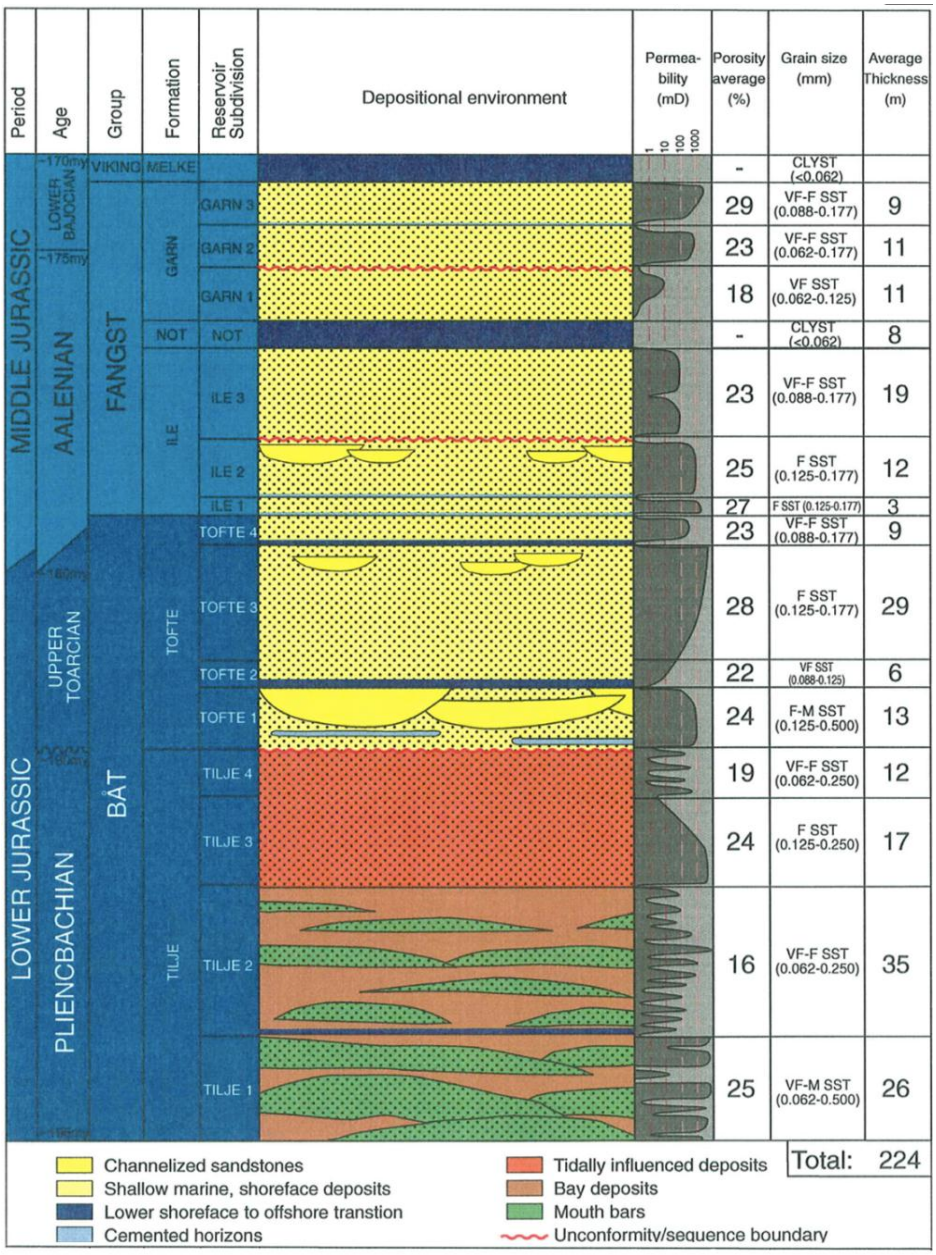

Figure 5: Stratigraphic sub-division of the Norne reservoir (Statoil, 2001)

2. Chapter Two – Input Data

2.1 Time Lapse Seismic Survey on the Norne Field

Time-lapse seismic survey has been carried out on the Norne field. The initial base survey was carried out in 1992 and subsequent surveys in 2001, 2003, 2004 and 2006. These monitor surveys have aided in optimizing the positioning of infill wells and generally increased the understanding of the reservoirs within the field. This has been done by the integration of well log data with the geophysical, geological and reservoir engineering data. The integration has also helped in fine tuning the dynamic reservoir model which effectively means a better prediction of remaining producible volumes and reduction in decision risks regarding drilling processes

2.1.1 Acquisition Repeatability

According to Osdal et al., 2006 seismic data over the Norne field was first acquired in 1992, as a conventional base survey. This survey has been subsequently followed with other successive monitor surveys. The scope and data available for this thesis focuses on four monitor surveys in 2001 (320 km^2), 2003 (85 km^2), 2004 (146 km^2) and 2006. Aerial extents for two of the surveys have been shown in figure 6 below.

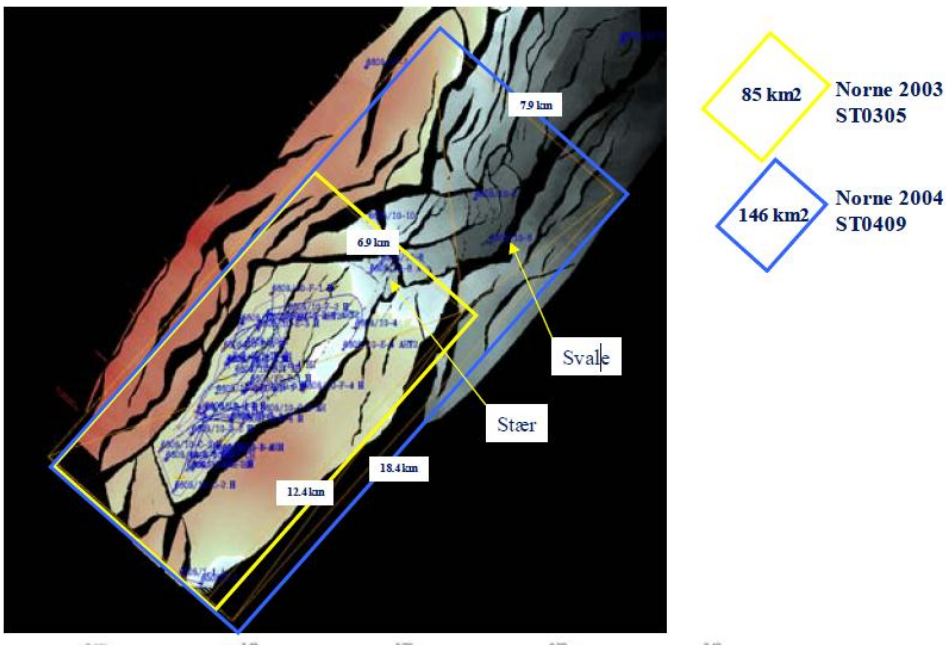

Figure 6: Aerial extents of seismic data for 2003 and 2004 surveys (Osdal et al., 2006)

The first conventional survey was acquired using a dual source and three streamers separated by 100 m. Subsequent monitor surveys were acquired with the Q-marine system from WesternGeco. The configuration for the monitor surveys are a six steerable streamers separated by 50m and a single source. The repeatability of time-lapse survey is considered very vital if it has to be used in effective monitoring of reservoirs. Inconsistencies in the data could pose a great challenge when comparing two surveys with low repeatability. This was the basis upon which the 2001 monitor survey has been considered as the base surveys due to repeatability issues with regards to the 1992 data, in this case feathering. The issue of feathering has been well documented by Osdal et al., (2006) when they mapped the difference between the Q-survey of 2003 and 1992 survey as well as the 2001 and 2003 (figure 7). The figure shows very high repeatability between the Q-surveys but much difference between the non Q-survey methods. Between the 2001 and 2003, the only portion of the field which has experience limited repeatability is the area under the Norne production vessel. Undershoot was done for this area with two survey ships instead of the conventional one, which were not Q-boats (Ouair et al., 2005).

Table 1: The acquisition parameters for 2001, 2003 and 2004 (Statoil, 2006)

Company	**WesternGeco**	**Vessel**		**Geco Topaz**
Survey date	August/Sept. 2001, June 2003, July 2004	**Survey type**		3D
Instruments	Triacq 5	**Tape format**		SEG-D
Filter settings	High cut	200 Hz	**Slope**	477 dB/oct
	Low cut	3 Hz	**Slope**	18 dB/oct
Record length	6144 ms	**Sample rate**		2 ms
Timing delay	64 ms	**Filter delay**		0 ms
Source array	1 X 5085 cu.in. airgun, operating at 2000 psi			
Source depth	6 m	**Shotpoint interval**		25 m
Receiver array	6 X 3200 m streamer, 240 groups per streamer			
Cable depth	8 m	**Group interval**		12.5 m (DGF)
Inline offset	122 m			
Source separation	n/a	**Cable separation**		50 m
Configuration	254 trace, 64 fold, 6 lines per boat pass, 25 m line spacing			
Polarity convention	Positive pressure at hydrophone recorded as a negative number			

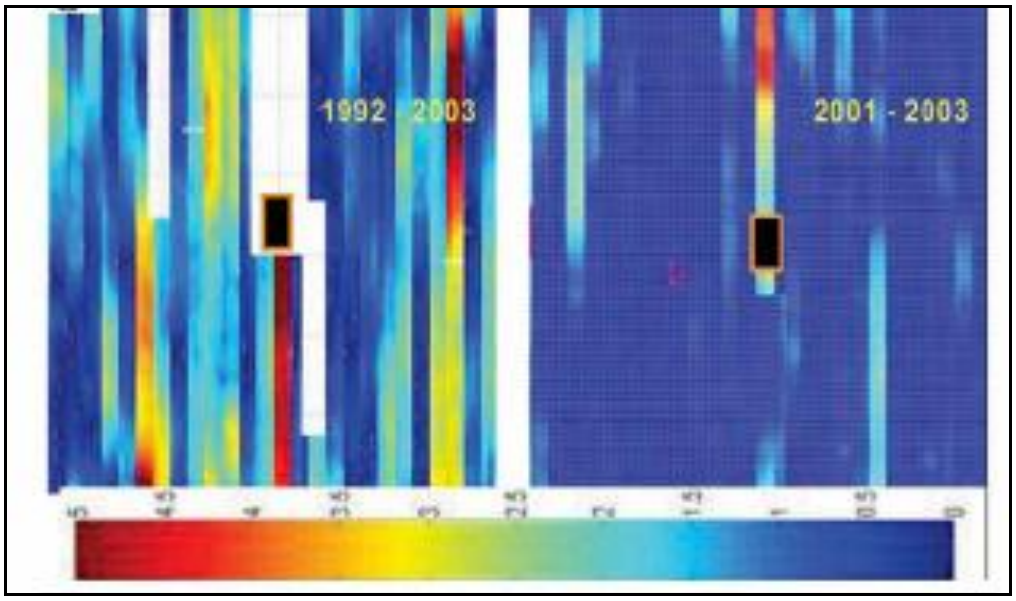

Figure 7: (Left)) Feathering difference between 1992 and 2003, (right) feathering difference between 2001 and 2003, The scale indicates areas of consistent repeatability at zero (0) and non-repeatability at five (5).

2.1.2 Processing

The Norne field data has basically been interpreted for OWC (Oil Water Contact) using the difference data i.e. subtracting one dataset from another. The Norne data has been known to be contaminated by diffracted multiples, which has been resolved by multiple attenuation and several radon passes. Figure 52 in the appendix below shows the effect of applying tau-p decon on the time-lapse. The decon helps remove the multiples but degrades the effect of the rising OWC. The solution applied to the above challenge during processing was a 2D SRME (Source Related Multiple Elimination) which preserved the time-lapse signal as well as removing multiples. The optimal result from the SRME was due to the very minimal feathering in the time-lapse acquisition process (Osdal et al., 2006).

The repeatability of traces in time-lapse analysis is very important. Ross et al., 1996, suggests that to correctly analyze time-lapse results the base and monitor surveys must be cross-equalized to correct for non-repeatable noise. This prevents non-repeatable noise from being interpreted as production or saturation effect. To make sure that only good traces are binned and compared it is important that non-repeating traces are discarded. This is observed in the NRMS (normalized root mean squared) maps shown in figure 53 in the appendix which indicate the difference where non-repeating traces are included as compared to when they are discarded.

The post-stack processing comprised of the following steps;

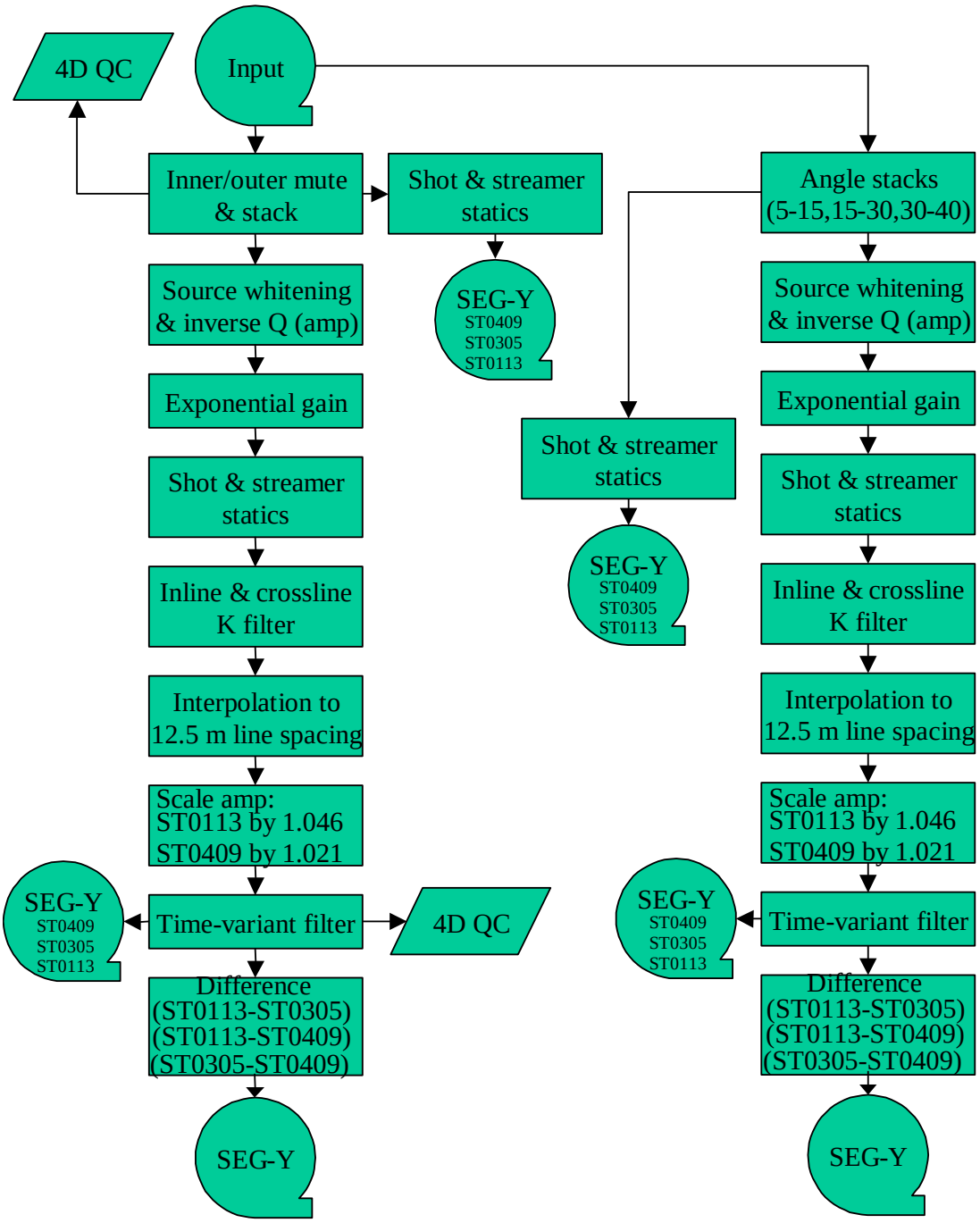

Figure 8: Graphical presentation of the post-stack processing steps (Statoil Norne processing report, 2006)

2.1.3 Previous Interpretation of Time-Lapse Data

Pressure and saturation differences due to production often lead to the differences in acoustic impedance from the field. Most of these changes are not very observable in individual surveys, but are interpretable using the 4D seismic difference cubes mostly along injector wells where water is used to flush the hydrocarbon in the reservoir. Seismic reflection amplitudes as well as seismic modeling are also compared with regards to the time-lapse effect. Seismic modeling is very effective in wells where there is repeated saturation logging (Osdal et al., 2006). The benefit of the repeated saturation logging has not been explored. Only single saturation datasets were available during the time of this research.

2.2 Well Data

Well logs provide information about the rock properties. Such properties are measured on a finer scale than the seismic data resolution. The well data also provide information about the rock formation such as lithology type, fluid saturation, stratigraphy etc. Well data can be used to produce a low-frequency model (< 10Hz) which is necessary if we are to obtain formation properties such as velocity and density by converting from relative acoustic impedance to absolute acoustic impedance (Oilfield review, 2008, Schlumberger). The low-frequency model which is important in resolving acoustic impedance would be discussed in further detail.

There were a few limitations with regards to the well data provided. Density and sonic logs are required to produce acoustic impedance for an inversion process but unfortunately most of the wells provided did not have sonic log data. There was a limitation therefore on the number of wells that could be used. Three wells were chosen; 6608/10-4, 6608/10-E-3H and 6608/10-F-1H. The latter well had a challenge with the density data within some part of the reservoir. The Gardner equation below (1) (Gardner et al., 1974) was used to generate the density (ρ) data within this well.

$$\boldsymbol{\rho = 0.23Vp^{0.25}} \qquad (1)$$

The transformation of the P-wave log into density log is possible but not as accurate as the measured data. This is because a careful observation of the actual density log from well 6608/10-F-1H showed some differences from the transformed density. Despite the changes in the measured and transformed data, the density log is important in achieving the acoustic impedance for the well.

2.3 Interpreted Horizons

Two interpreted horizons were provided within the reservoir of the field for the purposes of the time–lapse inversion process; Not and Åre Formations. The Åre Formation horizon marks the boundary of the Norne field with a graben interpreted between the E and G-Segments. The Not formation on the other hand has been interpreted on a much larger scale. This extends to areas well beyond the Norne main field. These horizons were used as a geometrical setting for a model building process during the inversion of the seismic data. 3-dimensional views of the two horizons have been presented below showing them from two different perspectives for each horizon.

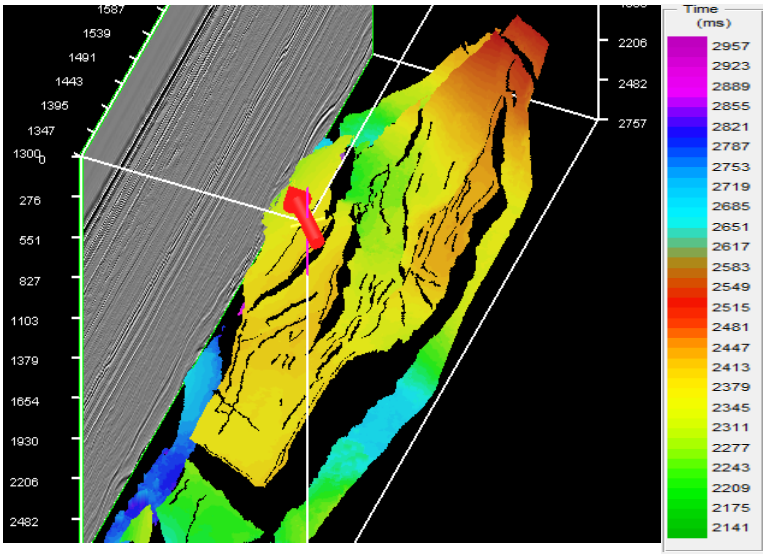

Figure 9: 3D display of Not Formation Horizon

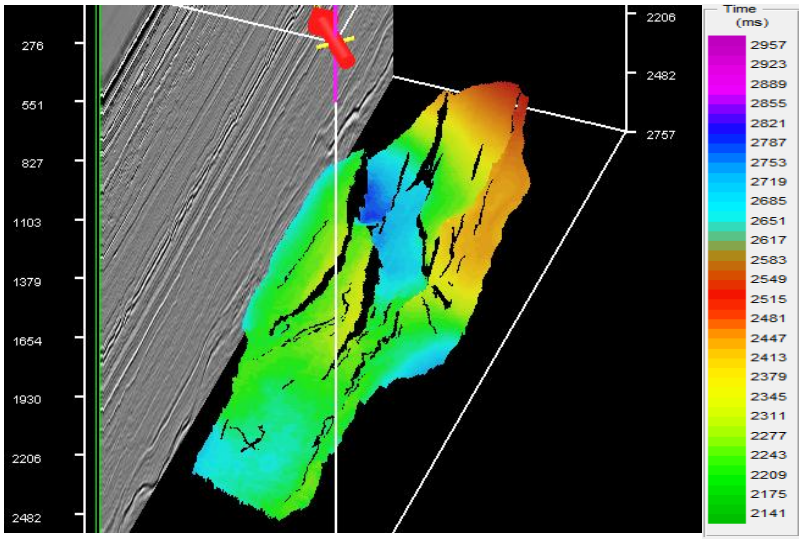

Figure 10: 3D display of Åre Formation Horizon

2.4 Production Data

The Norne field was discovered with original recoverable oil in place of 90.8 MSm^3 and original recoverable gas of 11.8 BSm^3. The production of oil started in 1997 and gas in 2001. The field has been developed with a Floating Production Storage and Offloading (FPSO) system.

Figure 12 shows an illustration of a cross-section of the field with an indication of present fluid contacts. The Norne main field is drained with horizontal wells which have been drilled into the oil leg in the reservoir. The drainage strategy for the field as at 2006 has been shown below in Figure 11. The initial strategy was to inject both gas and water above and below the reservoir respectively. This was stopped upon the realization that the Not formation, though thin, acts as a vertical barrier for the transmission of fluid flow. The strategy was therefore changed to the injection of both water and the produced gas from below the reservoir to maintain pressure within the reservoir. There was an increased injection rate from 42000 to 55000 Sm^3/d to sustain high pressure within the reservoir. The injection of the gas was stopped in 2005. The production of the field was based on the various segmentations caused by the various fault dispositions.

The highest production for both oil and gas has been recorded within the period under evaluation (2001-2006). The peak of production for the oil was in 2001 while that of the gas was in 2004 and 2005 (Figure 13).

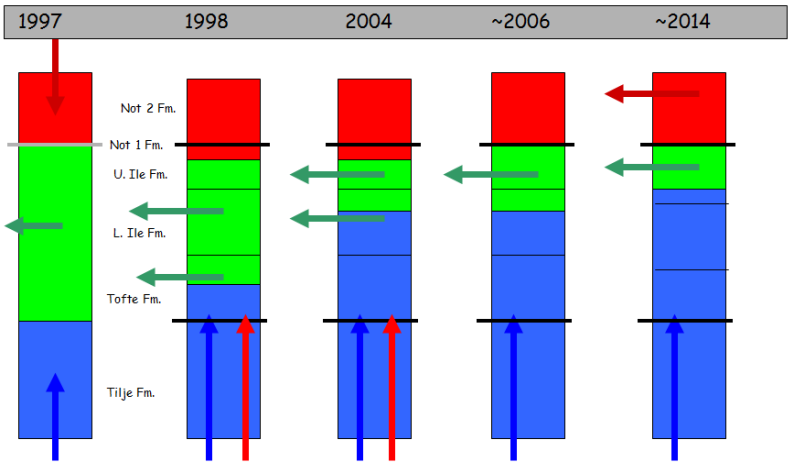

Figure 11: Norne 2010 drainage strategy

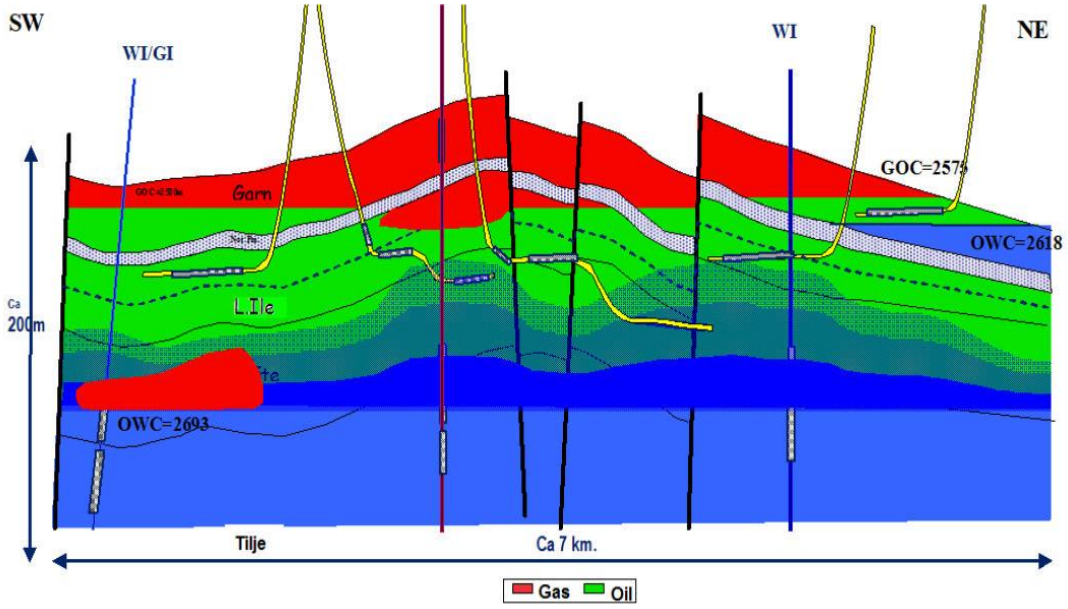

Figure 12: NE-SW running structural cross section through the Norne Field (Norne Annual Reservoir Development Plan, 2006)

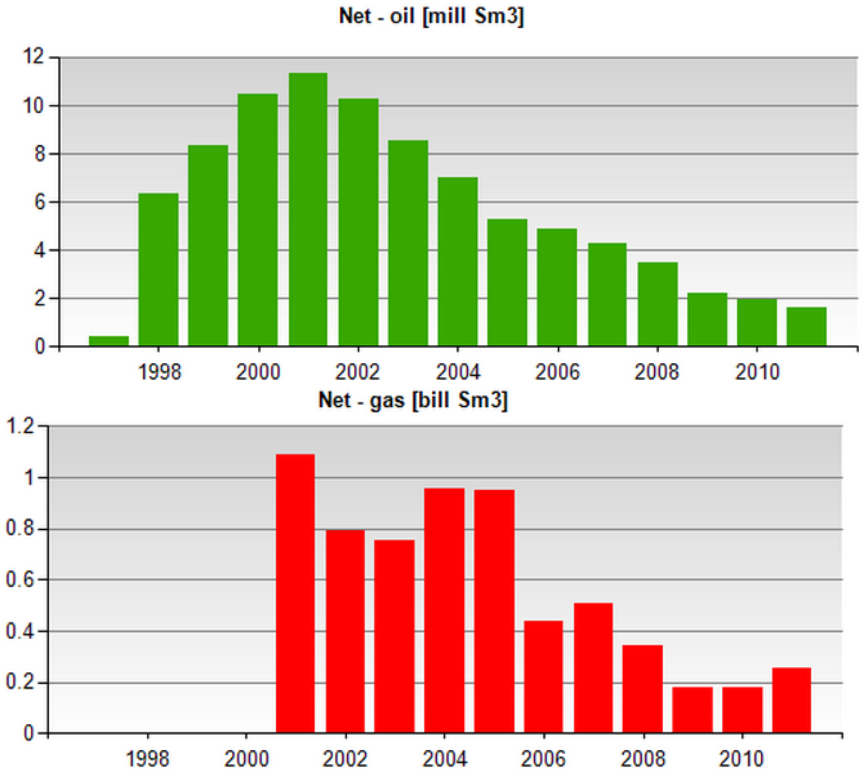

Figure 13: Total production of oil and gas from the Norne Field from 1997 to 2011 (NPD Factpages)

3. Chapter Three – Theoretical Background

3.1 Inversion Theory (Mathematical Background)

Menke (1989) classifies the inverse theory which is the mathematical base for seismic inversion, as made up of a set of methods which are used in the extraction of useful information from physical measurements. These various methods have their similarities and differences as well as their limitations during the extraction process. The data from which inversion can be carried out can be classified as either continuous or discrete. The inversion process can also help in the discrimination of different models. The principle of the inverse problem can be classified as;

$$d_i = \sum_{j=1}^{M} G_{ij} m_j \tag{2}$$

d, represents our data, **m**, model parameters and **G**, a data kernel (model) which relates the data to the model parameters. There are several methods for estimating the model parameters in the above equation (2). Some of the methods are; Linear Solution, Generalized Inverses, Maximum Likelihood etc.

The Linear Solution provides one of the simplest solutions to the inverse problem. The solution is based on the minimization of the length (error) between our observed (measured) data, $\mathbf{d}^{\mathbf{obs}}$ and predicted (forward modeled) data, $\mathbf{d}^{\mathbf{pre}}$. The error between the observed and the predicted is defined as;

$$e_i = d_i^{obs} - d_i^{pre} \tag{3}$$

This is represented graphically in figure 14. The best fit for our data is when the total error, *E*, in the data is kept at a minimum. The total error, ***E***, is the squared Euclidean length of the vector, ***e***.

$$E = \sum_{i=1}^{N} e_i^2 \tag{4}$$

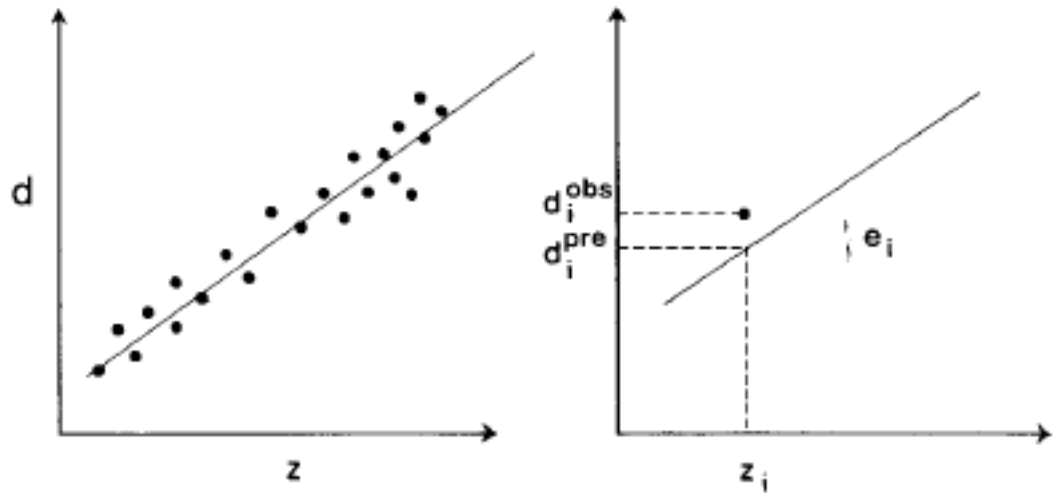

Figure 14 Illustration of the Least Squares Method in fitting a straight line through varied data points

This is called the least squares method and it effectively reduces the variation between our estimated model parameters and the predicted data. The solution thus becomes

$$m^{est} = \left[G^T G\right]^{-1} G^T d \tag{5}$$

The inverse of the data kernel $\left[G^T G\right]^{-1} G^T$ is represented by G^{-g} in the generalized inverse solution. The generalized inverse method focuses on the matrix of the data kernel more than the model parameter itself. It also seeks to enhance both the data and model resolution.

The maximum likelihood method as a solution for the inverse theory problem is a method of maximizing the probability of guessed values of mean and variance of our observed data. When this guessed probability value is close to being correct the $P(d^{obs})$, would be maximum and small when the guessed values are not close to $P(d^{obs})$. The maximum is located by differentiating $P(d^{obs})$ with respect to the mean and variance and setting the result to zero.

Tarantola (1987) and Gouveia (1996) gave a generalized probabilistic framework of the inverse problem when the goal is to obtain the posterior distribution of the model parameters when we have the prior distribution and the likelihood of observing the data.

$$\frac{\partial P}{\partial m_1} = \frac{\partial P}{\partial \sigma} = 0 \tag{6}$$

The maximum likelihood of the model parameters is the weighted least squares solution, where the weighting matrix, W_e is the inverse of the covariance matrix of the data

$$W_e=[\text{cov } \mathbf{d}]^{-1} \quad (7)$$

Another very important parameter which can be extensively used in the inverse solution finding process is a priori information according to Menke (1989). This is a sort of information which is not directly derived from the observed data but helps in the estimation of model parameters.

Sen and Stoffa (1995) categorized model-based inversion methods as follows; linear methods, iterative gradient-based methods, exhaustive search methods, random search methods, direct Monte Carlo methods and geostatistical sequential simulation methods. There are different inversion models which vary from each other based upon their mathematical background for estimating the model parameters.

The inversion process can best be illustrated by the figure 15 below.

Figure 15: Interactive Inverse Theory

In integrated reservoir characterization, impedance inversion process can be used to derive seismic attributes (P-impedance, Poisson's ratio, Vp/Vs etc.) as well as rock properties (lithology, porosity, pore fluids, saturations) when linked with the rock physics models and statistical techniques. The model parameters which can be estimated from an inversion process are dependent on the type of data available (pre-stack or post-stack seismic data)

Seismic inversion removes the wavelet effects which results in the estimation of reservoir properties yielding a better resolution. There are several models by which we can relate the model parameters (e.g. density, acoustic impedance, P-wave velocity etc) which we sort, to the dataset which we have measured. But these datasets are not devoid of noise thus we have to use models which will best be able to estimate the model parameters.

3.2 Seismic Data

3.2.1 Seismic Acquisition Theory

Seismic data is essential because it provides information about the reflectivity from the various formation surfaces as well as the differences in acoustic properties that helps in imaging the subsurface on a larger scale. Sequence stratigraphy can most likely be revealed from seismic sections while seismic cubes can provide information about horizontal heterogeneity through time slices.

Seismic exploration surveys are classified as an active method of geophysical exploration as it involves the artificial generation and measurement of seismic waves in the subsurface. The survey can be land or marine based. In land based surveys the source of seismic generation is mainly through the use of dynamites and vibroseis trucks with geophones as receivers which are usually buried in the ground in a line behind the trucks. In marine survey, the source of vibration is the air gun and the hydrophones are the measuring devices. The air gun is towed behind the survey ships and usually below the water surface. The receivers are also towed behind the acquisition vessel.

Seismic data starts with a source that emits acoustic pulses. The pulses spread out in all directions, the wave front, and are generally described by a ray path oriented perpendicular to the wave front. When the wave front hits an interface, some energy is reflected, some travels along the interface (refracted waves) and some penetrates into the next layer, transmitted waves (Avseth et al., 2005). In reflection seismic, the receivers measure the part of the acoustic pulse that reflects back to the surface.

The first arrival at the receivers is called the primary wave (which are the compressional, or P-waves) and the next arrival is called the secondary wave (S-waves or shear waves). These waves are measured using the equations stated below.

Compressional wave velocity, $V_p = \left(\frac{\lambda + 2\mu}{\rho} \right)^{1/2}$ (8)

Shear wave velocity, $V_s = \left(\frac{\mu}{\rho} \right)^{1/2}$ (9)

Where $\lambda = k - 2\mu/3$

The P-wave is recorded as a wavelet and forms the basis for reflection seismic data. The ideal wavelet is sinuous-shaped and relates to whether the body mass is compressed or expanded.

The reflected waves are due to the difference in acoustic impedances between two layers. Where there is no difference in impedance between two layers the waves are transmitted further downwards. The propagated waves are attenuated downwards as part of the energy is lost every time there is reflection. There are other properties of the earth which are convolved with the transmitted signal. The acoustic impedance (AI) which determines the reflection or refraction from the interface of the various layers in the subsurface is a product of the velocity (v) and density (ρ) i.e.

$$\text{AI} = \text{v}\,\rho. \quad (10)$$

The signals which are reflected to the surface are recorded as 'wiggles'. The wiggles are made up of peaks and troughs which indicated the conditions at the boundaries of reflection. A peak according to the Statoil (2006) processing report indicates a transition from a lower AI to a higher AI and a trough indicates a transition from a higher AI to a lower AI which is the SEG normal polarity. The amplitude of reflection from the boundaries are based on the reflection coefficient, R which is given by

$$R = \frac{v_{j+1}\rho_{j+1} - v_j\rho_j}{v_{j+1}\rho_{j+1} + v_j\rho_j} = \frac{AI_{j+1} - AI_j}{AI_{j+1} + AI_j} \quad (11)$$

Where v_j and v_{j+1} represent velocities in the first and second layers and ρ_j and ρ_{j+1} are densities in the first and second layers respectively.

The convolutional model is used to explain the basic theory behind the wiggle/seismic trace. This is a model in which a seismic trace S(t) is given by the convolution of an embedded wavelet w(t) with a reflectivity function r(t) plus random noise n(t), i.e.

$$S(t) = w(t) * r(t) + n(t) \quad (12)$$

Where S(t) is recorded seismic trace, w(t) is source wavelet, r(t) is earth's reflectivity and n(t) is additive noise. The above equation for the convolutional model is represented in the time domain but this can also be represented in the frequency domain. This is achieved by taking the Fourier transform of the various components of the time sequence except the noise aspect. The transform thus gives an indication of the noise and this is muted. Inversion can be thought of as the process of determining the reflectivity, r(t), given the seismic trace S(t) and an extracted wavelet w(t).

3.2.2 Time Lapse Seismic Theory

According to Landrø, 2010, there are various applications for 4D seismic surveys but the area where 4D survey has been most prolific is in the monitoring of changes in a producing clastic hydrocarbon reservoir. The effect of 4D is much more pronounced in clastic reservoirs than in carbonate reservoirs because of the stiffness of the carbonates. During the production of hydrocarbons there are reservoir parameters that might change; fluid saturation, pore pressure, temperature and subtle changes in layer thickness. The ability of a geophysicist to be able to link these changes to the seismic parameters in the life of a producing reservoir is most crucially provided by 4D surveys. To effectively recognize the changes which time-lapse survey bring we can analyse changes in amplitude or travel-time changes as shown in Figure 16.

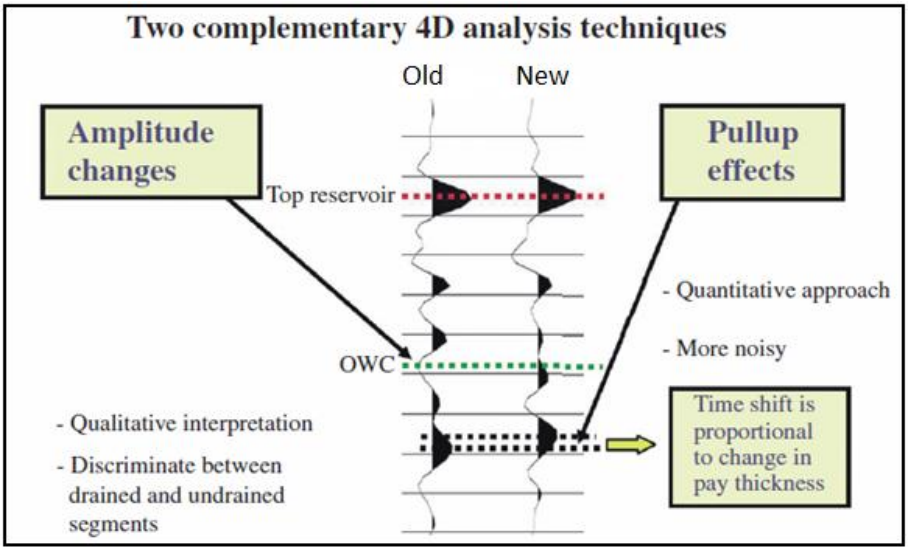

Figure 16: A display of two 4D analysis techniques (Landrø, 2010)

From the figure above, we observe that there are no amplitude changes at the top reservoir but huge amplitude changes at the oil-water contact (OWC). This is because there are differences in acoustic impedance which are generated due to new fluid saturation heights (production of hydrocarbons) which are identifiable in a seismic section. Due to its use in the identification of variation in fluid saturation, 4D seismic surveys have been applied in oil-water contact identification.

To be able to effectively monitor a reservoir and identify the changes in fluid saturation we need to be able to compare the base (initial) and monitor (time-lapse) surveys. The best way of doing this is by subtracting the monitor survey from the base survey which yields a difference that can be qualitatively and quantitatively measured. The differences which are observed in the survey can be put together in a new survey and this can give an indication of areas where there has been greater changes in fluid movement as opposed to areas with little movement. The various changes represent a 4D difference cube which is effectively used in monitoring a reservoir. (Landrø, 2010)

3.3 Seismic Wavelet

3.3.1 Wavelet Theory

The first step in the recording of seismic data is the generation of a seismic source signature which is represented by a seismic wavelet. The interest for an exact determination of the input signal in a seismic survey becomes important when we consider; Time lapse seismic, 4-C seismic and multiple attenuation (Landrø, Seismic data acquisition and imaging). The knowledge of the signature of a source signal means that we could use its inverse in a deconvolution process to remove the wavelet effect. This not usually the case and thus the source signature is estimated through a statistical process which will be described in the wavelet extraction process.

The wavelet is defined by its amplitude and phase spectrum. The amplitude spectrum is the plot of the amplitude vs. frequency and the phase spectrum is the phase-shift plot vs. frequency. Two wavelets can be described as in-phase or out of phase depending on their shape, symmetry and frequency. If the shape, symmetry and frequency match each other then they are in-phase but are out of phase if they have varied properties.

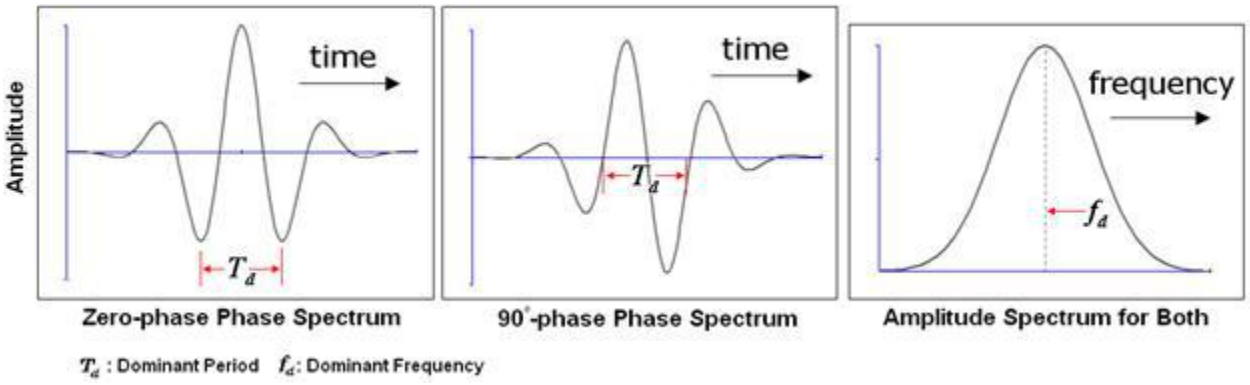

Figure 17: Amplitude and Phase Spectrum of theoretical wavelets (Hampson and Russell Articles, 2012)

3.3.2 Principles of Wavelet Extraction

Wavelet extraction is one of the most important procedures during an inversion process. An extracted wavelet representative of the seismic data leads to a good overall inversion result. There is the need to deconvolve the wavelet out of the measured seismic data. The issue of wavelet extraction in seismic processing is complex. Although numerous wavelet extraction methods have been devised, the following general statements can be made:

a) Purely deterministic: This means measuring the wavelet directly using surface receivers and other means.

b) Purely statistical: This means determining the wavelet from the seismic data alone. This procedure tends to have difficulty determining the phase spectrum reliably, but is applicable in some cases.

c) Use a well log: This means using well-log information in addition to the seismic data. In theory, this could provide exact phase information at the well location. The problem is that this method depends critically on a good tie between the log and the seismic. In particular, the depth-to-time conversion which converts the depth sampled log to two-way travel-time can cause misties which degrade the result.

Wavelets can and do change from trace to trace and as a function of travel-time. This means that the wavelet extraction process should be determining a large set of wavelets for each seismic section. In practice, attempting to determine variable wavelets can introduce more uncertainty than the data is capable of resolving. A practical and useful solution was to extract a single "average" wavelet for the entire section.

3.4 Principles of Crosscorrelation

The crosscorrelation of the base and monitor survey seeks to establish the similarity between two surveys. A correlation coefficient is assigned to the level of correlation and this is usually from zero (0) to one (1). A low coefficient indicates differences in the base and monitor surveys. Where the differences are within the production areas in terms of areas close to wells or in cross-section within the reservoir the changes would have to be maintained. Other areas outside of the productions areas would have to be calibrated out to match the base and monitor surveys. The

calibration is done for amplitude or time/phase shift. The importance of this is to establish that differences that are observed after the data volumes have been inverted are due to production effects and not due to acquisition or processing effects. This also establishes the basis for the time-lapse effect to be monitored since in as much as possible the base survey has been repeated. The most important part of the volume to cross-correlate is the reservoir section. The volumes beneath and above the reservoir can also be monitored for changes as the changes in the reservoir most probably would affect the over and under-burden materials.

This process of crosscorrelation is done by having a stationary reference trace from the base survey matched to a corresponding sliding trace from a monitor survey where the signal to noise ratio is the same. A lag is applied to the trace from the monitor relative to the stationary trace. The aligned traces are then multiplied together and summed to produce a total for the initial lag value.

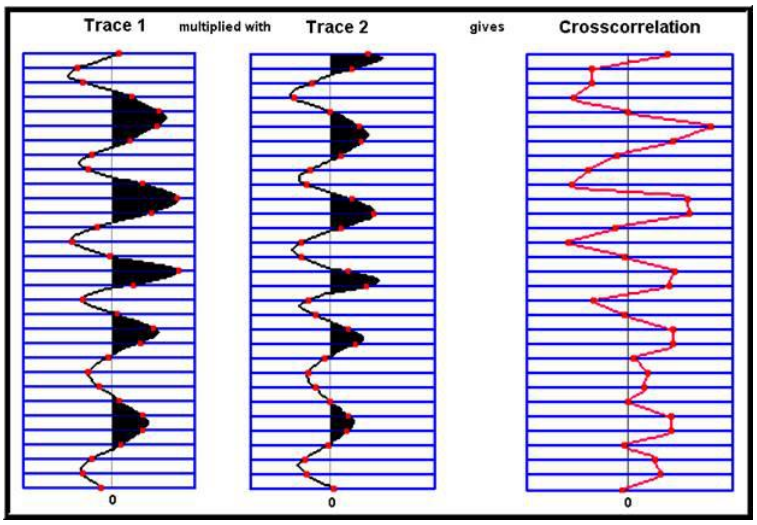

Figure 18: A crosscorrelation process where two traces are multiplied and summed (Hampson and Russell Articles, 2012)

The reference trace is then shifted down a sample and the process of multiplication and summation repeated as depicted in the figure below.

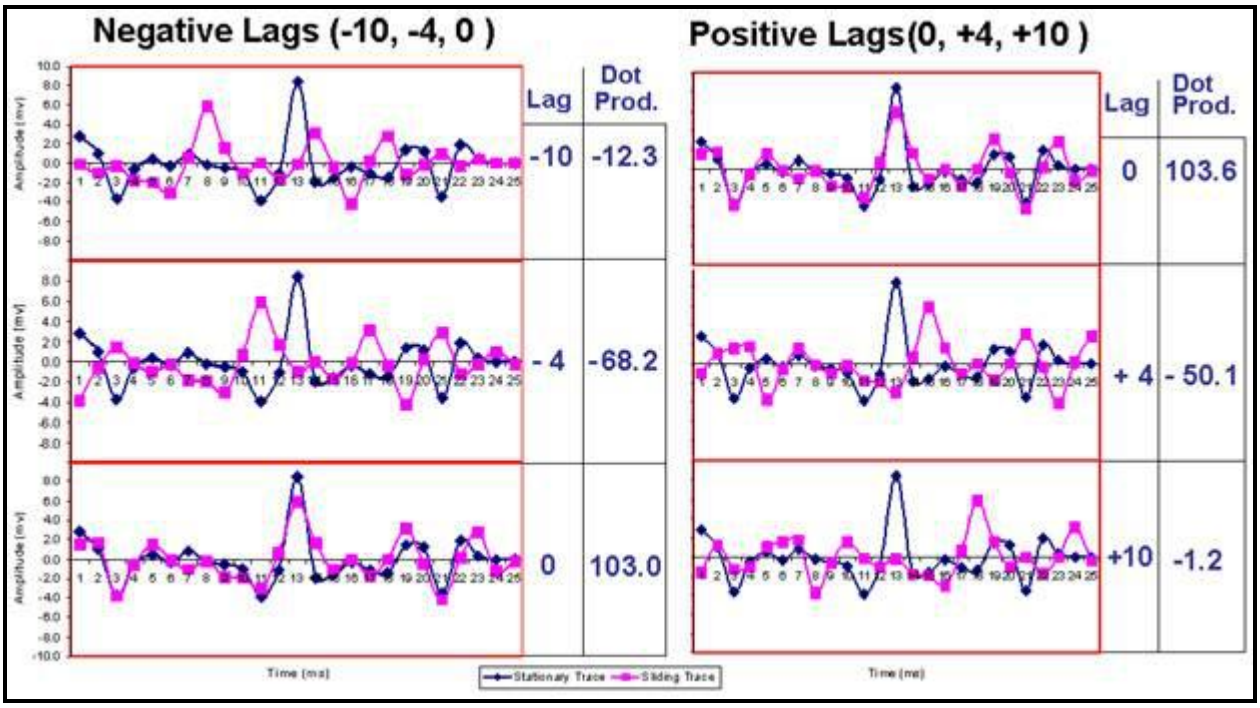

Figure 19: Multiplication and summation process with the highest dot product at zero lag (Hampson and Russell Articles, 2012)

The maximum dot product is achieved when there is a zero or minimum lag between the two traces. When two traces are identical a maximum crosscorrelation of 1.0 is achieved and this is called autocorrelation. In the case for a base and monitor survey where there are changes in the traces being cross-correlated, the normalized crosscorrelation coefficient is less than 1.0. A zero (0.0) crosscorrelation indicates no correlation between the two surveys and this could be either due to processing error or drastic changes in reservoir due to production. Two shifts are encountered when we cross-correlate; phase and time. Bishop and Nunns, 1994, helps resolve the different shifts by the application of the Russell-Liang technique (Hampson and Russell Articles, 2012).

4. Chapter Four - Workflow

The time-lapse analysis of seismic data in Pro4D includes a series of steps which will be explained in this chapter. The analysis according to the Pro4D guide has been modified according to this seismic data and it includes the following steps;

a) Comparing the seismic surveys carried out at various times in the field's production history
b) Calibrating the 3D seismic volume to remove differences which are related to seismic acquisition and processing.
c) Subtracting the calibrated seismic surveys and mapping the differences
d) Interpreting the calibrated 3D surveys and the difference survey to determine the areas of the field that have been changed during production.
e) Creating Time-Lapse Inversion with low frequency updates and 4D inversion
f) Analyzing the areas in the field where there have been changes and comparing it to production activity in those areas

4.1 Well Log Importation

Three wells were imported for the time-lapse inversion process. This, as has been explained provides the much needed low-frequency component. The wells give insight into the various formation measured properties.

The importation of the well data was done through the use of eLog application of the HRS. Well log measurements were imported into the application, in addition to their deviations, tops and check-shot corrections. Care was taken to append the various log properties to the appropriate well. A display of the density, sonic and gamma ray logs has been illustrated in figure 20 below.

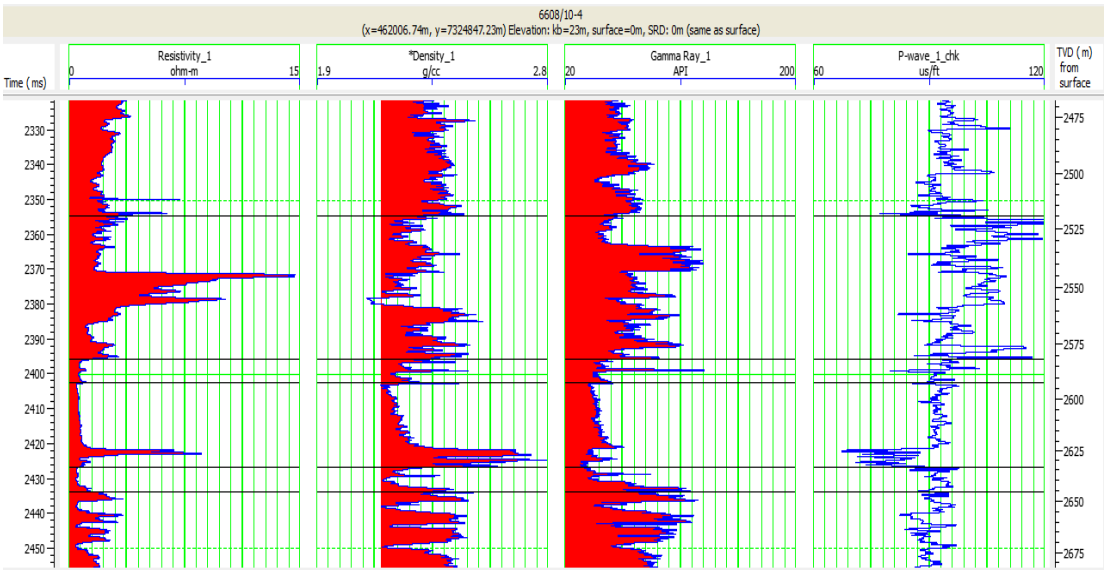

Figure 20: Log display of measured data from 6608/10-4

Check-shot corrections were carried out for all the wells and one of the corrections has been displayed in the figure 21 below.

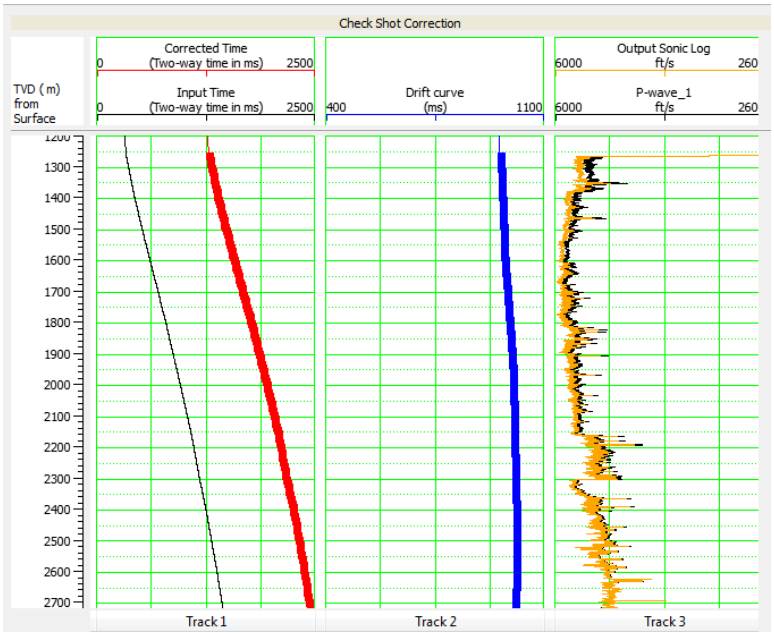

Figure 21: Check shot correction parameters and analysis window

4.2 Loading Seismic Data

The simultaneous inversion of base and monitor survey method requires the loading of all the time lapse surveys together as a group survey. This is the merging of various surveys which aids in the simultaneous analysis of these datasets in comparison with subsequent surveys. The base survey should be specified as the reference and its subsequent monitor surveys also specified so there is a basis for comparing them.

The loaded database is a little different from other merged volumes. This is because the group volume still maintains the individual surveys separate in the group but other surveys tend to merge traces for a particular location.

4.3 Crosscorrelation

A crosscorrelation between the two datasets performed for a 400 ms time window is shown in figures 22 and 23. The time window encompassed the reservoir as well as a few milliseconds above and below the reservoir. The crosscorrelation for the time window above and below the reservoir is due to the geometry of the reservoir and the possibility of having changes above and below the reservoir initiated by production effects. It is expected that the production related effects that can cause either the time or phase shifts would be evident if the base survey of 2001 and the last monitor survey of 2006 are cross-correlated. This gives the opportunity for any form of needed calibration to correct these effects outside the reservoir and production areas to be addressed.

The maximum crosscorrelation slice in the figure 23 shows a correlation range greater than 0.90 (ninety per cent) without any pre-inversion processing of these two datasets. This also shows the lowest correlation within the Norne field area to be about 0.80 (eighty percent), which on the average shows a good correlation requiring no further calibration. The patchy areas of green and yellow indicates slightly lower correlation while the bluish to pink colour indicate higher correlation. Within the Norne field the lower correlations are mostly around well locations in the E and G-segment and would not require any need to re-process these areas. These may be due to production-related effects and has to be preserved for the changes to be observed in the time

lapse evaluation. Other areas on the other hand around the south-western and north-eastern corners of the maps with lower correlation are areas out of the field area.

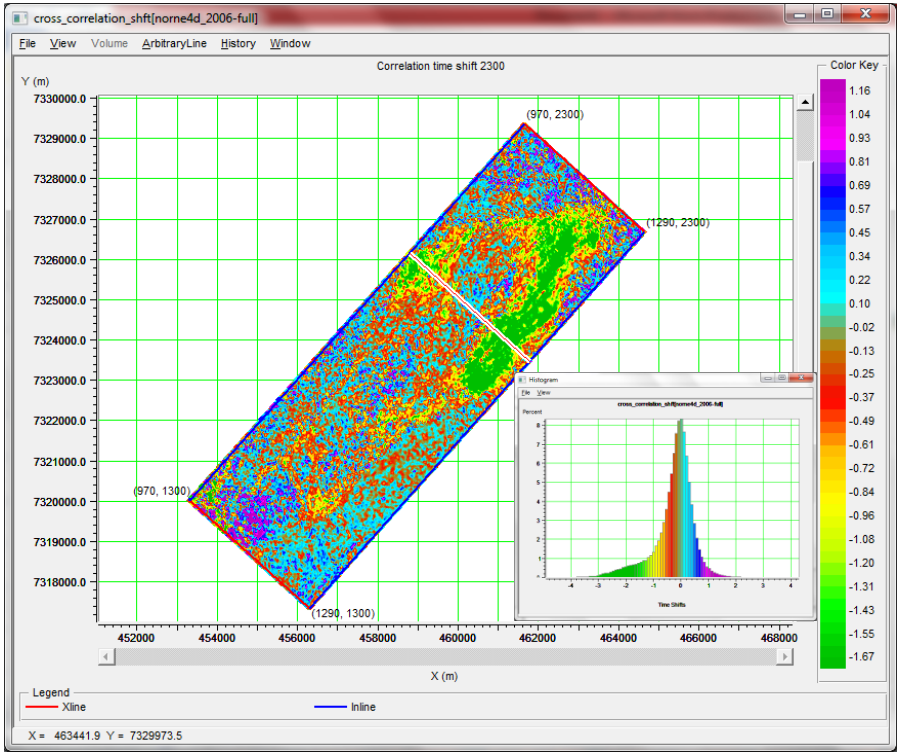

Figure 22: Time shift slice showing averagely low shifts (Insert is a histogram showing the time shift and its corresponding percentage for the datasets)

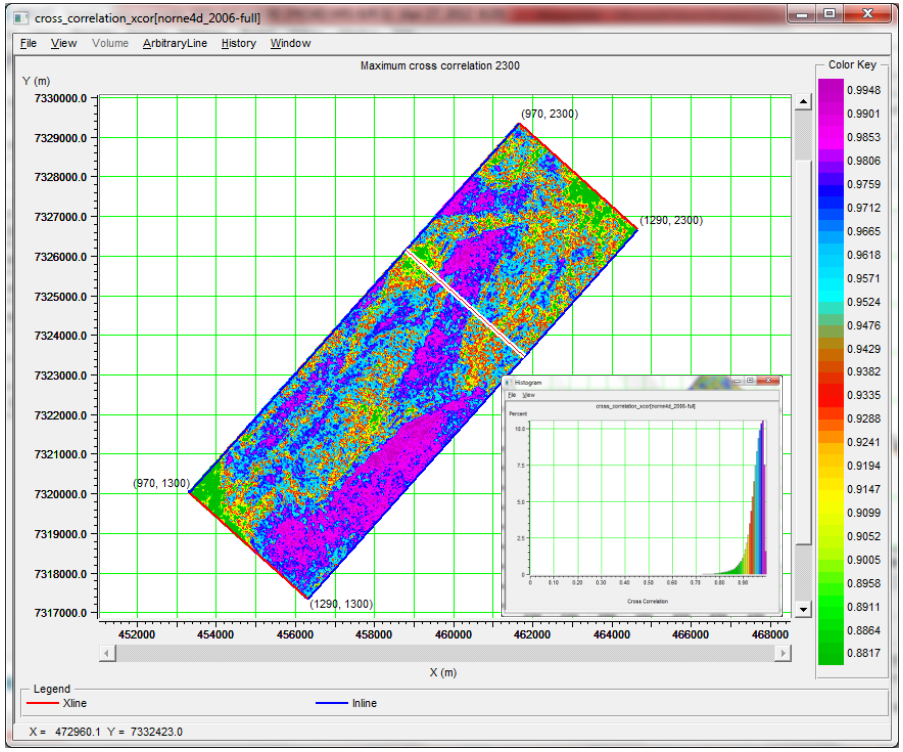

Figure 23: Map slice showing the crosscorrelational percentages for 2001 and 2006 (Insert is a histogram showing the crosscorrelation and its corresponding coefficient for the datasets)

A very low average of time shift between the 2001 base and 2006 monitor surveys is observed on the correlation time shift slice in figure 22. These shifts are located within the reservoir area. The time shifts correspond to the areas of least correlation on the crosscorrelation map slice. Due to the very minimal time shifts and a very high correlation there will not be any need for further calibration to correct for time and phase shifts.

4.4 Volume Difference

The volume difference analysis seeks to compare two volumes to see how and where they differ. This is based on total volume while the crosscorrelation compares on a trace by trace basis.

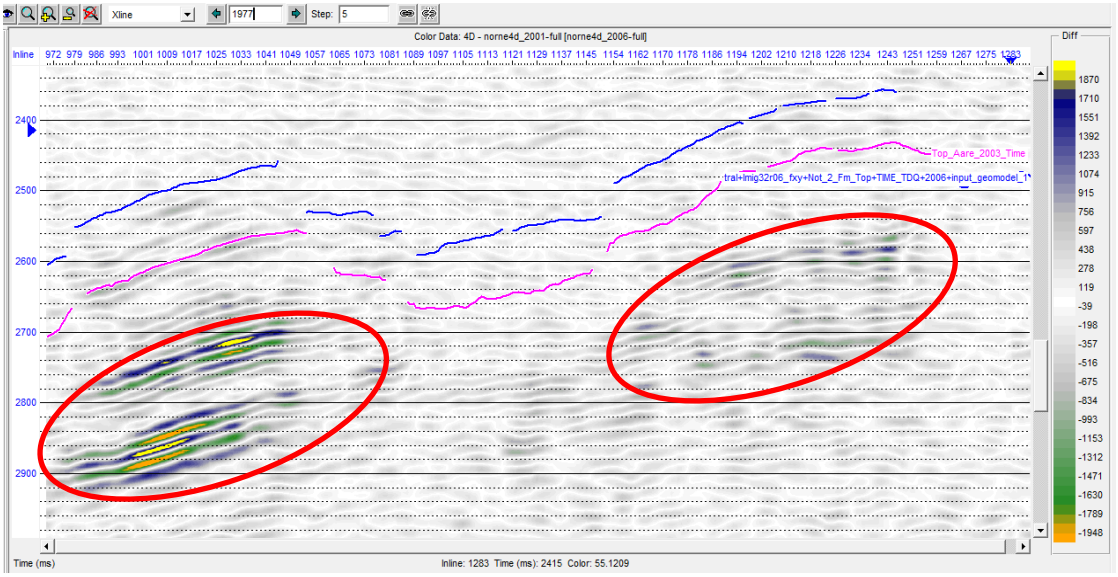

Figure 24: A cross-section through a difference volume at cross line 1977

Majority of the difference seen in the volume were located in the under-burden of the reservoir. These have been circled in figures 24 and 25 with a strong contrast in negative and positive differences.

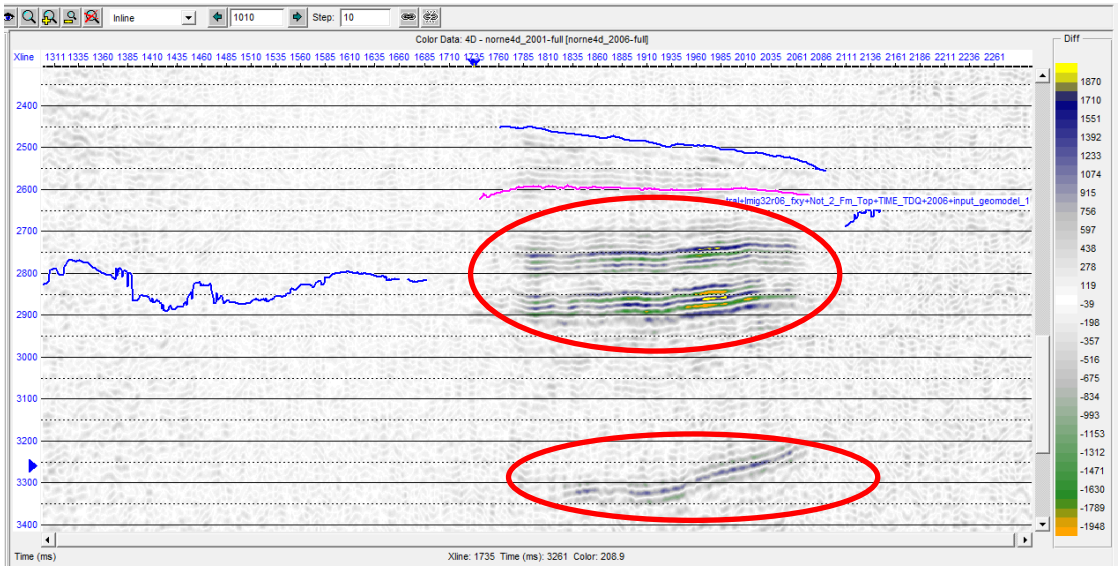

Figure 25: A cross-section through a difference volume at in-line 1010

4.5 Wavelet Extraction

Two wavelets were extracted from the seismic volumes as reference and monitor wavelets. The bandwidth matching function in wavelet extraction for time lapse seismic was used. The function creates an operator filter for the surveys that would match the survey's wavelet to a reference wavelet. These new wavelets are then applied to the surveys, which tend to remove any differences between surveys which are caused by different signal wavelets and enhancing the ability to observe production-caused differences.

The two wavelets extracted from the monitor and one of the monitor surveys are displayed in figure 26 below.

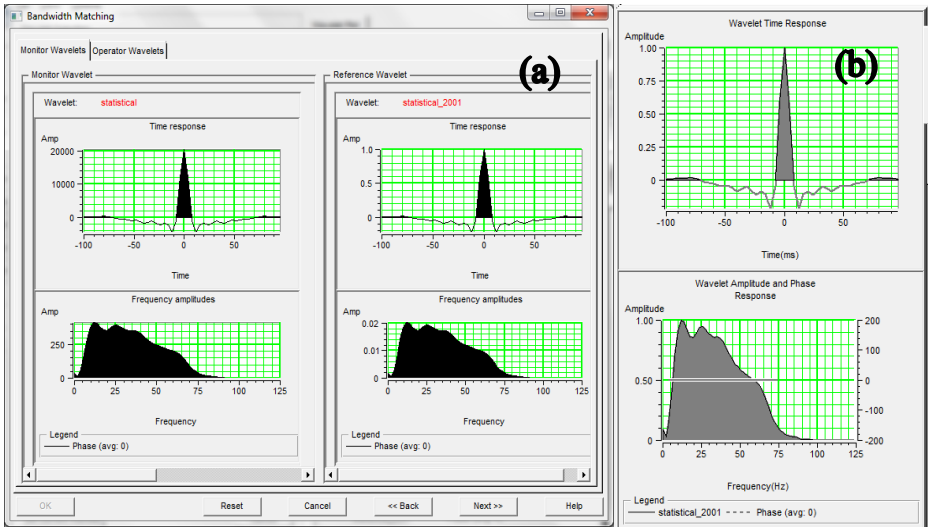

Figure 26: (a) Bandwidth matching wavelets for monitor and reference surveys showing time response and frequency amplitude (b) final wavelet for inversion

4.6 Loading Horizons

There were two main methods of getting horizons into Pro4D; importation of horizons or picking of horizons. Of these two, importation is usually preferred. This was used for the case of this inversion process. Two horizons were loaded into the seismic group volumes. These have been loaded and shown in fig. 9 and 10 above. The time based horizons were used because the seismic is also in time and the two would correspond with each other.

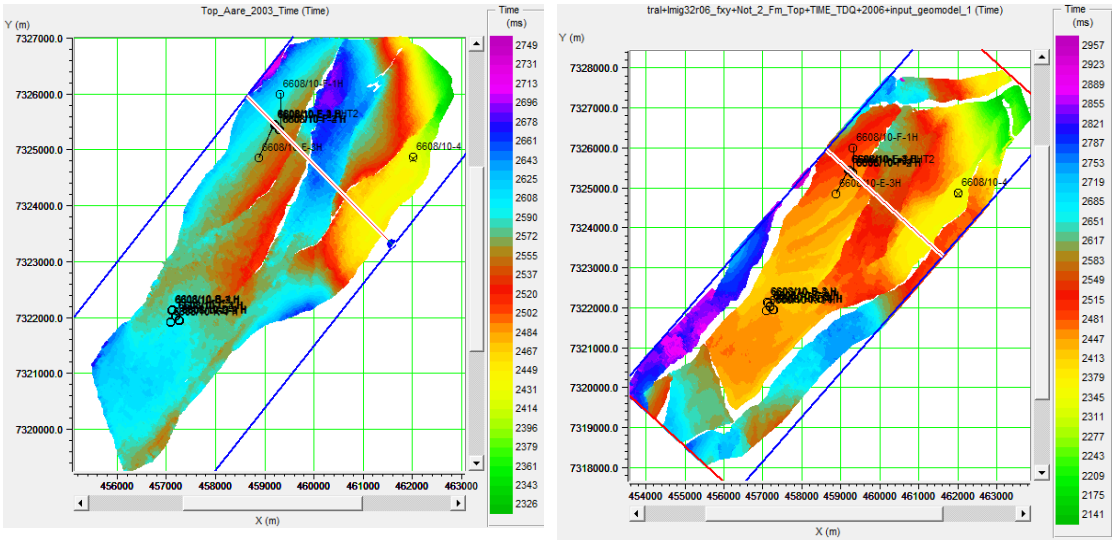

Figure 27: Map Slice of Top Not and Åre horizons in time. Colour legend represents depth, define the colour range

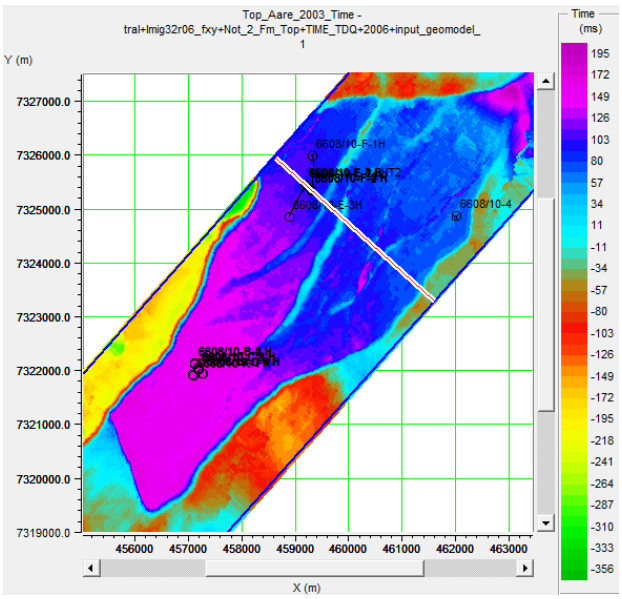

Figure 28: Isochron of the two horizons in time, giving an indication of the thickness in time of the horizon

Horizons are very important in the process because they act as a priori information for the building of the initial model. The final volume of inverted data takes its structure from the initial horizons that were loaded into the initial model.

4.7 Time-Lapse (4D) Inversion

The 4D inversion provides information about the acoustic impedance change between the base and monitor surveys. Time delays caused by velocity changes in the reservoir can negatively affect the inversion comparison. Time delay information can be used to enhance the inversion and thus provide information below the seismic bandwidth. This can be resolved with the provision of low frequency information from well information where scalars are multiplied with initial models. The initial model is built from the well log data and this most likely represents an initial guess at the velocity structure of the subsurface. This is a constraining factor during the inversion. The final inverted result is a velocity profile that may slightly deviate from the initial guess, while at the same time modeling the real data as closely as possible.

The initial model for the 4D inversion was built using the 4D inversion application in Pro4D. A model with a typical setup is chosen depending on the data available. For this purpose where post-stack data is being inverted the typical setup for acoustic impedance was used.

Wells which have been check-shot corrected and quality controlled checked were selected to be used. The wells used were discovery well, 6608/10-4, production well, 6608/10-E-3H and injector well, 6608/10-F1H. The grid for the base survey was used in accessing the model traces within the display and processing window for both base and subsequent monitor surveys.

Three logs were utilized in the building of corresponding log types for the model; P-wave, density and P-impedance logs. These are the logs required for the typical setup for an acoustic impedance model. The most recent of the edited logs are set as the active logs for the purpose of the inversion. The logs are combined with the imported horizons to be included in the model.

A filtering option was created by applying a smoother on the modeled trace in the output domain through a highcut frequency setup.

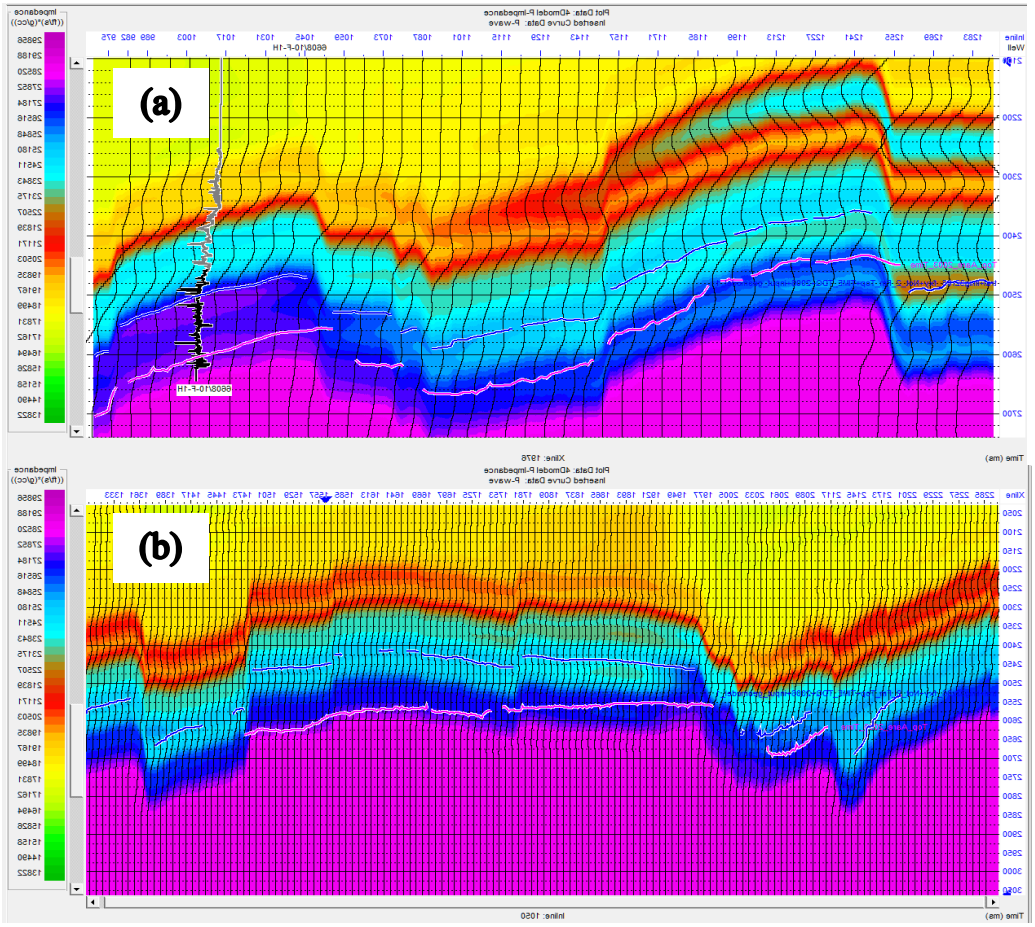

Figure 29: A cross-section through the initial model at (a) crossline 1976 with a P-wave inserted log and (b) inline 1050 with both showing the reservoir zone

The cross-sections above show the initial acoustic impedance through the model. The cross-line (a) in the figure above shows a section through the E-segment with its tilted fault block to the west of the section. The east of the section shows the G-segment at a higher elevation than the E also with a tilted fault block. The inline section (b) shows the E-segment with most of the formations within the reservoir area displaced by faults. A 3-dimentional representation of the model is shown below in fig. 30. These show slices through the volume with crossline (1977), inline (970) and a time slice at the two horizons; (a) approximately at Top Not and (b) approximately at Top Åre. Figure 30 shows higher impedance at base reservoir and lower impedance at the top reservoir.

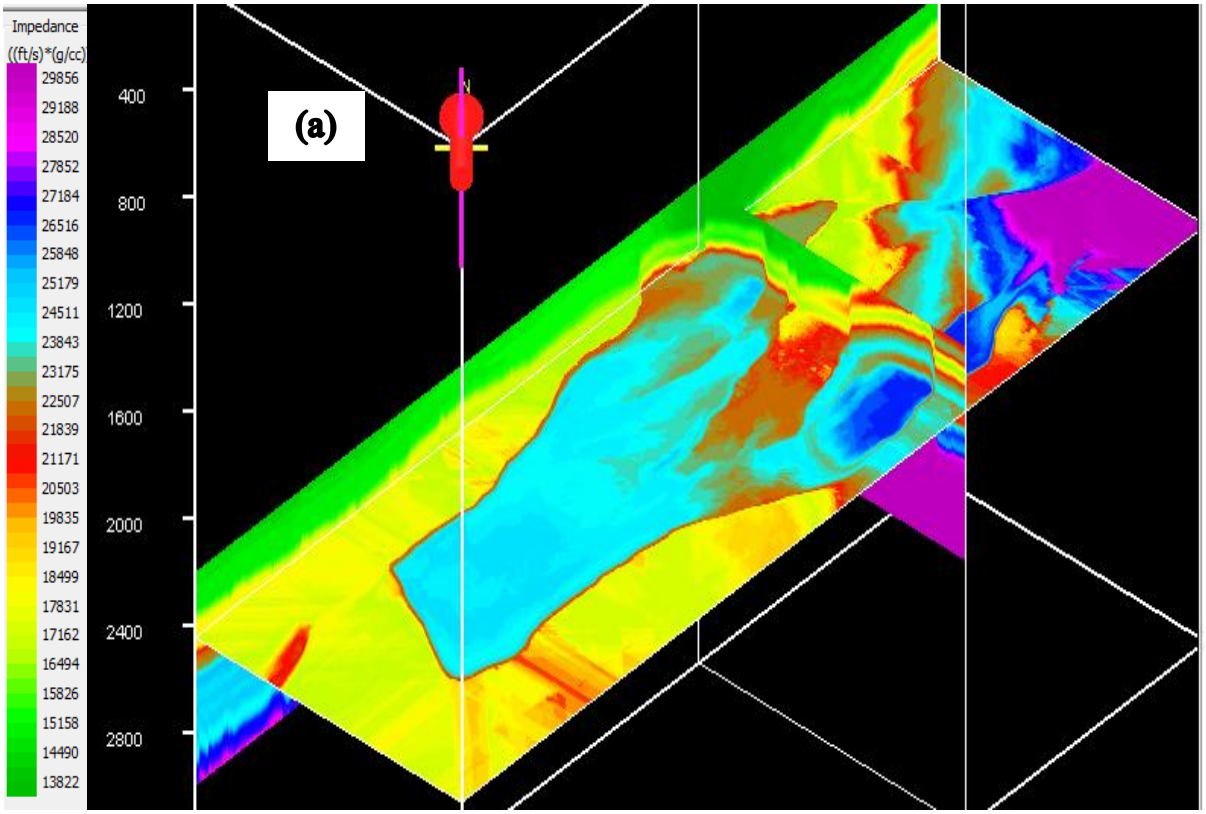

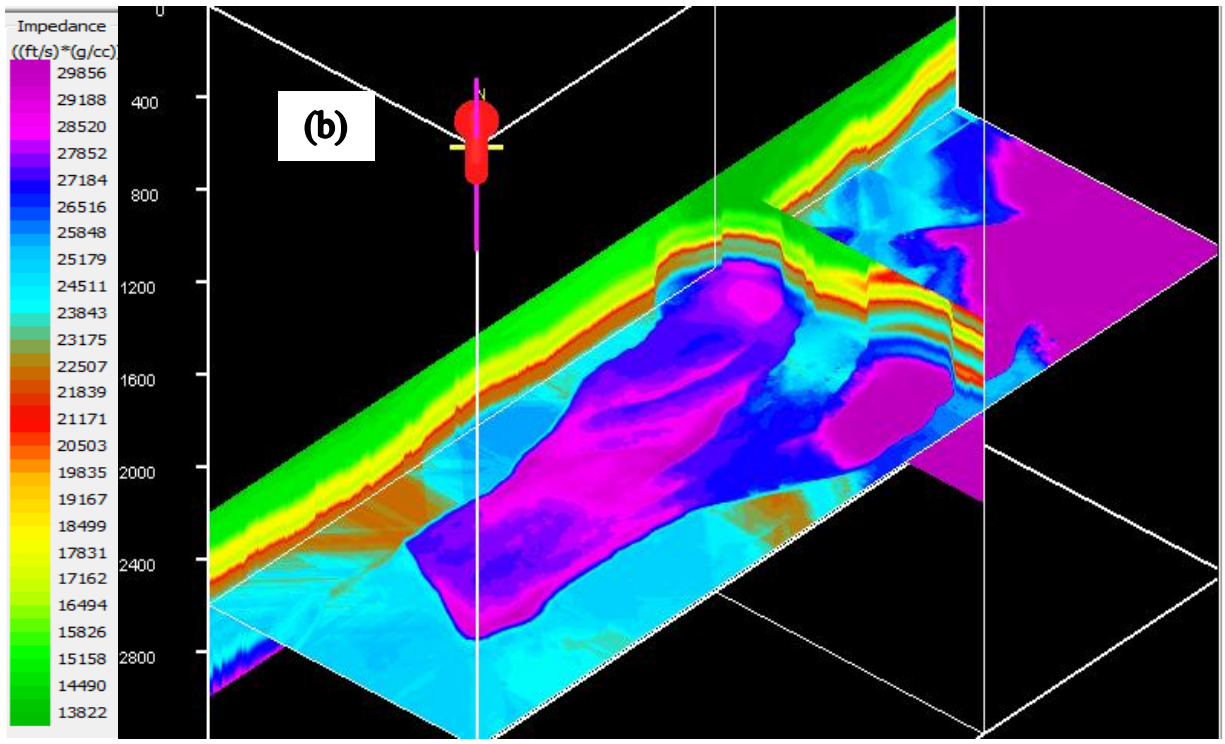

Figure 30: 3-D model representations through (a) Top Not and (b) Top Åre

A look at the frequency amplitude of the seismic data before the inversion (figure 31) indicates the lack of low frequency component which is typically associated with the seismic bandwidth. The low frequency component provided by well data is very vital for the inversion of post stack data.

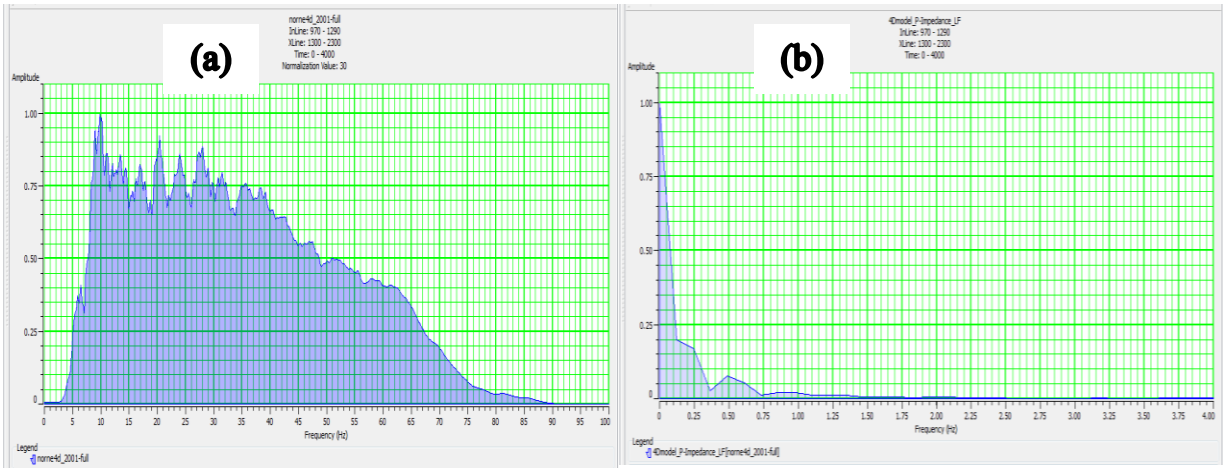

Figure 31: (a) Amplitude spectrum for 2001 seismic survey (b) Low-frequency component derived for 2001 survey

The above observation indicated the addition of the low-frequency component to the initial model built for inversion. The time-lapse P-impedance model had the low-frequency scalar added to it through the 4D inversion application. There are two ways of applying the scalar to it; horizon based or time-shift based. The horizon based method is much preferred since we have much more confidence and control over the horizons. A filter application is set for this process which tends to focus the bandwidth needed for the application of the scalars to the reservoir section of the seismic data required.

After the low frequency scalar had been applied, the inversion was performed with the selection of the appropriate seismic group and its corresponding impedance volume and the bandwidth wavelet created for the various seismic volumes. Various options can be used in the inversion of seismic data after the initial models have been built. The time lapse Pro4D application operates with the model based option. The model based is a generalized linear inversion (GLI) algorithm which attempts to modify the model until the resulting derived synthetic matches the seismic trace within some acceptable bounds. For each trace, a synthetic seismogram was calculated using the initial impedance guess and the known wavelet. That impedance was then modified gradually, until the resulting synthetic trace matched the real trace within some tolerance level (Hampson and Russell article, 2012).

The processing time window was also selected as it allows us to invert the volume needed in order for noisy areas within the volume not to overshadow the reservoir zone. The hard constrain option was chosen since this limits the amount of deviation of the inverted model from the initial model.

5. Chapter Five – Results and Discussion

5.1 Well and Seismic Correlation

The main objective of the seismic well tie correlation process is to be able to extract the best possible wavelet to be used in the inversion. Correlating our synthetically generated seismic data with the acquired seismic is vital in the model building process which eventually leads to inversion. The main objective of the seismic well tie correlation process is to be able to extract the best possible wavelet to be used in the inversion. The correlation is based on the convolution of the extracted wavelet, the sonic and density log datasets to generate synthetic seismic data, which are zero-offset based. The synthetic seismic data is then compared with an extracted composite trace close to the well location from the acquired seismic volume. The convolved zero-offset based synthetic traces have been plotted in blue and the extracted composite traces close to the well have been plotted in red. The acquired seismic is plotted in black from the figure below.

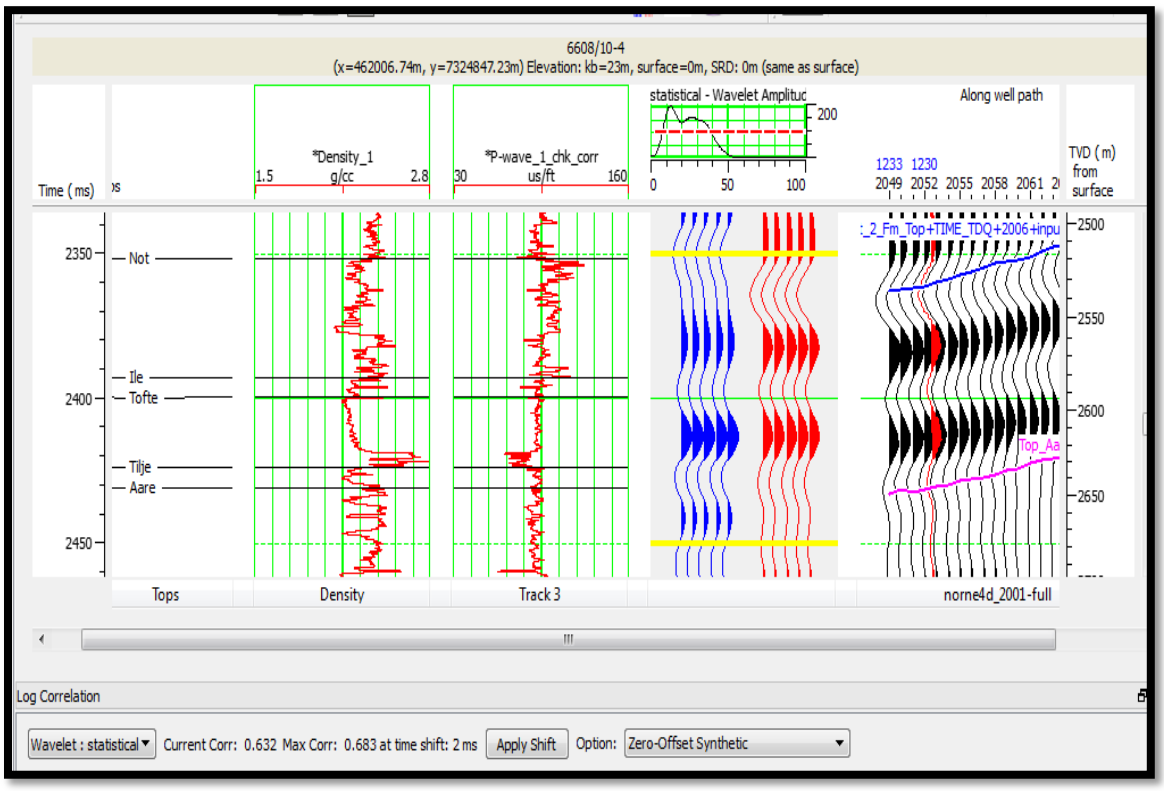

Figure 32: Log correlation for well 6608/10-4 showing the synthetic seismic generated from wavelet and well data (blue trace) and sampled seismic data close to the well (red) and a correlation co-efficient of 63%

The important part of this process is to be able to identify how much correlation exists between the synthetically generated seismic and the extracted composite seismic.

The correlation co-efficient is based on a time window match between the two seismic traces. The few milliseconds below and above the reservoir section of the Norne seismic data has been added to the actual reservoir and the correlation co-efficient is 63 % for well 6608/10-4 (Figure 33) and 6608/10-F-1H (figure 35). A much higher percentage of correlation (81%) is observed for well 6608/10-E-3H (figure 34). Three things were checked to make sure that the log correlation was done in the right way; reservoir centered time window, appropriate wavelet and an optimized shift in time.

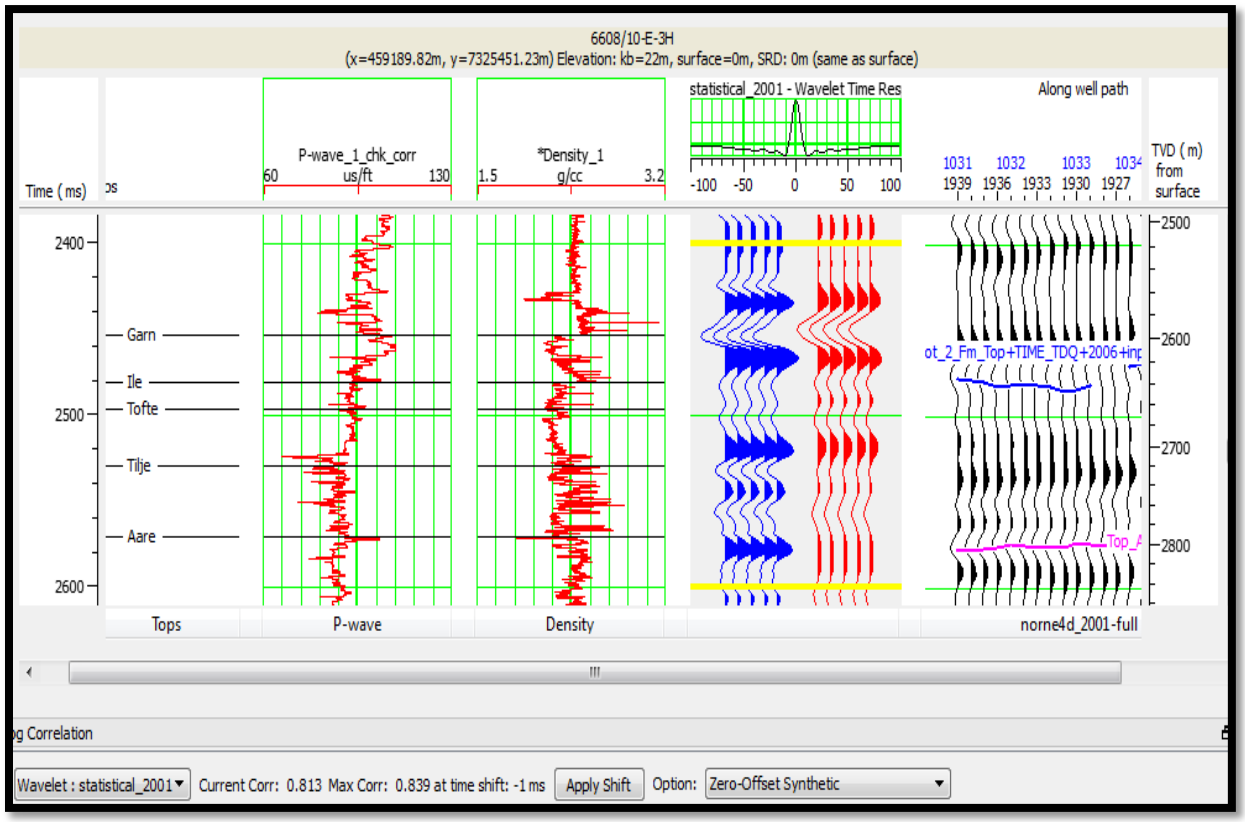

Figure 33: Log correlation for well 6608/10-E-3H showing the synthetic seismic generated from wavelet and well data (blue trace) and sampled seismic data close to the well (red) and a correlation co-efficient of 81%

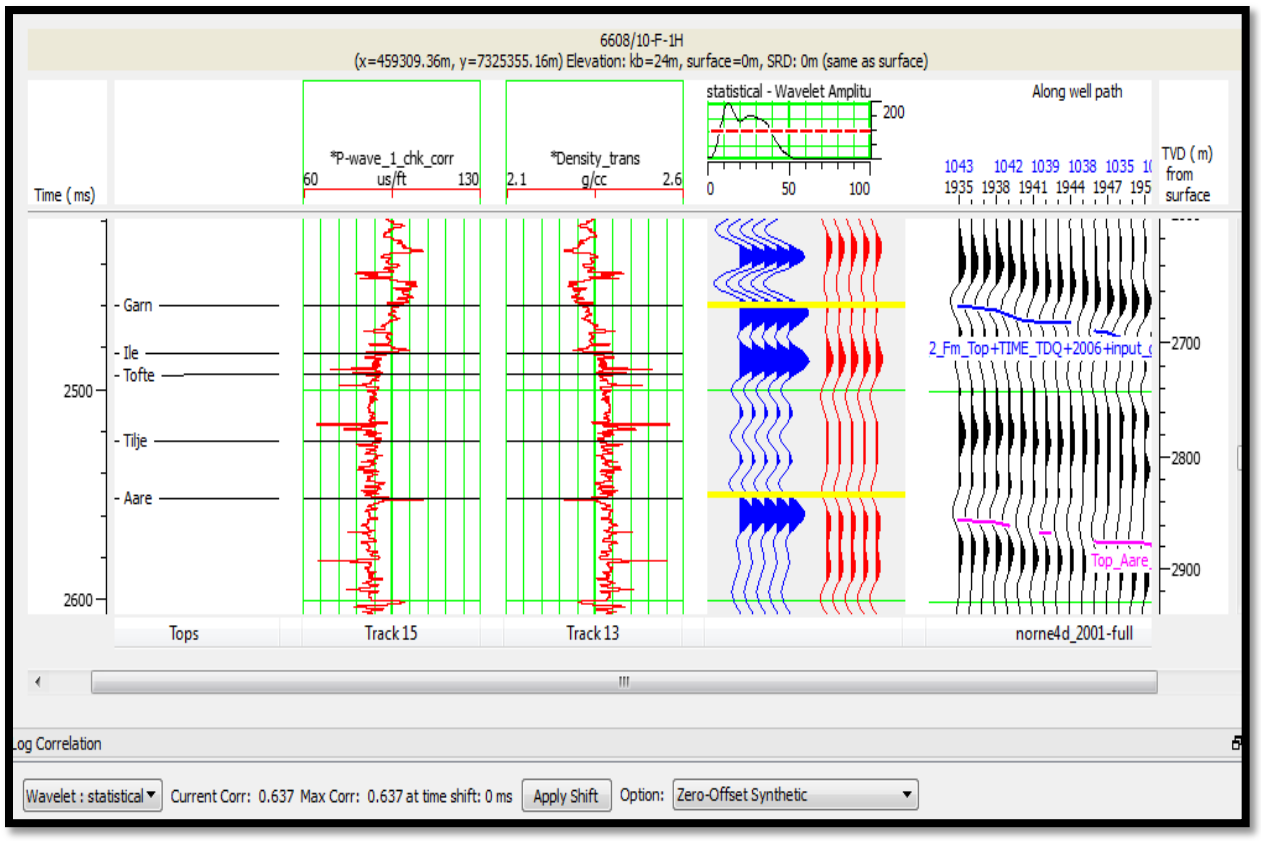

Figure 34: Log correlation for well 6608/10-F-1H showing the synthetic seismic generated from wavelet and well data (blue trace) and sampled seismic data close to the well (red) and a correlation co-efficient of 63%

5.2 Attribute Analysis

There are several attribute analyses which can be carried out on time-lapse data to find out the effects which have been recorded in monitor surveys. Horizon based analysis is one of the most important parameters used where attributes are analyzed between the interpreted horizons.

5.2.1 Difference in NRMS

NRMS is a measure of amplitude level in the difference trace normalized by the average of the base and monitor traces. Kragh and Christie, 2002 defined this as the difference between two datasets. A perfect match gives a value of zero (0). Where crosscorrelation has been dealt with during the acquisition and processing stage, as in this case, a difference in the NRMS gives an indication of an effect which is more related to the production of hydrocarbons. The NRMS is calculated by

$$NRMS = \frac{2 * RMS(a-b)}{RMS(a) + RMS(b)} \tag{13}$$

where *a* is the monitor survey and *b* is the base survey. In this case the base survey (2001) has constantly been subtracted from the monitor surveys which are alternated between the surveys carried out in 2003, 2004 and 2006. The confidence imposed in the NRMS results is established in the fact that areas within the horizon based analysis where there has been very minimal hydrocarbon production shows very little variation while segments with significantly high production show effect in the result.

Differences in the various analyzed maps slices within the field show that there are variations in the NRMS of the monitor and base surveys. These changes have been illustrated in the figures 35, 36 and 37. These figures show a comparison of the NRMS difference between the common base survey and different monitor surveys. The observed differences between (2003 and 2001) and between (2004 and 2001) in figure 35 shows that there has been an increase in impedance especially in the areas on the map that have the ellipsis; the E-segment and G-segment. The increase in impedance is very much observed around the well locations in these segments.

Excellent communication in the reservoir implies that the most important changes which have occurred are due to vertical and horizontal flow movement of fluids below the Not formation.

This is due to the sealing ability of this layer. A change in figure 35 is represented below with a positive impedance change across it.

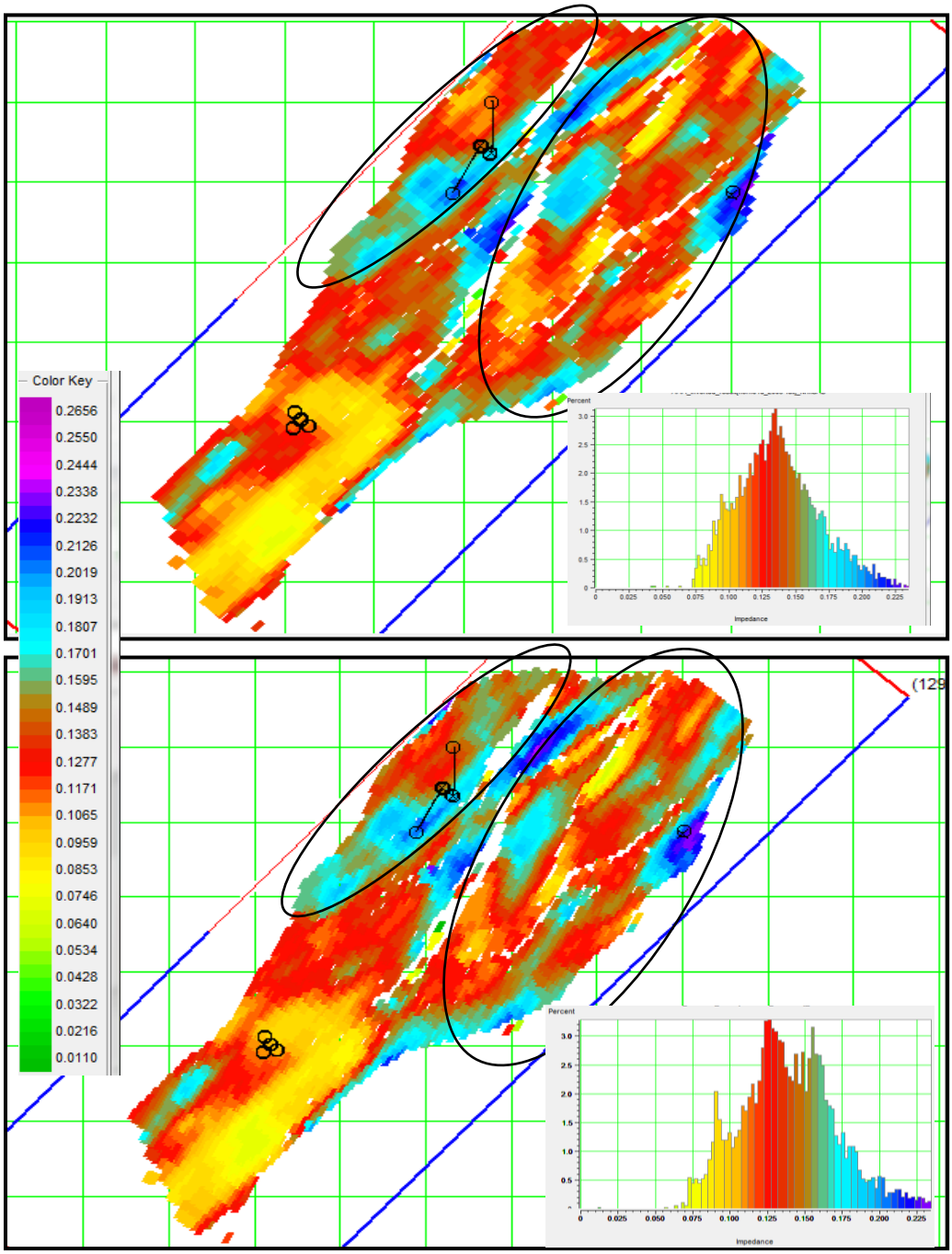

Figure 35: (a) NRMS difference between base (2001) and first monitor (2003) and (b) NRMS difference between base (2001) and second monitor (2004)

Figure 36 shows the NRMS difference between surveys 2003 and 2001 as well as 2006 and 2001. The areas of significant changes observed in the previous figure 35 have being observed much clearer in this figure. These areas are represented in the ellipsis on the maps and the most significant again is the E-segment.

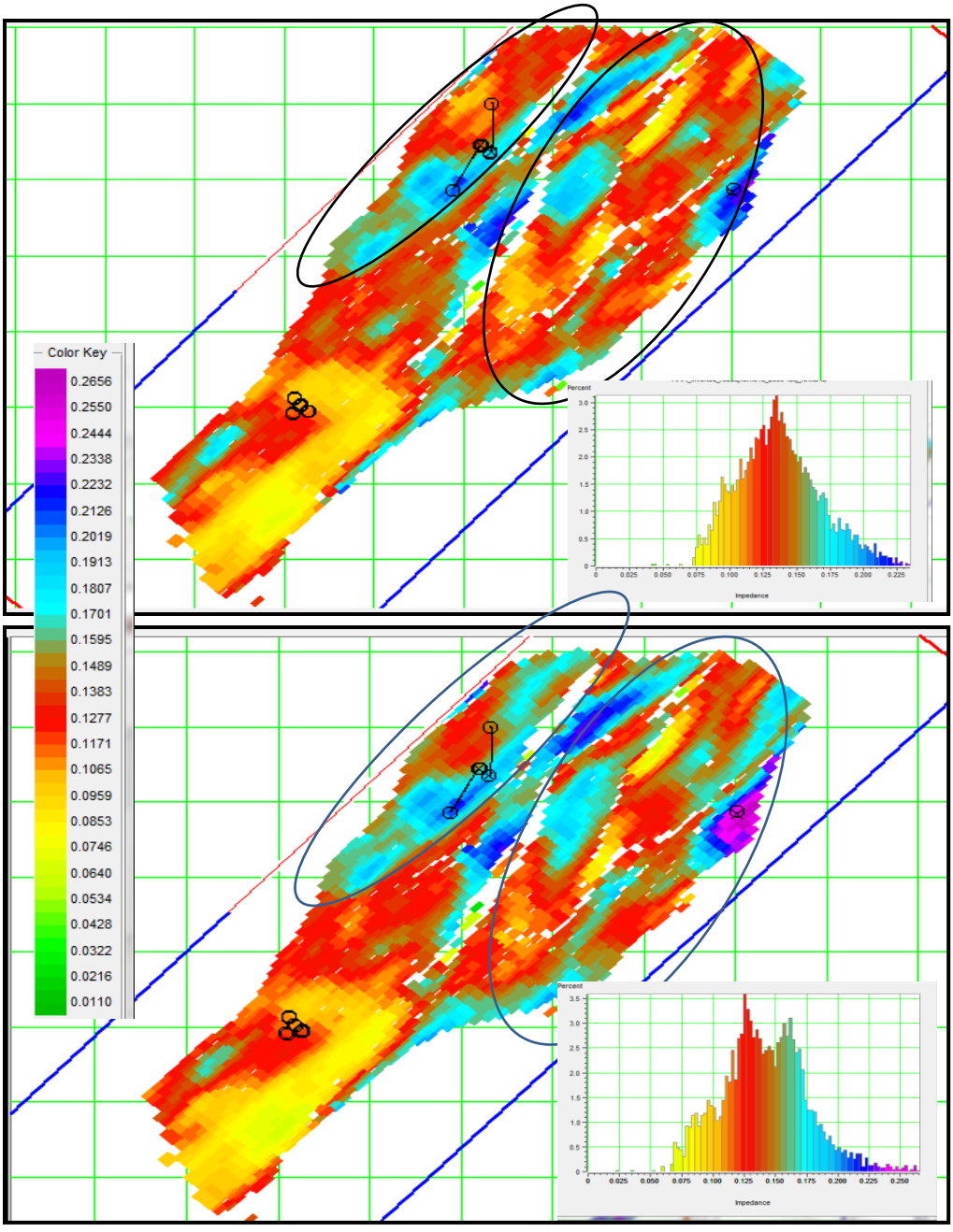

Figure 36: (a) NRMS difference between base (2001) and first monitor (2003) and (b) NRMS difference between base (2001) and second monitor (2006)

The compared difference between monitors 2006 and 2004 and base 2001 has been shown in figure 37 below. The areas within the circle indicating segments E and G, still show much higher difference in the impedance change.

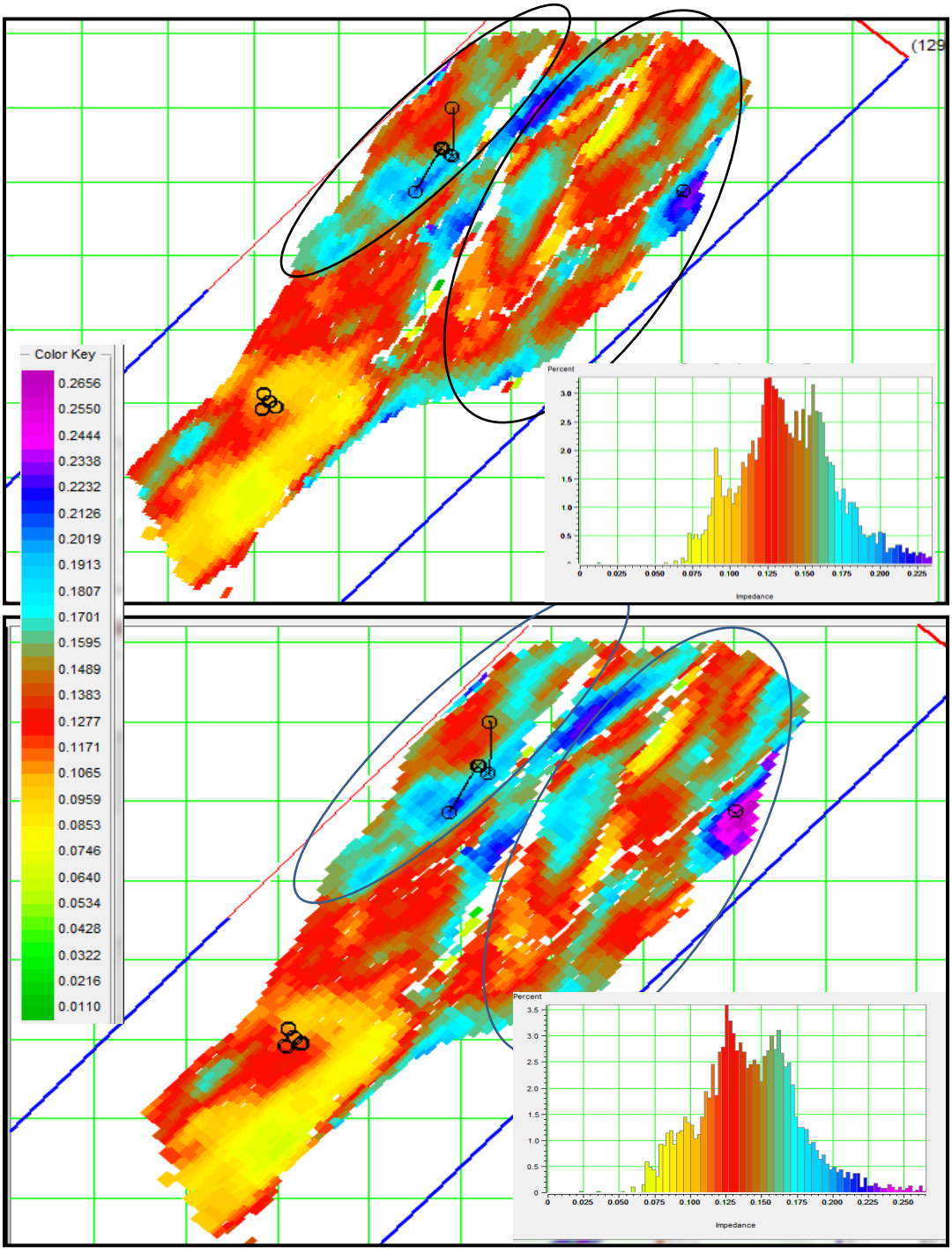

Figure 37: (a) NRMS difference between base (2001) and first monitor (2004) and (b) NRMS difference between base (2001) and second monitor (2006)

The E-segment (top left ellipse) has had increased impedance in the NE and SW parts of the ellipse while the well in the G-segment (lower right ellipse) shows the most change. There are changes in other parts of the field, but a careful look at the geometry and the changes that have occurred indicate that these changes mostly occur within the lower sections of the tilted horsts.

Water injection well F-1H is located at the northern end of the E-segment where the geometry of the block tilts down. The impact of the injector well is observable in the gradual change in the difference from one monitor to the other. The area around the injected well is systematically increasing in the velocity difference indicating the presence of a migrating fluid front with much higher impedance than the initial fluid being replaced. This is quite significant because the area around producer wells located at the southern end of the segment has not experienced such intensity of change.

A statistical histogram plot of impedance versus percentage of the difference in NRMS for the various surveys has been attached to the various data slices (figures 35, 36 and 37). The histograms show a consistent change with respect to time. The difference in NRMS for 2003 and 2001 in figure 35 shows a singular peak in impedance. This change is centered at an impedance change of 0.135. The statistical histogram difference plot for NRMS in the subsequent monitor (2004 and 2001) shows another peak at the higher end of the impedance scale in addition to the initial peak seen in the 2003and 2001 statistical plot. This gives an indication of much higher changes between the 2004 monitor and 2001base surveys. The final histogram which is seen on the monitor 2006 and base 2001 has the highest percentage change as well as increased impedance with a double peak also occurring.

5.2.2 Amplitude Changes

The average amplitudes for the various inverted volumes were analyzed within the reservoir. The Not and Åre interpreted horizons were used as upper and lower limits for the amplitude analysis. The results for this analysis have been presented in the figure below. From the data slices for the volumes there are noticeable changes within the field. Most of these changes are concurrent with those observed in the NRMS analysis. Increases in average amplitudes for the reservoir region are observable within these slices.

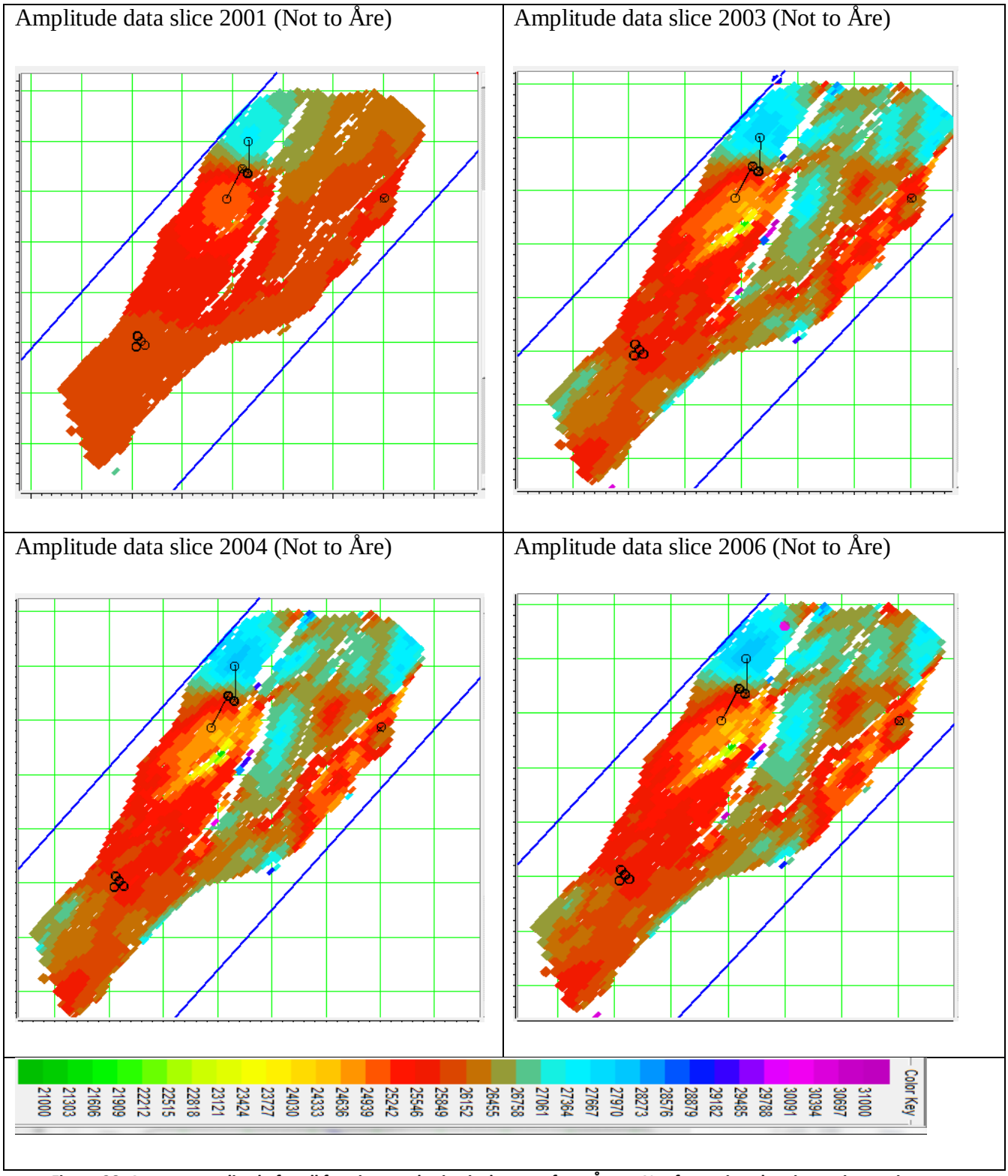

Figure 38: Average amplitude for all four inverted seismic datasets from Åre to Not formation showing an increasing impedance with monitor vintages especially within the E-segment

5.2.3 Seismic Amplitudes

Seismic amplitude analysis of the field impedance shows an increase across the Not formation and a rapid decrease below the Not formation in the figure below. This was identified as the gas filled part of the sandstone with amplitude differences seen across the horst structure. There is a gradual increase in the amplitude of the seismic trace down into the reservoir with the highest amplitudes within the reservoir occurring just above the Åre formation which marks the limit of the reservoir base. This is interpreted as the water-filled part of the reservoir with the negative and lower amplitudes associated with the gas and the oil-filled parts of the reservoir respectively.

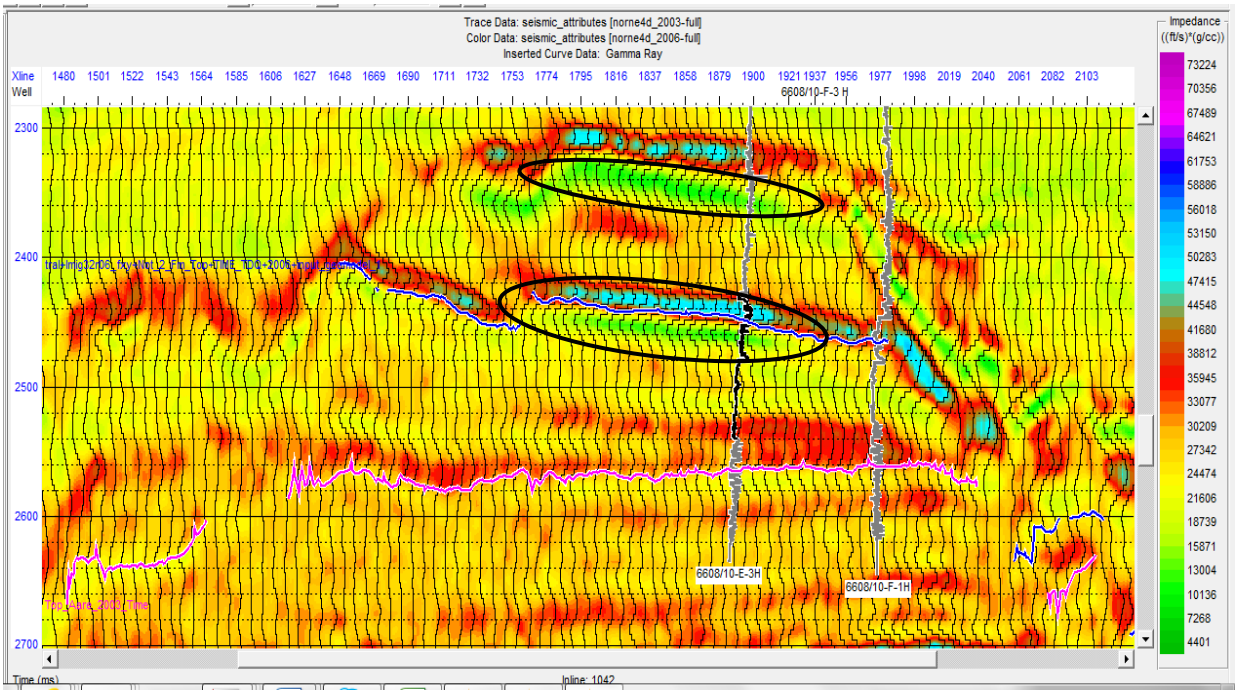

Figure 39: A cross-section of inline 1042 showing seismic amplitude of high and low impedance within the Not formation and below it in the inserted ellipsis

5.3 Geological Interpretation of Cross-Sections

5.3.1 Faults

The inversion confirmed fault structures within the field with a further indication of fluid mobility and migration possibilities. The most pronounced fault indications where those bounding the horsts in the field. This is observed in the difference in impedances of the inverted data for base and monitor surveys where different fluid saturations are seen on either sides of the

juxtaposing faults as in figures 40. The difference in impedance amplitudes across the fault gives an indication of a non-communicating fault, indicating that the faults are not just structurally juxtaposing the adjacent fault blocks, but are also acting as fluid barriers in some cases. The fault is indicated with a black line across the section and this is located within the E-segment of the field. The horst viewed from an inline perspective shown in figure 41, shows listric faulting with the sediments of the rotated fault block being much higher compacted than the E-segment horst. The impedance across the bounding faults are also seen as sealing since the differences in impedance across the faults are not the same after an impedance based interpretation of the various horizons. The sealing nature of the fault further confirms the segmentation of the field based on these major faults.

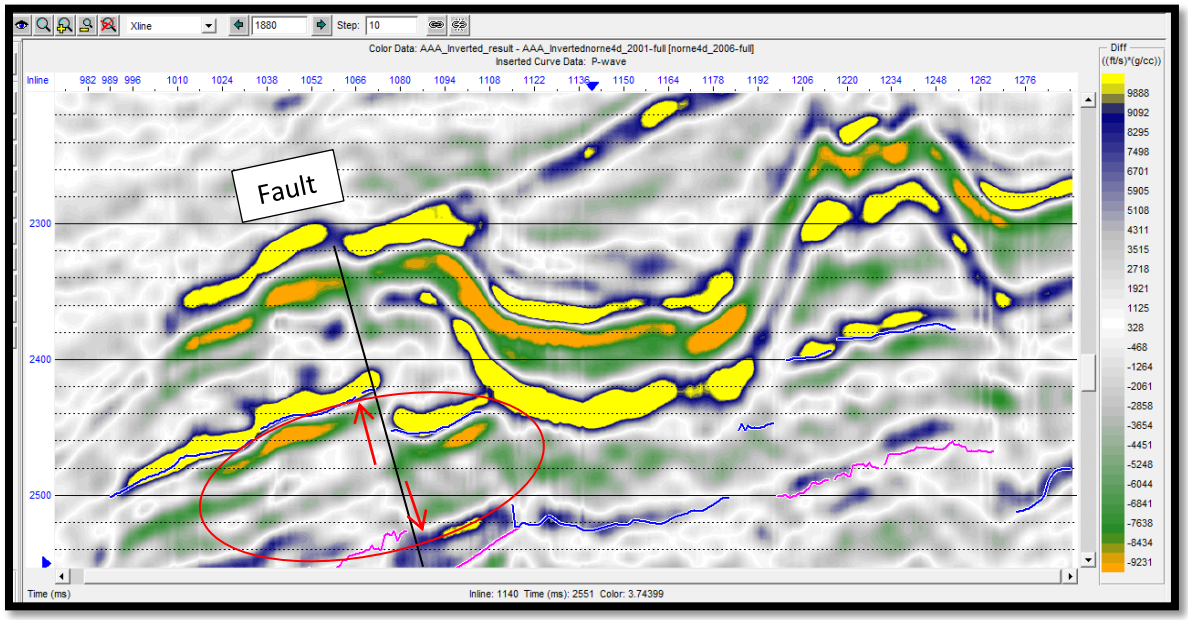

Figure 40: Cross-section through X-line 1880 showing a fault with different impedance build-up across it within circle

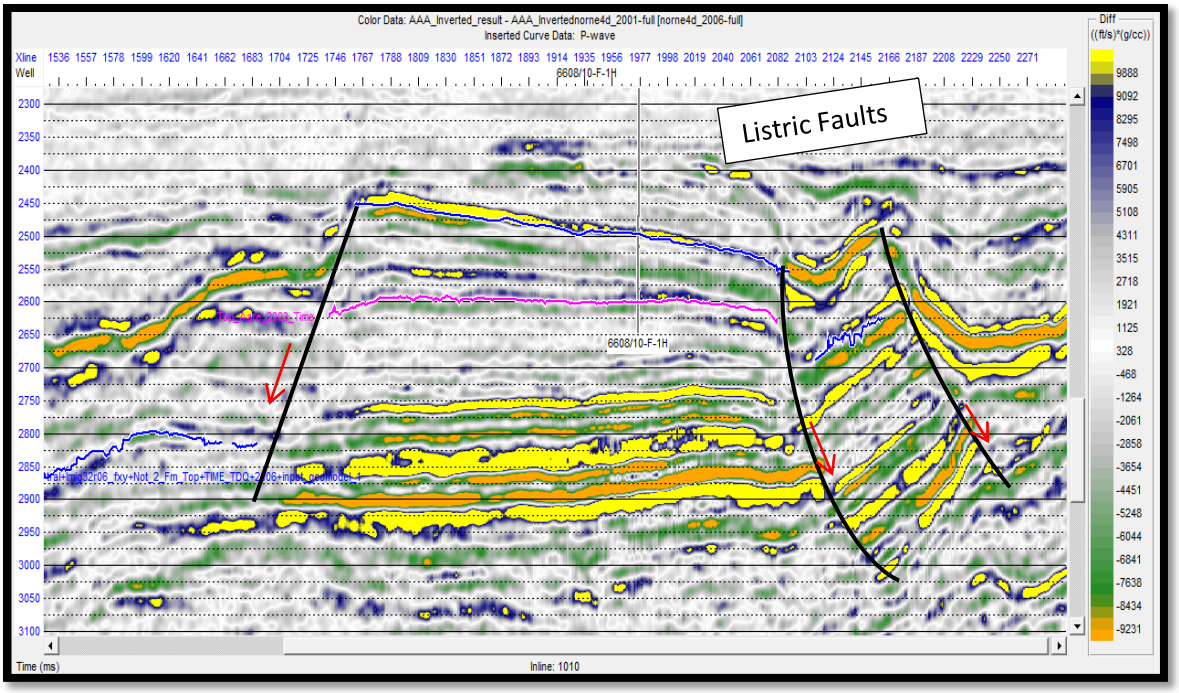

Figure 41: A cross-sections through inline 1010 showing listric faulting and a normal fault. The wedge shape off the reservoir is also revealed in this section

Minor faults observed within the field were seen to be also acting as fluid barriers as there is an inhomogeneous fluid front migration across the field. These faults serve as local fluid barriers which most probably reduces the fluid sweep efficiency in the field as the general fluid fronts within the reservoir are inhomogeneous, with these local fluid barriers affecting fluid movements and drainage of the field.

5.3.2 Stratigraphy

The well data from the field gives an indication of the various stratigraphic units up until the base of reservoir section. The various attributes analyzed for the time-lapse inversion have all given confirmation of some of the stratigraphically important lithologies within the group. The Not formation which is a hard event within the reservoir has been recognized in all of these attributes and inverted vintages of the base survey as well as the subsequent monitors. The Not formation though thin is noted for its sealing capability because of its shale content. The

impedance change across the Not formation and stratigraphically below it can be attributed to different properties. The impedance change across the Not is lithologic while that below it within the Ile and Tofte are fluid related (gas) as seen in Figure 39. The seismic attribute and impedance difference cross-sections above give indication of the Not as well as the presence of the lower density gas in the reservoir. The Ile, Tofte and Tilje formations show changes in impedance for the inverted time-lapse survey. This gives an indication of fluid front movement and the good communication within the reservoir.

5.4 Production and Injection Impacts on Time Lapse inversion

The field started producing with a self-sustaining pressure which dropped after a few years of production. The drainage strategy of the field indicated water and gas injection below the reservoir to increase the pressure within the field. The injected water replaces the produced oil in the lower sections of the tilted fault blocks while the gas cap was kept intact. This is shown in figures 43- 46 below where we can see a steady change in the impedance difference from one monitor to the other in the inserts. A plot of the well oil production total (WOPT) from production wells E-3AH and E-2H in the E-segment are shown in figure 42 as well as the well water injection total (WWIT) from wells F-1H and F-3H. The WWIT for the data available for this segment indicates a higher volume of injection as opposed to the WOPT. The injected water with a higher density replaces the produced oil with a lower density which explains the reason for the changes which have been observed in the NRMS difference data slices in the previous figures. There are observable changes also within the G-segment, containing oil with no gas cap. Likewise the E-segment, the changes within the G also occurs within the lower tilt of the fault blocks. The graben area between the E and G segments also show some changes in both the data slice and the cross sections.

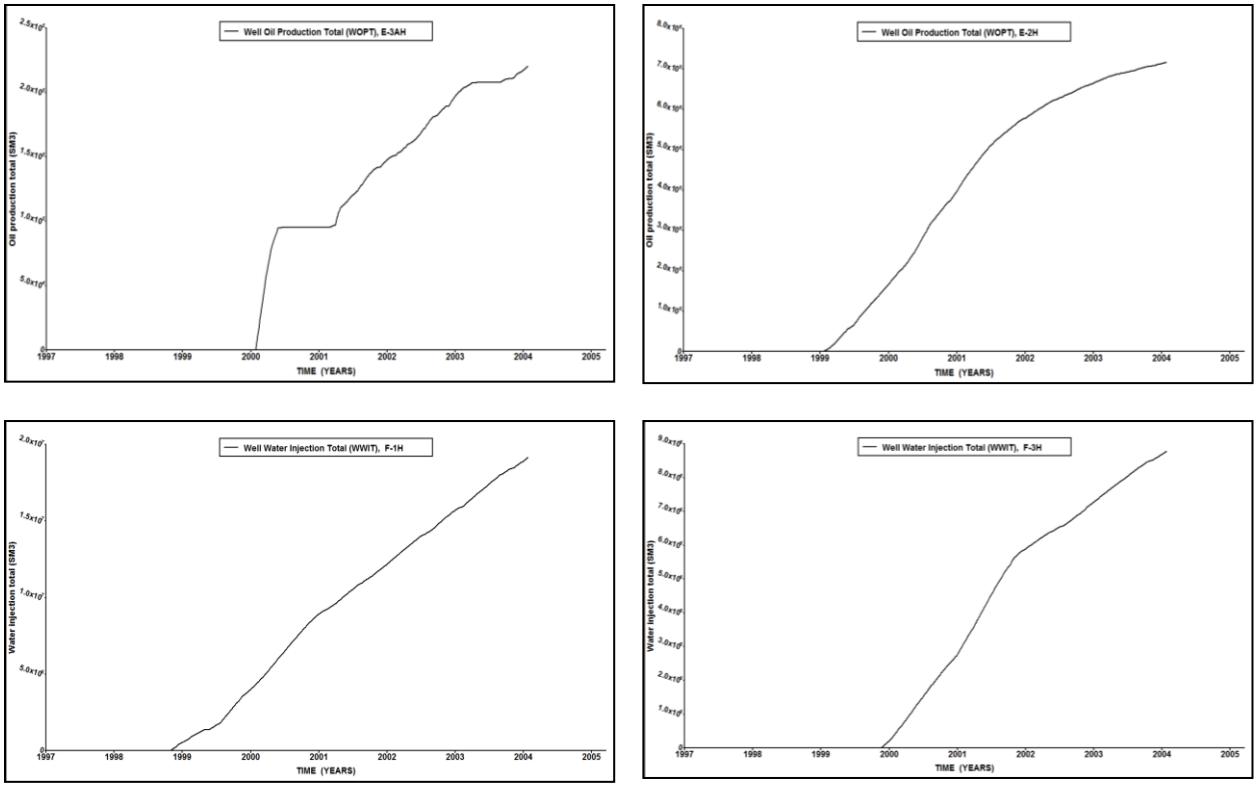

Figure 42: Well Oil Production Total (WOPT) vrs Time in years for 6608/10-E-3AH (Top left) and 6608/10-E-3H (Top right). Well Water Injection Total (WWIT) vrs Time in years for 6608/10-F-1H (bottom left) and 6608/10-F-1 (bottom right)

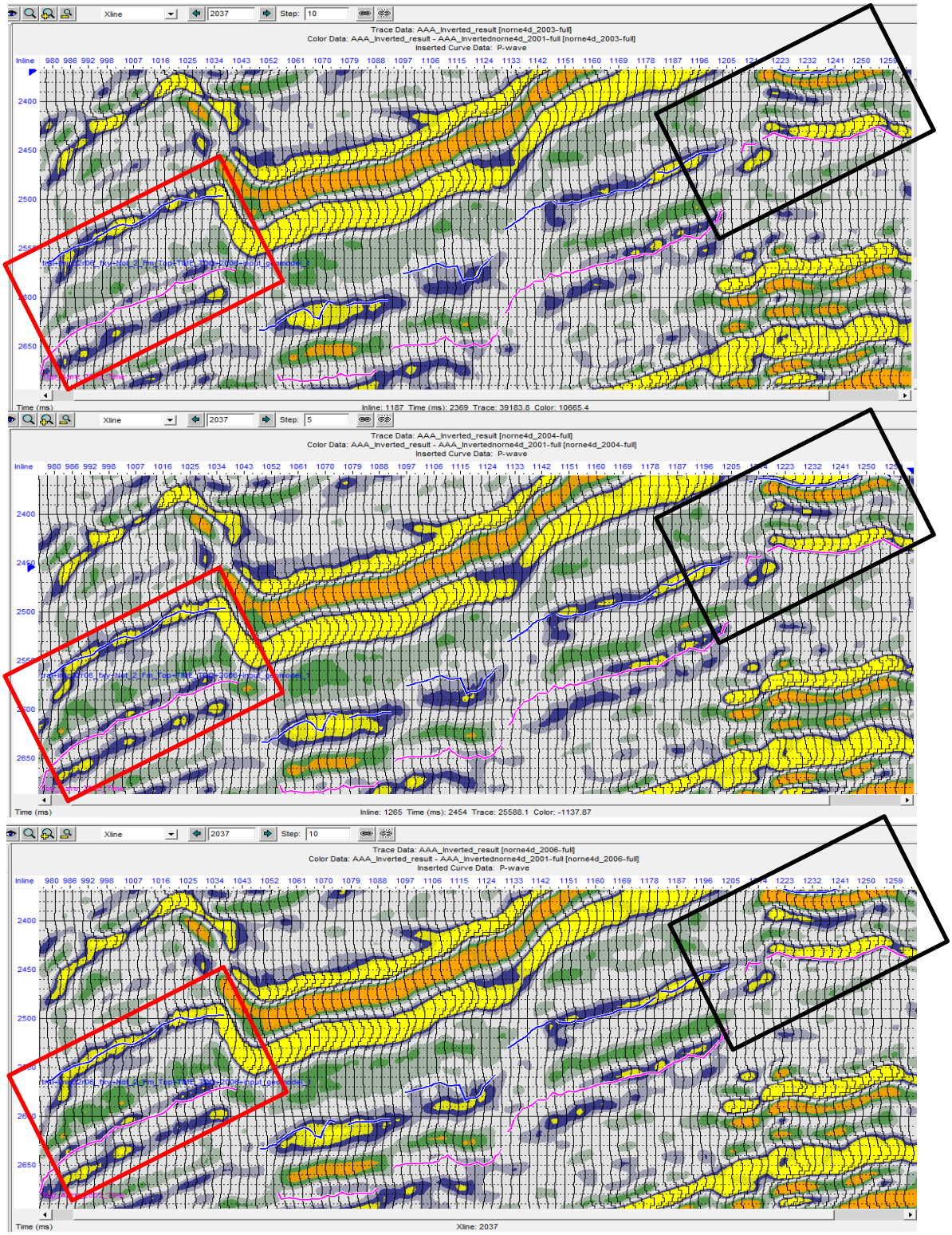

Figure 43: A cross-sectional through cross-line 2037 showing the change in impedance within the reservoir section of the E and G-segments, red and black insert respectively. The difference in impedance changes from the first monitor 2003 (top), 2004 (middle) and 2006 (bottom)

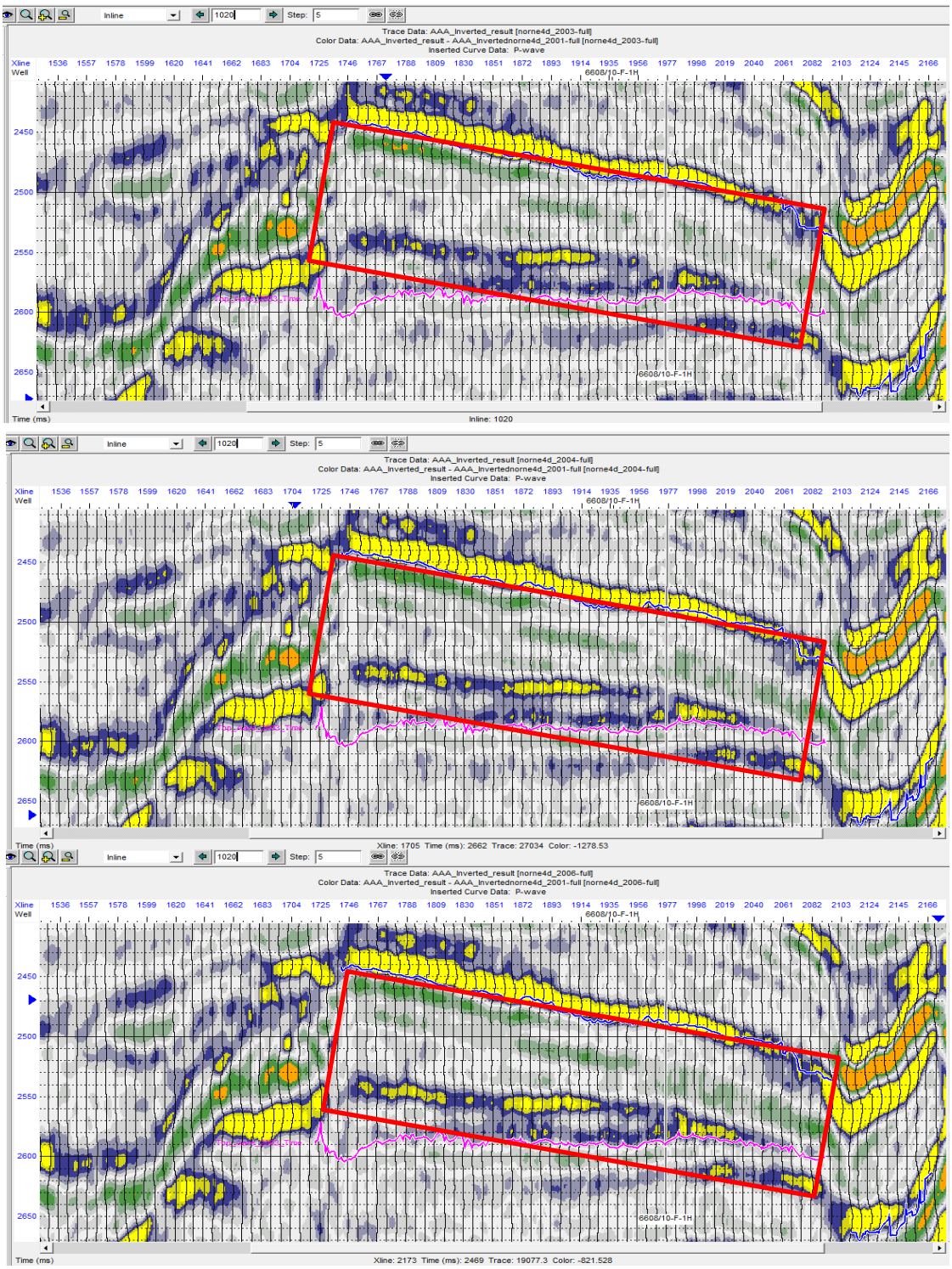

Figure 44: A cross-sectional analysis through inline 1020 showing the gradual increase in impedance within the reservoir section (red box). The difference in impedance changes from the first monitor 2003 (top), 2004 (middle) and 2006 (bottom)

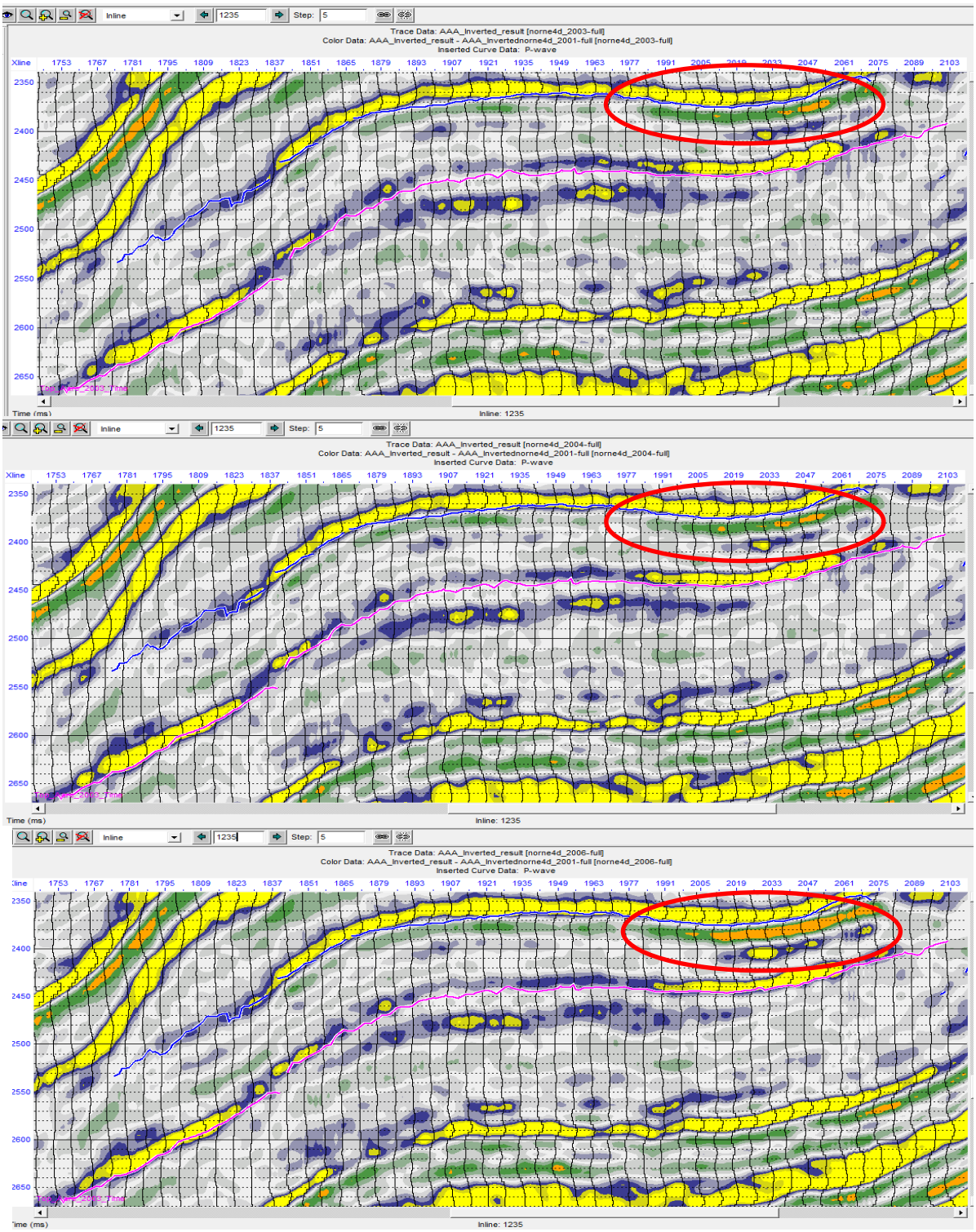

Figure 45: A cross-sectional through inline 1235 showing the change in impedance within the reservoir section of the G-segment. The difference in impedance changes from the first monitor 2003 (top), 2004 (middle) and 2006 (bottom)

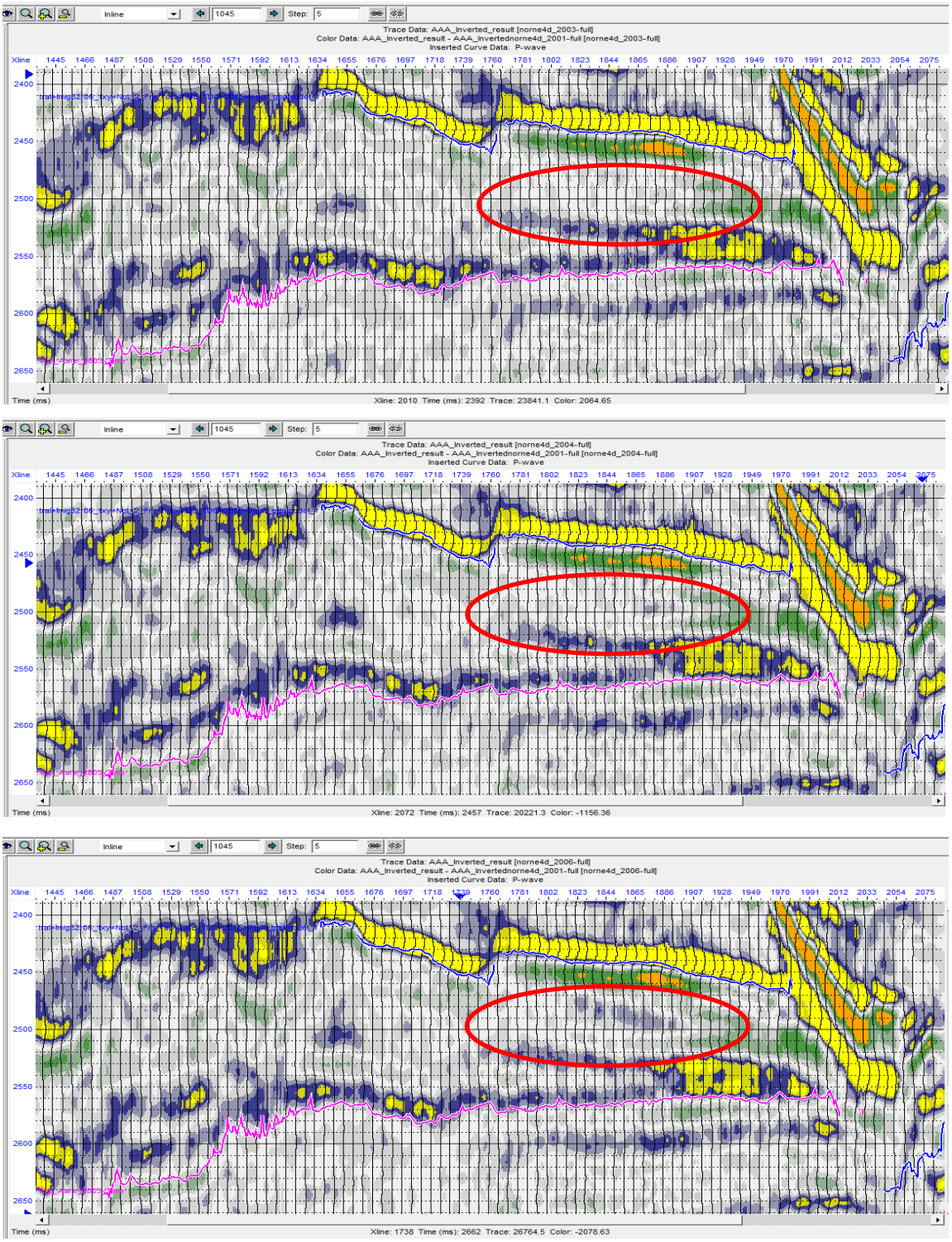

Figure 46: A cross-sectional through inline 1045 showing the change in impedance within the reservoir section of the E-segment. The difference in impedance changes from the first monitor 2003 (top), 2004 (middle) and 2006 (bottom)

6. Chapter Six - Conclusion

6.1 Conclusion

The time–lapse inversion of the Norne post-stack seismic data has revealed the impacts of production, dynamic fluid changes across main identified geologic structures, fluid front 'migration', fluid communication across structures and segments and other identified stratigraphic elements. Inversion is one of the most important processes being carried out in reservoir management and optimization of hydrocarbon production today in the industry.

The aim of the research was to track various fluid movements within the field and its impact on the reservoir as well as identify areas with the potential of hydrocarbon accumulation. There is a possibility of identifying these untapped resources because these resources are most likely located within isolated patches of the reservoir where neither water/gas injection will be able sweep them to the producer wells.

The methodology of concurrently inverting seismic data for base and several subsequent monitors has significantly reduced the potential error which could have been associated with the time-lapse inversion. Differences associated with the inverted volumes were easily tracked since all the volumes were inverted together with same parameters. Re-gridding of base and monitor surveys before crosscorrelation minimized the error associated with crosscorrelating different surveys volumes on associated seismic trace level and also increased the repeatability confidence in the compared volumes. The choice of a single initial model for base and monitor surveys rather than individual models for all surveys seems to have worked very well since it improves efficiency and reduces the number of iterative processes for tracking changes. The bandwidth matching wavelet generated for the inversion provided the needed optimized frequency range for both base and monitor surveys.

The time lapse inversion proves to capture major to minor details of production changes within the Norne field when comparing the base and monitor inverted volumes. The presence of high impedance at the injector wells gradually intensifies with observation within the monitor surveys. The increase in impedance is indicative of the water flooding within the reservoir. Comparatively low changes observed within some areas of the field show very minimal changes due to water injection influence and the possibility of untapped accumulations within less

communicating sections of the reservoir. The communication barriers may be due to stratigraphic and structural displacements within the field. The WWIT for F-1H shows a much higher rate than F-3H, this implies a much higher impedance anomaly at the former than the latter. This is the case seen in the NRMS difference data slices. Furthermore, it was observed that other segments of the Norne field (C, D, G) has experienced little water replacement when compared to the E-segment. This probably indicates that the E- segment has been much produced compared to other segments with high drainage points compared with the other segments. The C-segment shows a much pronounced change in RMS (root mean squared) velocity figure 58, despite this the segment has not reflected prominently the change in the velocity on the general impedance change map slice. Increasing amplitude and acoustic impedance are a response to the changing fluid gradient due to production as the water level rises to replace the hydrocarbon zones within parts of the Norne reservoir.

It was observed that the drainage pattern within each of the segments seems to indicate that the segments are not in communication and the fluid spill points are delimited by the bounding Norne fault systems as shown in the various impedance difference cross-sections. The time lapse section captures the spatial fluid accumulations across each segment of the Norne field within parts of the horst /fault systems.

It is also assumed that preserved hydrocarbon saturation 'pockets' bypassed by the water front indicate areas which retained their impedance contrast after production across each of the segments. It therefore implies that correlating the amplitudes of the inverted sections indicates a reasonable contrast in identifying zones of bypassed hydrocarbon or re-migrated saturated hydrocarbon zones. The advantage in this is that it provides an additional opportunity to optimize infill well locations, especially in other segments where little production impacts were observed and subsequently understanding the migrating water front's due to production drive.

Despite its extensive use in the industry it must be stated that inversion has a degree of uncertainty like any other modelling process and it is therefore non-unique. The source of the uncertainty could be one of many, ranging from acquisition and processing related parameters to the inversion. There is therefore the need to constrain the process with appropriate quality control measures from the initial stages to the end. For this research the accuracy of inversion could have been slightly compromised with the limitation in the number of wells which had

check shot data for correction application as well as generating density data for the reservoir section for one of the wells as stated previously.

The time-lapse inversion of the Norne field has shown that acoustic impedance inversion can aid in the tracking of fluids within the reservoir and thus can be effectively used as a stand-alone method or in combination with other formation evaluation methods in reservoir management.

7. Chapter Seven - References

7.1 References

1. Asquith and Gibson (1983), Basic Well Log Analysis For Geologist, AAPG, USA
2. Avseth, P., Mukerji, T., Mavko, G., (2005), Quantitative Seismic Interpretation: Applying Rock Physics Tools to Reduce Interpretation Risks, Cambridge University Press.
3. Bishop, T. N. and Nunns, A. G., (1994), Correcting amplitude, time, and phase mis-ties in seismic data, Geophysics, vol. 59, No. 6, June 1994, p. 946-953.
4. Blystad, P., Brekke, H., Færseth, R.B., Larsen, B.T., Skogseid, J. and Tørudbakken, B. (1995), Structural elements of the Norwegian continental shelf, Part II: The Norwegian Sea Region, Norwegian Petroleum Directorate Bulletin 8.
5. Brekke, H., Sjulstad, H.I., Magnus, C. and Williams, R.W. (2001), Sedimentary environments offshore Norway – An overview. In: Martinsen, O. and Dreyer, T. (eds.), Sedimentary Environments Offshore Norway – Paleozoic to Recent, NPF Special Publication 10, pp. 7–37 (Norwegian Petroleum Society and Elsevier Science B.V.).
6. Clayton, C. 1994. Origin of Natural Gas in Mid-Norway. Statoil Order DTJO13425
7. Dalland, A., Worsley, D. & Ofstad, K. 1988: A lithostratigrafic scheme for the Mesozoic and Cenozoic succession offshore mid- and northern Norway. NPD-bulletin No 4. Oljedirektoratet.
8. Faleide, J.I., Tsikalas, F., Breivik, A.J, Mjelde, R., Ritzmann, O., Engen, Ø., Wilson, J. and Eldholm, O. (2008), Structure and evolution of the continental margin off Norway and the Barents Sea, Episodes 31, 82–91.

9. Faleide, Jan Inge; Bjørlykke, Knut & Gabrielsen, Roy H. (2010), Geology of the Norwegian continental shelf, In Knut Bjørlykke (ed.), Petroleum Geoscience: From Sedimentary Environments to rock Physics, Springer Science Chapter 22. s 467 - 499
10. Gardner, G.H.F., Gardner, L.W., and Gregory, A.R., (1974), Formation velocity and density – the diagnostic basics for stratigraphic traps: Geophysics, 39, 770-780.
11. Gouveia, W., (1996), Bayesian seismic waveform inversion: parameter estimation and uncertainty analysis. Unpublished PhD. Thesis, Colorado School of Mines.
12. Greaves, R. J., and Fulp, T. J., (1987), Three-dimensional seismic monitoring of an enhanced oil recovery process: Geophysics, 52, no. 9, 1175-1187.
13. Kragh, E. D., and Christie, P., (2002), Seismic repeatability, normalized rms, and predictability: The Leading Edge, 21, 640–647.
14. Lafet, Y., Duboz, P., Deschizeaux, B., Lefeuvre, F., and Hubans, C., (2005), 4D Stratigraphic inversion of the Girassol field-Towards a more quantitative approach, 67th EAGE Conference and Technical Exhibition, Madrid, Expanded Abstract C018
15. Landrø, M., (2010), 4D Seismic, In Knut Bjørlykke (ed.), Petroleum Geoscience: From Sedimentary Environments to rock Physics. Springer Science
16. Landrø, M., (2011), Seismic data acquisition and imaging course handbook
17. Lindseth, R.O., (1979), Synthetic sonic logs – A process for stratigraphic interpretation, Geophysics, 44, 3-26.
18. Lorenzen, R.J.L., (2000), Inversion of Multicomponent Time-lapse Seismic Data for Reservoir Characterization of Vacuum Field, New Mexico, Ph.D Dissertation, Colorado School of Mines.
19. Norne and Urd Annual reservoir development plan, (2006), Statoil

20. Osdal B, Husby O, Aronsen HA, Chen N and Alsos T., (2006), Mapping the fluid front and pressure buildup using 4D data on Norne Field, The Leading Edge.

21. Ouair, Y.E.I. and Springer, M., (2005), Integrated reservoir management approach: From time-lapse acquisition to reservoir model update at the Norne field. IPTC 10894, International Petroleum Technology Conference, Doha, Qatar, 21-23 November 2005. doi: 10.2523/10894-MS

22. Plan-for-Development-and-operation-reservoir-geology-support-Documentation

23. Ross, C. P., Cunningham, G. B., and Weber, D. P., (1996), Inside the cross-equalization black box: The Leading Edge, 15, 1233–1240.

24. Reports/Statoil_Norne_2006_Processing_Reports

25. Sarkar, S., Gouveia, W., and Johnston, D., (2003), On the inversion of time-lapse data: 73rd Annual International Meeting, SEG, Expanded Abstracts, 1489–1492.

26. Sen, M., and Stoffa, P. L., (1995), Global Optimization methods in Geophysical Inversion. New York: Elsevier

27. Statoil, (1991), Regional Haltenbanken Study, Volumes 1 & 2

28. Statoil, (2001), PL128-Norne Field Reservoir Management Plan.

29. Statoil (2006), Annual reservoir development plans Norne Field.

30. Tarantola, A., (1987), Inverse Problem Theory: methods of Data Fitting and Model Parameter Estimation, New York: Elsevier

Internet Resources

31. http://factpages.npd.no/factpages/default.aspx, accessed on 9th, May, 2012

32. Articles from Hampson-Russell Assistant accessed on 20th May, 2011

33. http://www.ocean.slb.com/docs/psiv-b1/seismic_inversion_readingbetween.pdf

7.2 Appendix

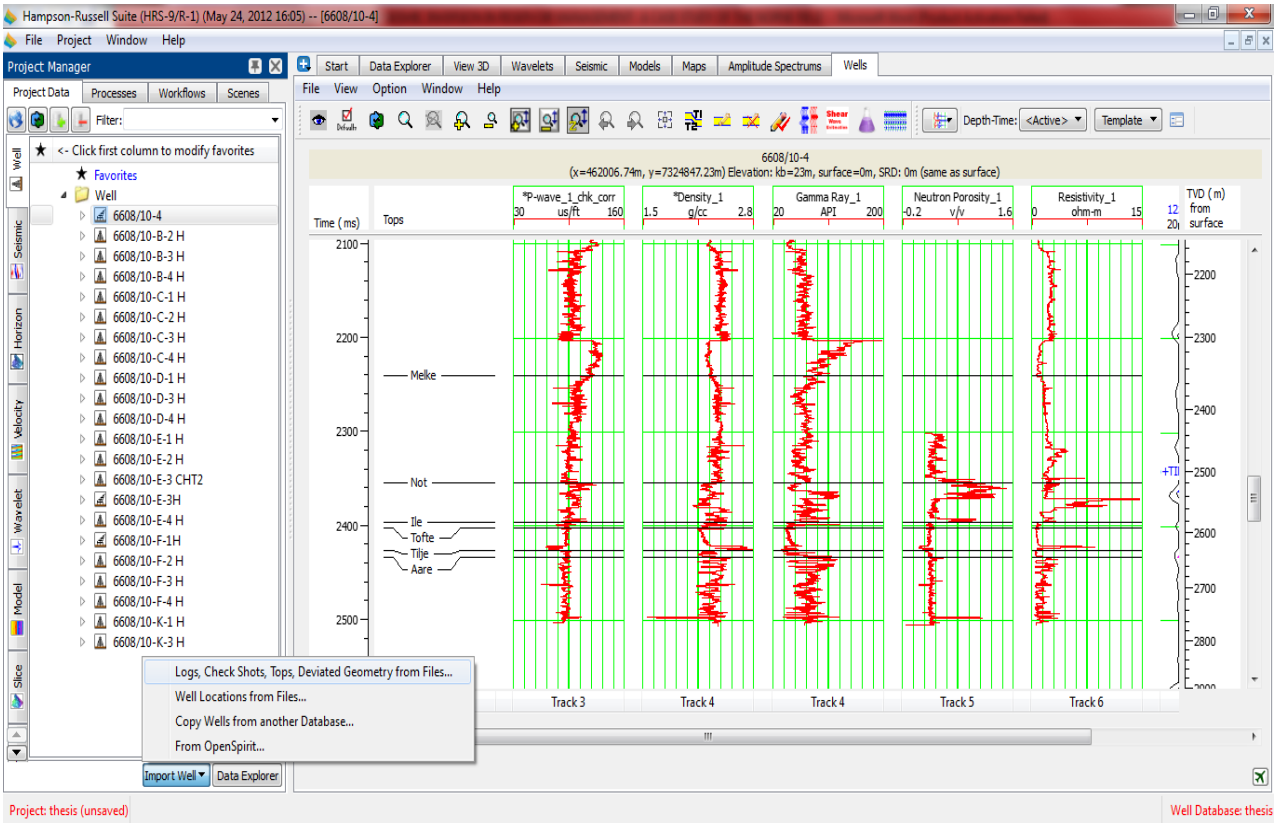

Figure 47: Import window showing the well data option to load

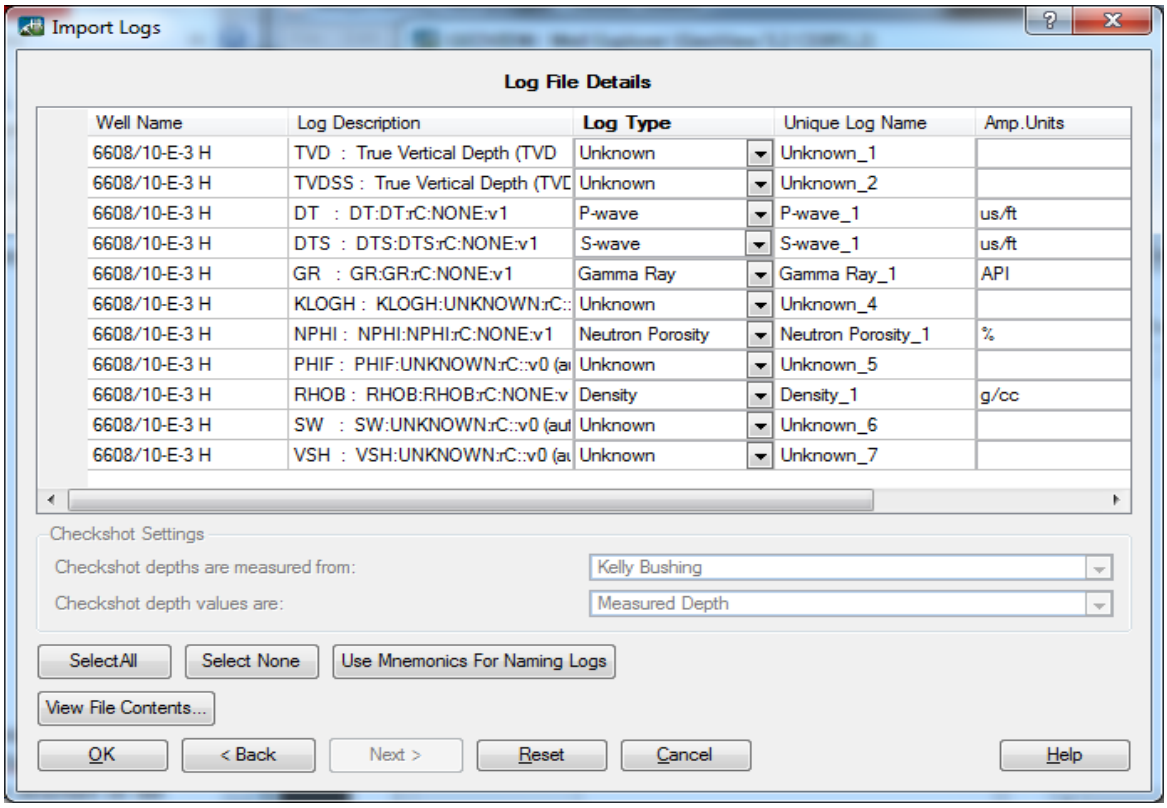

Figure 49: Log type and log description match

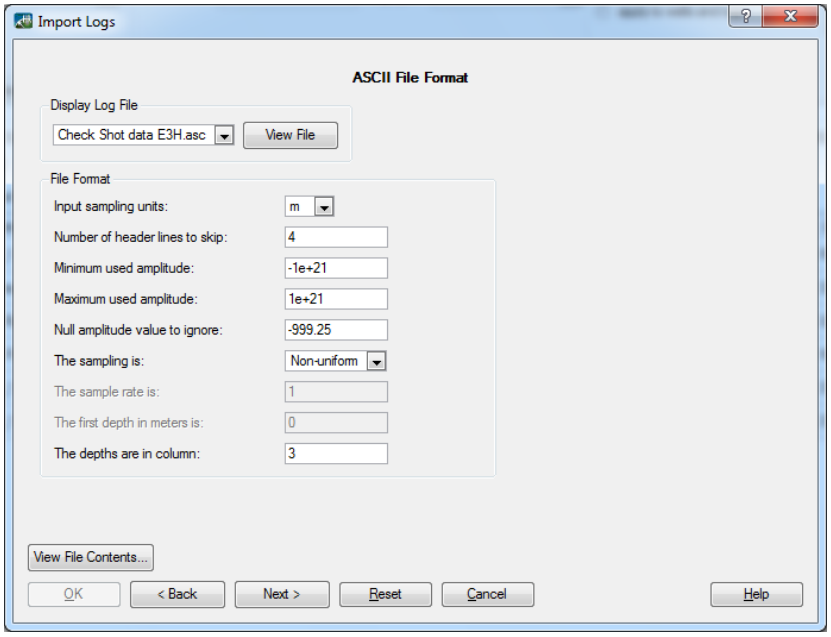

Figure 48: Input parameters for deviated geometry

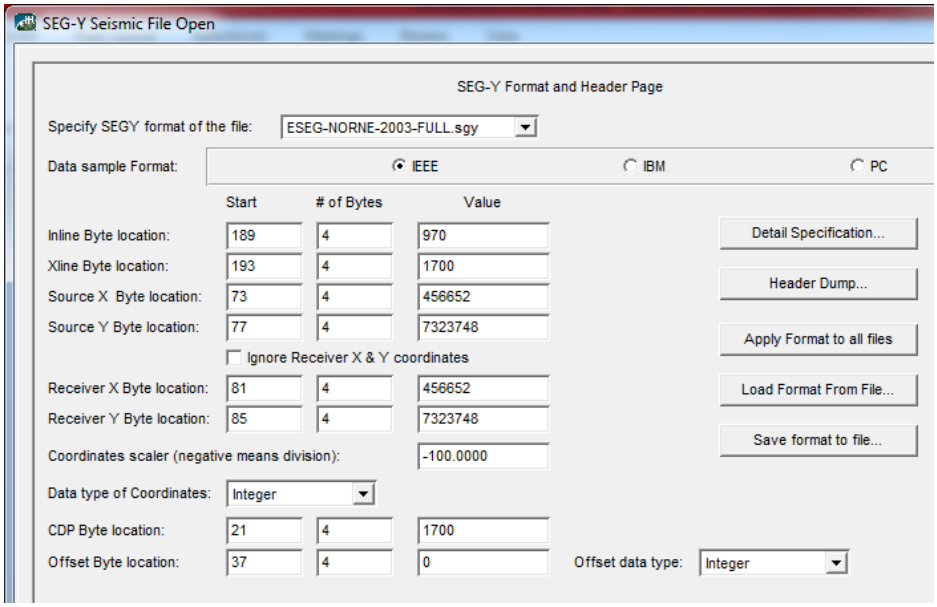

Figure 50: Parameter window for loading seismic data

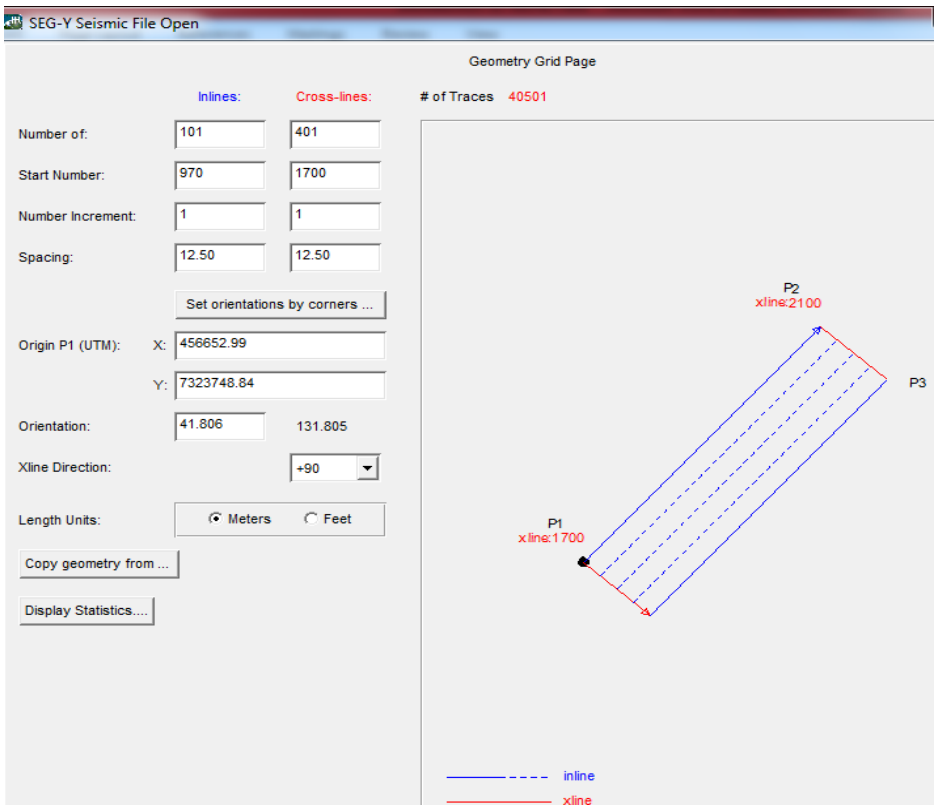

Figure 51: Parameters of loaded seismic data showing an overview of the field

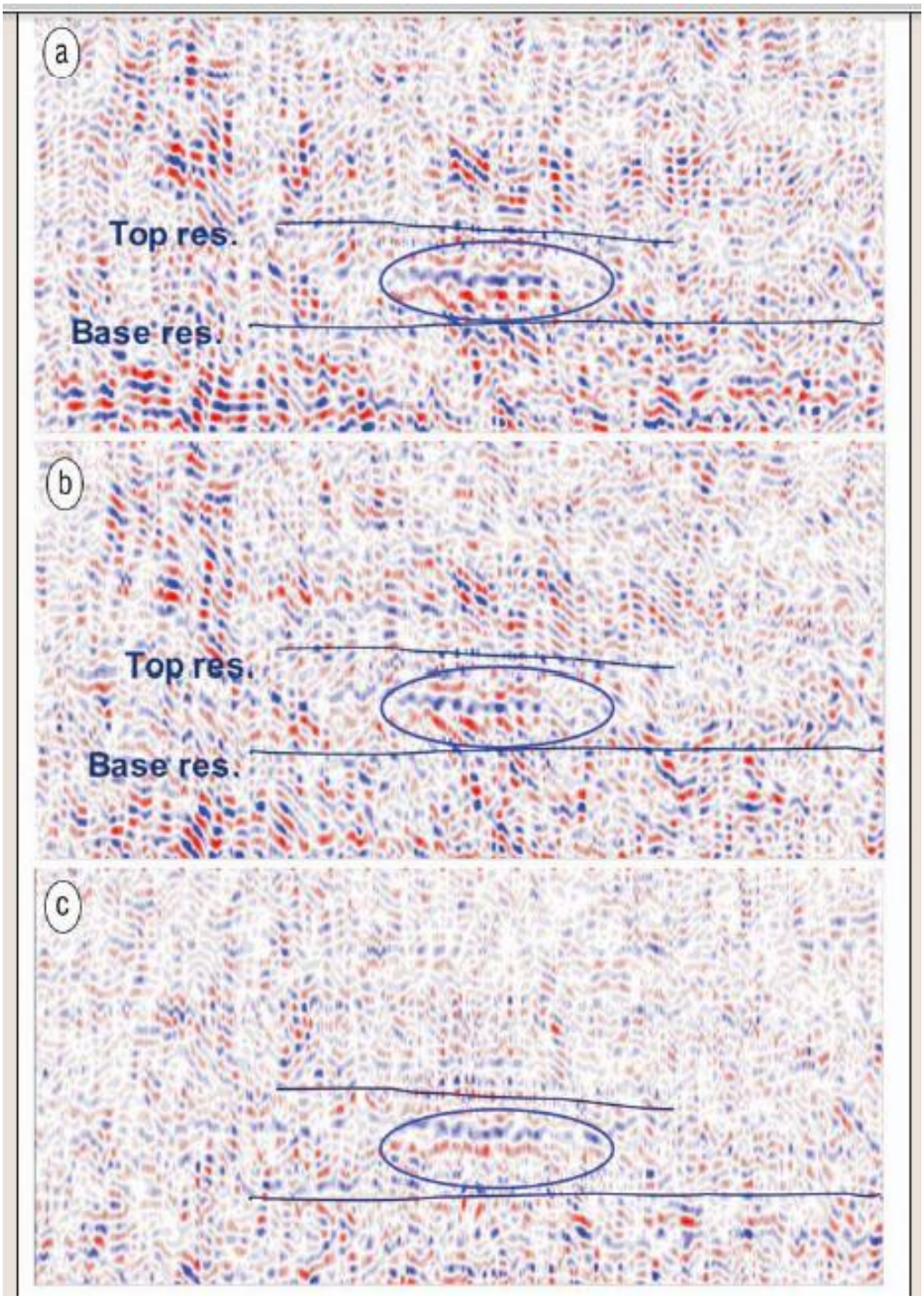

Figure 52: (a) Radon stack, (b) Radon and Tau-p (c) Radon and 2D SRME. Blue circle highlights the 4D effect of a rise of the OWC (Osdal et al., 2006)

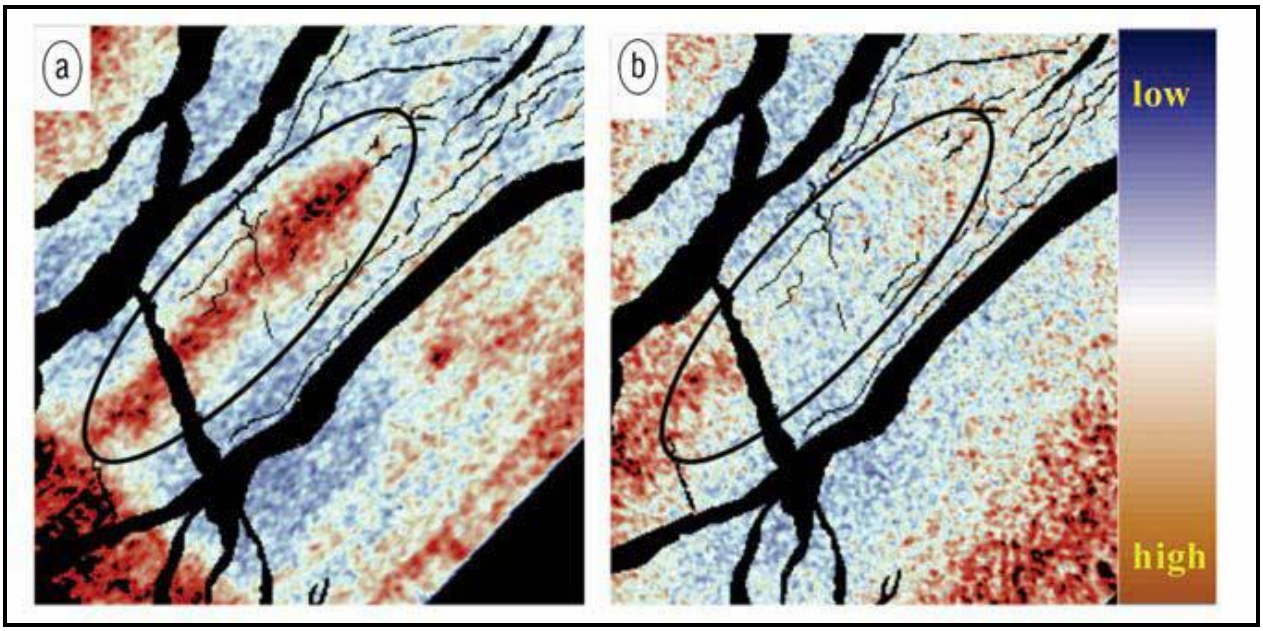

Figure 53: The NRMS map showing an overfold area with (a) all data used in the processing and (b) binning applied and non-repeating traces discarded

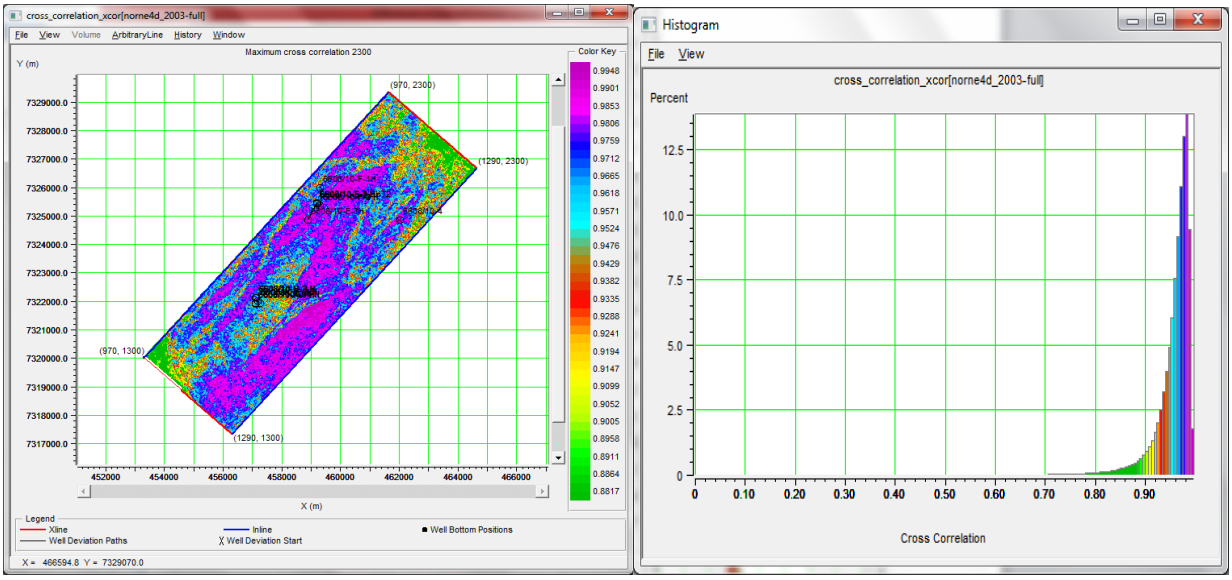

Figure 54: (Left) Map slice showing the cross-correlational percentages for 2001 and 2003, (Right) Histogram showing the crosscorrelation and its corresponding coefficient for the datasets

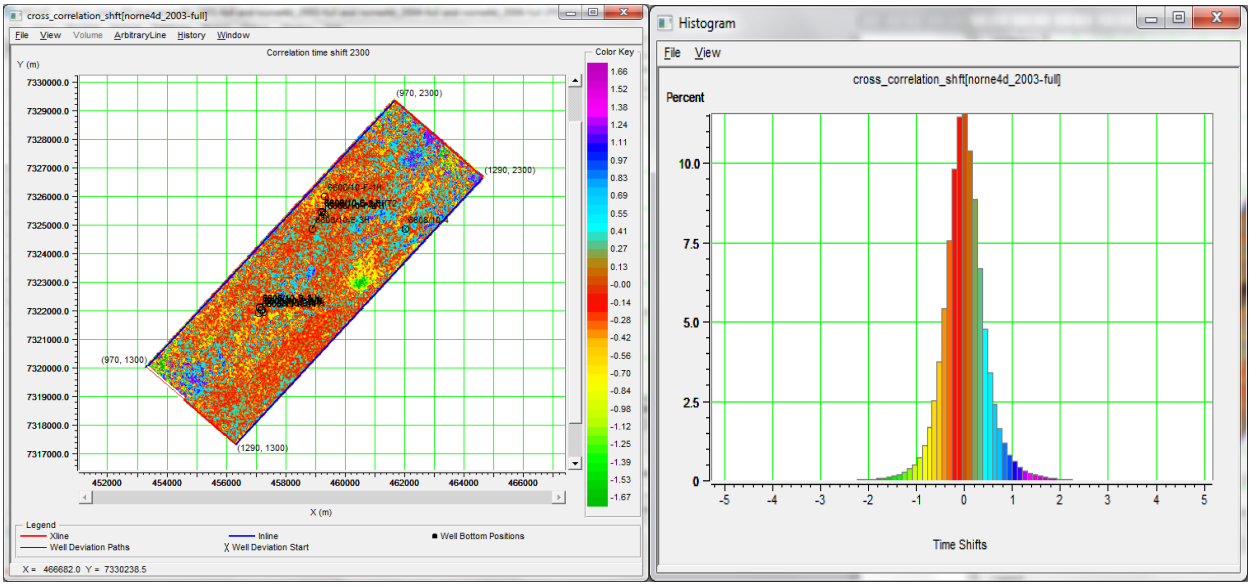

Figure 55: (Left) Time shift slice showing averagely low shifts, (Right) Histogram showing the time shift and its corresponding percentage for the datasets

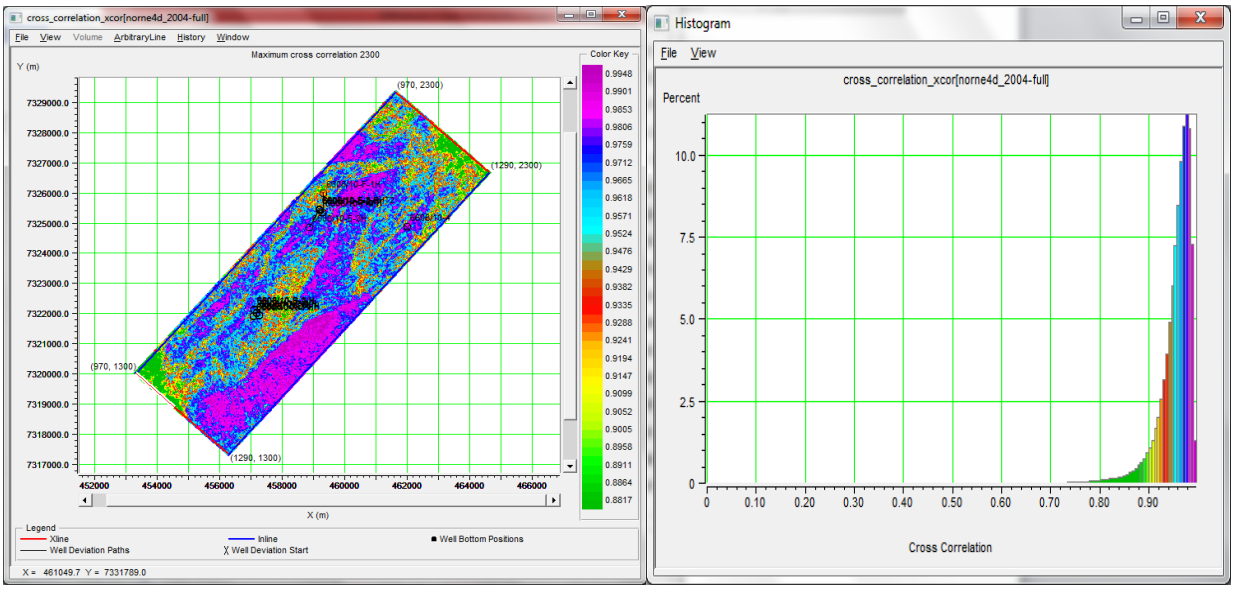

Figure 56: (Left) Map slice showing the cross-correlational percentages for 2001 and 2004, (Right) Histogram showing the crosscorrelation and its corresponding coefficient for the datasets

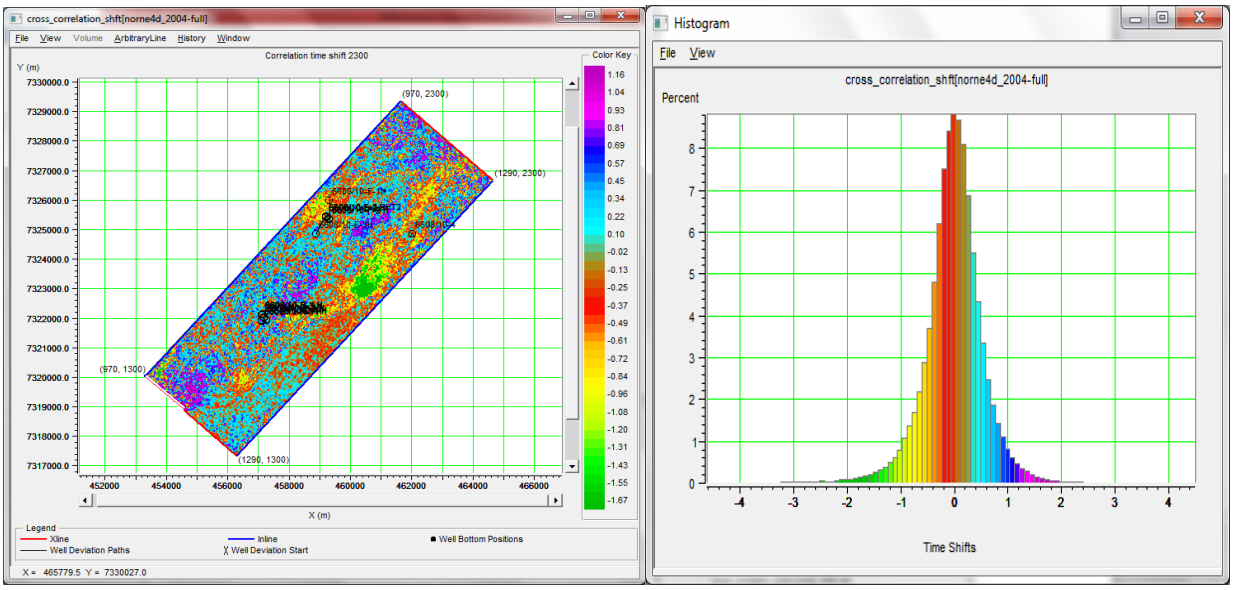

Figure 57 (Left) Time shift slice showing averagely low shifts, (Right) Histogram showing the time shift and its corresponding percentage for the datasets

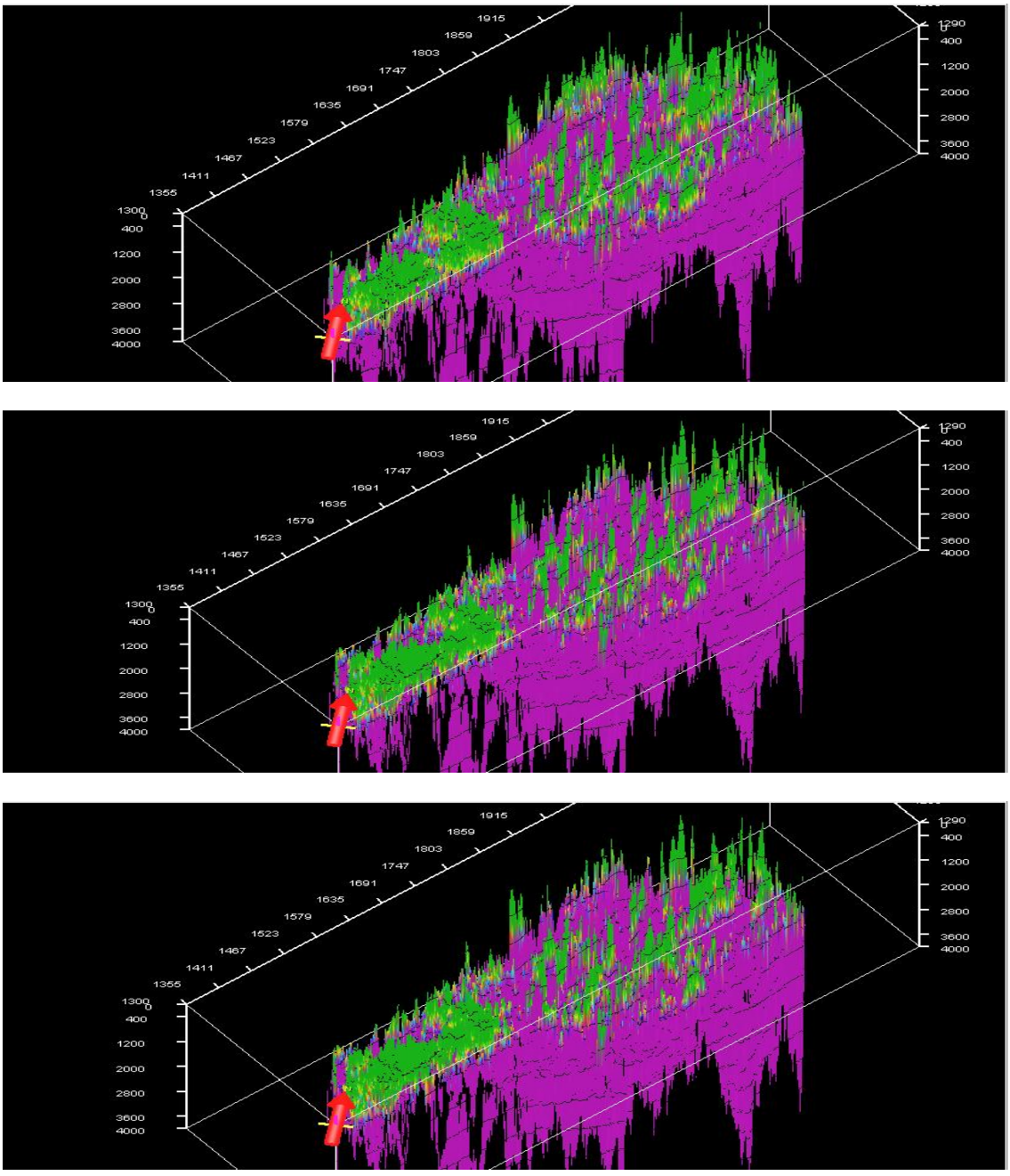

Figure 58: (Top) RMS velocity difference between 2003 and 2001 (Middle) RMS velocity difference between 2004 and 2001 (Bottom) RMS velocity difference between 2006 and 2001